2010

Expression and functions of renin isoforms

Di Xu
University of Iowa

EXPRESSION AND FUNCTIONS OF RENIN ISOFORMS

by

Di Xu

An Abstract

Of a thesis submitted in partial fulfillment
of the requirements for the Doctor of
Philosophy degree in Genetics
in the Graduate College of
The University of Iowa

May 2010

Thesis Supervisor: Professor Curt D. Sigmund

ABSTRACT

Renin is an enzyme that catalyzes the rate-limiting step in the production of angiotensin peptides, and is thus a key regulator of processes controlled by angiotensin such as blood pressure, hydromineral balance, and metabolism. Our laboratory and others have previously identified a novel isoform of renin (icRen) which, as a result of the utilization of an alternate first exon, lacks the signal peptide and first third of the pro-segment of classical secreted renin (sRen). This alternate icRen isoform thus remains within the cytoplasm of the cell, but is constitutively active. Here, we report that while sRen is the predominant form of renin expressed in most tissues during development, icRen is the predominant form of renin within the adult brain. Thus, we hypothesized that sRen and icRen play distinct physiological roles in adult mice.

To examine this hypothesis, we have utilized the Cre-LoxP system to selectively delete either isoform globally or within selected cell types such as neurons and glia. We have successfully developed a “sRen-flox” model, in which endogenous mouse sRen isoform can be selectively deleted, while not affecting endogenous icRen production. Breeding these mice against the E2A-Cre, Nestin-Cre, and GFAP-Cre mouse lines resulted in global-, neuronal-, and glial-specific knockouts of sRen, respectively. Physiological characterization of resulting mice has uncovered postnatal lethality, hypotension, renal atrophy, vascular dysfunction and decreased body weight and white adipose in the global knockouts. Depletion of sRen from only neuronal or glial cells does not appear to alter any of these phenotypes at baseline. From these data, we conclude that while peripheral sRen is of primary importance to blood pressure regulation, hydromineral balance, and metabolism, central expression of this isoform is unimportant. Further, comparison of our results to published findings from global total renin knockout models indirectly supports a role for icRen in the brain. We are currently

in the process of generating icRen-flox and subsequent knockout mice, which will be useful models to directly analyze the physiological role(s) of icRen.

Abstract Approved: _____
Thesis Supervisor

_____
Title and Department

_____
Date

EXPRESSION AND FUNCTIONS OF RENIN ISOFORMS

by

Di Xu

A thesis submitted in partial fulfillment
of the requirements for the Doctor of
Philosophy degree in Genetics
in the Graduate College of
The University of Iowa

May 2010

Thesis Supervisor: Professor Curt D. Sigmund

Graduate College
The University of Iowa
Iowa City, Iowa

CERTIFICATE OF APPROVAL

_____

PH.D. THESIS

_____

This is to certify that the Ph.D. thesis of

Di Xu

has been approved by the Examining Committee
for the thesis requirement for the Doctor of Philosophy
degree in Genetics at the May 2010 graduation.

Thesis Committee: _____
Curt D. Sigmund, Thesis Supervisor

_____
Michael G. Anderson

_____
Jim J. Lin

_____
Anton P. McCaffrey

_____
Kamal Rahmouni

_____
Richard J. Smith

_____
Baoli Yang

To my grandparents, who are the roots of my large family, from where my deepest love grows.

To my grandfather, Yiqian Zhang, who has been and will always be my strongest motivation for participating in biomedical research.

To my parents for their selfless love and support.

To my husband for his love, care, and for being my best company.

“The highest education is that which does not merely give us information but makes our life in harmony with all existence.”

Rabindranath Tagore

ACKNOWLEDGMENTS

Pursuing the Ph.D. degree in Genetics at the University of Iowa has been one of my life-changing decisions. I was privileged to meet many professors, classmates, colleagues and friends who have provided tremendous support during my study and life here. First and foremost, I would like to show my deepest gratitude to my thesis advisor, Dr. Curt D. Sigmund, for his guidance and patience throughout my training to become a professional scientist. This dissertation would not have been possible without his support. I would also like to express my appreciation to my thesis committee members, Drs. Michael G. Anderson, Jim J. Lin, Anton P. McCaffrey, Kamal Rahmouni, Richard J. Smith and Baoli Yang, for their valuable advice on my dissertation.

I am indebted to many of my past and present colleagues from the Sigmund laboratory. They have witnessed my failure and success in experimental practices, and helped me grow and learn in a scientific and enjoyable environment. I offer my sincere gratitude to fellow graduate students, Dr. Xiyou (Joe) Zhou, Dr. Andreas Beyer, Dr. Hana Itani, Dr. Carmen Halabi, Dr. Matthew Dickson, Eric Weatherford, Jinlu Cai and Christopher Pelham. It was great pleasure to work and discuss science with them. Special thanks to Joe, who led me through my rotation project and taught me various experimental molecular biology approaches. I am also grateful to postdoctoral fellows: Drs. Koji Sakai, Robert Bianco, Willem (Toy) de Lange, Huiping Li, Justin Grobe, Pimonrat Ketsawatsomkron, Giulianna Borges, Sungmi Park and Mark Santillan for their technical and intellectual support. I would like to specifically thank Justin and Giulianna for their collaboration in the physiological experiments and inspiring comments on my paper and dissertation drafts. Additionally, I owe my sincere gratitude to research scientists Drs. Xuebo Liu, Henry Keen and Severine Groh for sharing their experiences with me and guiding me through the dissertation. I specifically appreciate the collaboration with Dr. Xuebo Liu on the icRen project. Last but not least, I would like to thank Debbie Davis for

performing animal surgeries, Ella Born for keeping the lab in order, Xin Tian for helping with experiments and Vickie Akers for administrative support.

I have been honored over the years to have collaborated with a variety of individuals in and out of the University of Iowa. I would like to express my appreciation to the Gene Targeting Facility for the generation of the knockout mice, the Transgenic Animal Facility for performing genotyping, Drs. Martin Cassell and Khristofor Agassandian from the Department of Anatomy and Cell Biology for performing immunohistochemistry in the brain, Drs. Nobuyuki Takahashi and Feng Li from the University of North Carolina for their advice on subcutaneous saline injection, and Drs. Ariel Gomez and Maria Sequeira Lopez from the University of Virginia for the renal immunohistochemistry.

I would also like to acknowledge the grants from NIH (P01HL084207 to Dr. Curt D. Sigmund) and AHA (0910035G to myself) to fund this project, and to promote our understanding of human diseases.

My family has been a tremendous support during my Ph.D. study. They have been the source of strength, courage and inspiration during frustration and happiness. I owe my thanks to my parents, who have been my role models for life values. I was away from home since I was middle school-age. They have always been there listening to me and giving me advice to keep me on the right track. I am also thankful to my husband for his generous love and encouragement, and for being my best friend in the journey of life.

ABSTRACT

Renin is an enzyme that catalyzes the rate-limiting step in the production of angiotensin peptides, and is thus a key regulator of processes controlled by angiotensin such as blood pressure, hydromineral balance, and metabolism. Our laboratory and others have previously identified a novel isoform of renin (icRen) which, as a result of the utilization of an alternate first exon, lacks the signal peptide and first third of the pro-segment of classical secreted renin (sRen). This alternate icRen isoform thus remains within the cytoplasm of the cell, but is constitutively active. Here, we report that while sRen is the predominant form of renin expressed in most tissues during development, icRen is the predominant form of renin within the adult brain. Thus, we hypothesized that sRen and icRen play distinct physiological roles in adult mice.

To examine this hypothesis, we have utilized the Cre-LoxP system to selectively delete either isoform globally or within selected cell types such as neurons and glia. We have successfully developed a “sRen-flox” model, in which endogenous mouse sRen isoform can be selectively deleted, while not affecting endogenous icRen production. Breeding these mice against the E2A-Cre, Nestin-Cre, and GFAP-Cre mouse lines resulted in global-, neuronal-, and glial-specific knockouts of sRen, respectively. Physiological characterization of resulting mice has uncovered postnatal lethality, hypotension, renal atrophy, vascular dysfunction and decreased body weight and white adipose in the global knockouts. Depletion of sRen from only neuronal or glial cells does not appear to alter any of these phenotypes at baseline. From these data, we conclude that while peripheral sRen is of primary importance to blood pressure regulation, hydromineral balance, and metabolism, central expression of this isoform is unimportant. Further, comparison of our results to published findings from global total renin knockout models indirectly supports a role for icRen in the brain. We are currently

in the process of generating icRen-flox and subsequent knockout mice, which will be useful models to directly analyze the physiological role(s) of icRen.

TABLE OF CONTENTS

LIST OF TABLES

LIST OF FIGURES

CHAPTER 1

INTRODUCTION: RENIN AND HYPERTENSION

Hypertension

Hypertension is one of the most prevalent diseases in the world. With its related cardiovascular diseases (CVD), hypertension accounts for 20% of deaths worldwide[1]. In the US, hypertension affects about 144 million people (73.6 million with hypertension and 70 million with prehypertension), which accounts for approximately 30% of adults according to the National Health and Nutrition Examination Survey (NHANES). Hypertension is an established risk factor for diabetes, obesity, coronary disease (e.g. atherosclerosis), stroke, heart failure and renal defects. Studies have shown that for every 10 mmHg increase of systolic blood pressure, there is a doubling of the risk of having a heart attack, stroke, or renal failure[2,3]. Chronic hypertension can also lead to severe blood vessel damage in the eye, brain, heart, and/or kidney[4]. According to the 2009 update from the American Heart Association, 69% of people experiencing their first heart attack, 77% of people affected with their first stroke, and 74% who have congestive heart failure suffer from hypertension[5]. In addition, hypertension is the 13th largest cause of death in the United States (American Heart Association, 2005)[6], not counting the mortality of other cardiovascular diseases secondary to hypertension. Research from the Centers for Disease Control (CDC) suggests that hypertension related morbidity and mortality are likely to grow as the population ages, based on the fact that the prevalence of hypertension directly correlates with age (7.3% of 18-39 year-olds, 32.6% of 40-59 year-olds and 66.6% of >60 year-olds are affected)[7].

Hypertension is defined as a systolic blood pressure (SBP) >= 140 mmHg and/or a diastolic blood pressure (DBP) >=90 mmHg in humans. This definition is not age-adjusted, and simply applies to individuals without antihypertensive treatment. Between normal blood pressure and hypertension, there is also a spectrum of pre-

hypertension, when SBP/DBP falls in to the range 120-139 mmHg/ 80-89 mmHg. When an individual's resting blood pressure climbs up to more than 160/100 mmHg, he or she will be diagnosed with stage 2 hypertension or malignant hypertension (as opposed to stage 1), which could be life-threatening, and is in urgent need of medical intervention.

Causes and Treatments of Hypertension

Hypertension is divided clinically into primary and secondary hypertension. Primary hypertension is also called essential hypertension, to which no single cause has been designated to be responsible for all cases. Primary hypertension accounts for 80% of all hypertensive cases. In contrast, secondary hypertension is a result of a definable clinical condition such as pheochromocytoma or renal artery stenosis. Primary hypertension is a complex disorder. Its heterogeneity is demonstrated in two aspects. The first aspect is phenotypic heterogeneity, as indicated by the diversity of antihypertensive treatments that are effective among patients. For instance, some patients that have elevated sympathetic nerve activity may be responsive to β-adrenergic blockers, while some others that are volume expanded could be better treated with diuretics. The second aspect is its genetic heterogeneity, in which multiple genes contribute to a blood pressure phenotype. For example, the renin-angiotensin system is a group of gene products that play pivotal roles in blood pressure regulation. It is noteworthy that in addition to genetic contributions, environmental factors (such as smoke, stress and diet) also have a significant impact on the development of primary hypertension.

Unlike its primary counterpart, secondary hypertension can be monogenic or multifactorial. It can also be a result of other physiological changes or environmental challenges. Causes of secondary hypertension include secretion of excess aldosterone, hormonal changes (e.g. oral contraceptives), adrenocortical hyperfunction (e.g. Cushing's syndrome), mental/emotional changes or damage to the central nervous

system (e.g. increased intracranial pressure or tumor). Environmental risk factors for hypertension include being overweight, not being physiologically active, stress, tobacco consumption, alcohol consumption, salt overload, low potassium diet, vitamin D deficiency and certain chronic conditions (e.g. high cholesterol and sleep apnea).

Available pharmacological therapy for hypertension includes approaches to target renal fluid retention, vascular resistance, heart rate and cardiac contractility. The categories of drugs used to treat hypertension include diuretics, α-adrenergic receptor blockers, β-adrenergic receptor blockers, calcium channel blockers (CCB), direct vasodilators (e.g. nitroglycerin), angiotensin converting enzyme inhibitors (ACEi, e.g. captopril[8]), angiotensin type 1 receptor blockers (ARB, e.g. losartan[9]) and newly developed renin inhibitors (e.g. aliskiren[10]). Although a broad range of drugs exist, most monotherapies suffer from ineffectiveness and a significant number of side effects[11,12]. For instance, β-blockers (especially atenolol) are associated with mortality and stroke in elderly patients[13]. Moreover, ACEi and ARB therapies reduce renal perfusion pressure and increase volume retention as a byproduct of lowering systemic blood pressure. Further, diuretics alone tend to lose effectiveness in aged patients. Thus, diuretics are commonly used along with ACEi's and ARB's to minimize side effects[14]. Still, a significant number of individuals with primary hypertension are less responsive to these treatments. According to research from the Baylor College of Medicine, only 27% of Americans who are on antihypertensive treatments successfully have their systolic blood pressure under 140 mmHg[15]. Additionally, it is documented that among individuals with hypertension, 78.7% are aware that they have it, but only 69.1% are currently under treatment, with the remaining 30.9% not taking any antihypertensive medicine (NHANES 2005–06)[16]. Even within the 69.1% who are receiving treatments, there is an issue of compliance to the therapy, presumably due to concerns about ineffectiveness and side effects[17]. All these taken together are reasons to conduct basic

research on hypertension to further understand its mechanism and work toward better clinical therapies.

Physiological Regulation of Systemic Blood Pressure

The four major organs/tissues that participate in blood pressure regulation are the brain, heart, kidney and vasculature. The brain is the site where peripheral cardiovascular information is integrated and processed. Although the cardiovascular system is able to manage blood flow and heart rate on its own, additional signals from the brain ensure precise and quick responses of the cardiovascular system to physiological or environmental cues. Moreover, the central nervous system contributes to the chronic regulation of blood pressure[18]. For example, extensive studies from our group and others have found that interference with the renin-angiotensin system in the brain leads to alteration of systemic blood pressure[19-23].

Many nuclei that control cardiovascular function are located in two general areas of the brain (Figure 1), the hypothalamus (which includes the Paraventricular Nucleus, PVN) and brain stem (which includes the Nucleus Tractus Solitarius, NTS and Rostroventrolateral Medulla, RVLM). Upon physiological stimuli (such as thirst, restraint stress *etc.*), they send out nerve signals or hormones to peripheral tissues (e.g. heart, kidney and vascular bed) to fine-tune blood pressure and fluid homeostasis. Vasopressin, an example of a neurohormone, is a peptide that is synthesized in the hypothalamus and stored in the posterior pituitary gland. Its discharge into the circulation is elevated upon dehydration in order to preserve water through its action on the kidneys. Direct sympathetic (and parasympathetic) stimulation of cardiovascular organs also contributes to the central regulation of blood pressure. The NTS is a site to integrate signals from chemoreceptors and mechanoreceptors from the peripheral (for instance, lung, heart, blood vessels and intestines). Physiological changes (such as altered blood pressure and heart rate) are detected via baroreceptors and

chemoreceptors at the carotid bodies and aortic arch and signals are relayed to the NTS. The NTS then activates glutamatergic neuronal projections to the CVLM (Caudalventrallateral Medulla). Postsynaptic GABAergic neurons in CVLM then suppress nerve firing in RVLM to affect sympathetic nerve activity to peripheral organs (such as heart, kidney and vasculature) to alter heart rate, renin secretion from JG cells, and vasoconstriction[24].

The heart controls blood flow through regulating stroke volume and heart rate. The relationship between blood flow and blood pressure is defined as: Arterial Pressure = Blood Flow (cardiac output) x Vascular Resistance, where Cardiac Output = Stroke Volume x Heart Rate[25]. A bradycardic effect mediated through the brain could potentially slow down the heart beat and thus lower the blood pressure. In contrast, a tachycardic effect could contribute to increased blood pressure assuming the stroke volume remains unaltered. Under normal physiological conditions, the autonomic nervous system tightly regulates heart rate over a range of blood pressures. Antihypertensive treatments such as β-blockers have been utilized to suppress sympathetic outflow to the heart in order to decrease heart rate and contractility. The interaction between hypertension and cardiac function is mutual. In both animals and human, hypertension is frequently linked to cardiac hypertrophy.

The kidney has a profound influence on blood pressure mainly through its regulation of plasma volume and composition (e.g. electrolyte and water reabsorption). Under normal physiological conditions, the kidney regulates blood volume by managing the amount of urine that is produced. Urine formation involves three steps: glomerular filtration, reabsorption and secretion[25]. The kidney consists of structural units named nephrons. Glomeruli are the structures in nephrons responsible for initial fluid and electrolyte filtration and protein retention. Other structures in the nephron, such as the proximal tubules, loop of Henle and collecting duct are sites for reabsorption and secretion. Diuretics work in the kidney to promote water excretion. Therefore, they

have been used to treat hypertensive patients to decrease blood volume and pressure. On the other hand, antidiuretic hormone (ADH, also named Arginine Vasopressin) acts to expand plasma volume by eliciting insertion of aquaporin-2 channels into the apical membrane of collecting duct cells to facilitate water reabsorption. The kidney is also a major site for the synthesis of renin. Conventionally, renin is formed in and secreted from Juxtaglomerular (JG) cells of the afferent arteriole of glomeruli. Its secretion is mediated by multiple physiological stimuli, including low blood pressure, increased sympathetic activation and decreased plasma Na concentration[26].

The vasculature is directly responsible for blood pressure changes via vasoconstriction and vasodilation. Small changes in the diameter in a blood vessel lead to large changes in vascular resistance (Resistance α (viscosity x length)/radius^4). Under normal physiological conditions, resistence vessels (e.g. arterioles) are the primary regulators of blood pressure. Conduit arteries (such as aorta, carotid arteries and femoral arteries) contribute less to blood pressure regulation except in disease states such as atherosclerosis. Because vascular resistance is positively linked to arterial blood pressure, antihypertensive drugs such as calcium channel blockers and α-adrenergic receptor antagonists have been employed to decrease vascular resistance by reducing vasoconstriction. Vascular responses are mediated by a variety of pathways, of which an important example is Angiotensin-II type 1 receptor (AT1R) induced vasoconstriction [27]. Global AT1R knockout mice exhibit decreased blood pressure[28,29], which is probably (at least partially) due to lack of vascular AT1R, as Crowley S.D. *et al.* have demonstrated that renal AT1Rs are only partially responsible for maintaining normal blood pressure and that systemic AT1Rs are equally important for blood pressure regulation[30]. Nitric oxide (NO), in contrast, diffuses from vascular endothelial cells to smooth muscle cells, and buffers blood pressure through vasodilation[31]. Endothelial Nitric Oxide Synthase (eNOS) knockout mice exhibit enhanced blood pressure variability compared to wild-type controls[32].

Renin-Angiotensin System (RAS)

The RAS is known to influence many aspects of blood pressure regulation, including sympathetic output, vascular contraction, electrolyte/fluid homeostasis and cardiac cell development. As depicted in Figure 2, in the RAS, the aspartyl protease renin cleaves the substrate angiotensinogen (AGT) into a decapeptide, angiotensin-I (Ang-I). Angiotensin-I is further digested into angiotensin-II (Ang-II) by angiotensin converting enzyme (ACE), and two amino acids at the carboxyl terminal of Ang-I are removed. The octapeptide Ang-II is generally considered the main effector of the RAS, and binds to angiotensin type-I receptor (AT1R) or type-II receptor (AT2R). Once activated, membrane bound AT1R at the cell surface of target tissues will, depending on cell type, cause vasoconstriction, increase heart rate and blood pressure, promote fluid and sodium intake behaviors, and cause renal sodium reabsorption. In contrast, AT2R plays an antagonistic role, as it typically facilitates vasodilation and decreased blood pressure[33,34].

Notably, there have been numerous studies indicating that the RAS is more complex than originally described[35]. ACE2 is a prolyl endopeptidase that removes one amino acid of Ang-I from its carboxyl end to generate Ang-(1-9), which is subsequently processed into Ang-(1-7) by ACE. Alternatively, ACE2 is capable of producing Ang-(1-7) directly from Ang-II. Ang-II is the term for Ang-(1-8). In addition, it has been suggested that alternative enzymes may be involved in Ang-II generation besides renin and ACE. Examples of those enzymes include tonin, cathepsins and kallikrein. However, when one considers that 1) tonin is a slow-acting enzyme, 2) cathepsin D is only active in a low pH environment (e.g. lysosome), and 3) kallikrein mainly liberates kinins (bradykinin and kallidin) from kininogen and also generates plasmin from plasminogen, it is likely that renin is the main enzyme that cleaves AGT *in vivo*[36]. AGT is the only known substrate for renin[37]. The renin-angiotensinogen reaction is the rate-limiting step in Ang-II generation, as ACE is relatively abundant. Chymase is a serine protease that may also play a role in

converting Ang-I to Ang-II. It is mainly expressed in mast cells, and was reported to be involved in renovascular hypertension (RVH) in Goldblatt rat models[38]. Ang-II has a half life of 30 seconds in plasma. Ang-II can be metabolized by aspartyl aminopeptidase A into Ang-III (Ang-(2-8)), which lacks one N-terminal amino acid when compared to Ang-II. Ang-III could be further cleaved into Ang-IV by an arginyl aminopeptidase N. Studies have shown that both Ang-III and Ang-IV could be physiologically active in certain tissues, in particular, the brain[39,40]. Ang-III has been determined to induce pressor responses[41] and Ang-IV is involved in learning and memory[42]. Last but not least, prorenin (or inactive renin) has attracted considerable attention in recent few years because of the novel finding of a prorenin/renin receptor and its potential in clinical therapy.

The full-length precursor of renin is preprorenin which is composed of a pre-segment (the signal peptide for secretion), a pro-segment that covers the active enzymatic site of renin under normal conditions, and mature active renin. After entering the Endoplasmic Reticulum (ER), preprorenin is processed into prorenin. The prorenin is either secreted constitutively out of cells or packaged into secretory granules, where its pro-segment is proteolytically cleaved to generate active renin. Notably, the plasma level of prorenin is ~10 fold higher than that of mature renin[43]. Several research groups have shown that prorenin and renin both are able to bind to the prorenin/renin receptor[44], and the binding of prorenin to the receptor leads to a conformational change of prorenin which allows it to be enzymatically active without cleaving off the pro-segment[45]. Presumably, prorenin binding to the receptor leads to the unfolding of the pro-segment out of the active site of the enzyme, thus allowing substrate entry. Interestingly, Stankovic AR *et al.* have demonstrated that renal vasodilator response to captopril (ACE inhibitor) in diabetic patients correlates better with the prorenin plasma levels than that of renin[46]. Soon after the discovery of the prorenin/renin receptor, handle region peptides (HRP) were designed as receptor antagonists. The HRP is a

subset of the prorenin sequence that is able to competitively bind to the receptor, preventing prorenin from binding[47,48]. This may provide potential therapeutic approaches to cure hypertension. It should be noted, however, the role of HRP and prorenin receptor remains controversial due to lack of consistent results from other investigators.

So where are various members of the RAS expressed, and where do they function? In the systemic RAS (also known as the conventional or circulating RAS), angiotensinogen is expressed by liver hepatocytes and delivered into the circulation[49], whereas renin is predominantly released by renal Juxtaglomerular (JG) cells near the afferent arteriole of the glomerulus and released in to the renal interstitium where it eventually is taken up into the blood stream. ACE is an membrane-bound ectoenzyme that is particularly abundant in lung endothelial cells[50,51]. With the substrate (angiotensinogen) and enzyme (renin) available, Ang-I is produced in the circulation and subsequently processed by ACE on the endothelial surface to generate blood-borne Ang-II. AT1R receptors are located in many target organs, such as brain[52,53], kidney[54], blood vessels[55] and adrenal glands[56], and binding of Ang-II elicits interaction with downstream signal transduction pathways including MAPK[53], STAT3[57], NADPH oxidase[58] and the insulin receptor axis[59].

In addition to the circulating RAS, some organs express all the components of RAS locally. As a result, Ang-II is generated within local tissues and functions to mediate local cardiovascular responses and/or water/electrolyte homeostasis. Among the tissues that express a local RAS, are brain[60], kidney[61,62], adrenal gland[63,64], vasculature[65-67], adipose pads[68-70], pancreas[71], gonads[72] and placenta[73]. The tissue-specific RAS is of particular importance in pathophysiology, because Ang-II generation is not always correlated with circulating RAS activity[74]. In fact, experimental studies have demonstrated that ACE inhibitors with a higher tissue affinity exhibit better antihypertensive efficacy than those with lower tissue affinity[74,75]. Moreover, ACE

inhibition is also effective in hypertensive patients with normal or even low systemic RAS levels[76,77]. Thus local tissue RAS may be the most efficacious target for antihypertensive and vasoprotective drugs.

Brain RAS and Blood Pressure Regulation

Central Nervous Control of Blood Pressure

Tonic activity of the central nervous system plays an essential role in blood pressure maintenance through the autonomic nervous system and various hormonal systems. The autonomic nervous system is composed of both sympathetic and parasympathetic systems. While both sympathetic and parasympathetic systems are involved in blood pressure regulation, most current studies are in favor of the idea that the sympathetic nervous system is more influential than the parasympathetic nervous system[14]. This is also reflected by the fact that α and β-adrenergic blockers of the sympathetic system are used more often in antihypertensive treatments. Admittedly, parasympathetic stimulators (muscarinic receptor agonists) and blockers (muscarinic receptor antagonists) are used in the clinic, but with less emphasis on cardiovascular therapeutic application[78]. The central nervous system employs a series of centrally or peripherally-located receptors to monitor blood pressure fluctuations and blood composition. Among these are baroreceptors, chemoreceptors and osmoreceptors. Baroreceptor is a type of mechanoreceptor that senses the vascular stretch at the aortic arch and carotid bodies due to elevated blood pressure or conversely, low blood pressure, while chemoreceptors are sensitive to vascular O_2 deficiency, CO_2 and H^+ excess. Upon physiological changes, baroreceptors elicit a change in the tone of afferent nerves which connect to a core set of cardiovascular-control nuclei in the brain stem including Nucleus Tractus Solitarius (NTS), Rostroventrolateral Medulla (RVLM) and Caudal Ventrolateral Medulla (CVLM). Subsequently, enhanced or suppressed sympathetic signals are delivered via postganglionic efferent nerves to target organs in

order to maintain consistent blood pressure. For example, in an experiment with acute intraperitoneal (IP) injection of phenylephrine, blood pressure in the animal increases as a result of enhanced α-adrenergic receptor stimulation. The increase in blood pressure is then detected by baroreceptors and causes increased firing of aortic depressor nerves and carotid sinus nerves to the CNS. The baroreflex system will then decrease heart rate. In hypertensive animals and patients, the baroreflex is often reset to a higher pressure or its sensitivity is blunted[79].

In addition to the brain stem, another pivotal site for blood pressure regulation is the hypothalamus, where the Paraventricular Nucleus (PVN) is located. The synthesis and secretion of the antidiuretic hormone arginine vasopressin (AVP) from magnocellular neurons in PVN are key steps of blood pressure regulation such that change in osmotic and volume homeostasis could have direct impact on systemic blood volume and pressure[80]. The amount of peripheral AVP in the circulation is proportional to plasma osmolality, as osmoreceptors in the organum vasculosum of the lamina terminalis (OVLT), subfornical organ (SFO) and medial preoptic nucleus (MnPO) in hypothalamus are responsible for sensing osmolality changes[81]. AVP mainly acts through three receptors. V1 receptors mediate vascular constriction via increased cytosolic free calcium. V2 receptors mediate antidiuretic effects by eliciting translocation of aquaporin-2 water channels to the apical plasma membrane of the tubular epithelial cells in renal collecting duct and enhancing water retention[82]. The V3 receptor is less well understood and may be involved in adrenocorticotropic hormone release. The PVN also projects Ang-II-responsive nerves to RVLM and NTS. Indeed, the RAS interacts with the Hypothalamus-Pituitary Axis (HPA) at several levels. First, it is well documented that Ang-II stimulates AVP release[83]. Secondly, it has been supported by several studies that Ang-II facilitates secretion of HPA hormones via paracrine mechanisms. Ang-II is able to influence growth hormone (GH), luteinizing hormone (LH), thyroid stimulating hormone (TSH), prolactin (PRL) and adrenocorticotropic hormone (ACTH) at the HPA[84-86]. Finally,

Ang-II is related to depression that also involves HPA in rodent models[87,88]. Other sites that have effects on blood pressure include the Amygdala (fight-or-flight defense response) and Hippocampus. Both of these are beyond the scope of this dissertation and will not be discussed further. In summary, neuronal regulation confers not only the ability to adjust short term cardiovascular control in a precise manner, but also the capability of governing long-term cardiovascular and blood pressure regulation.

Brain RAS

Ample studies from animal models have demonstrated that the brain RAS is an indispensible component of systemic blood pressure control. First, CNS delivery of renin[89,90] and AT1R[91] antisense oligos independently led to suppression of brain RAS signaling and subsequently decreased blood pressure. Secondly, various experimental hypertensive models including the spontaneous hypertensive rat (SHR)[92], (TGR mRen2) transgenic rat[93] (an overexpression model with mouse ren2 gene, which is a tandem duplication of ren1 in some 2-gene mouse stains, such as 129 and DBA), the Dahl salt-sensitive rat[94] and the deoxycorticosterone acetate-salt (DOCA-salt) rat[95] exhibited elevated blood pressure associated with increased central sympathetic nerve activity. Notably, ACE inhibition in the brain successfully prevented and reversed DOCA-induced hypertension[21,96-98]. Additionally, rats with brain-specific overexpression of human ACE, developed by Nakamura *et al*., exhibit increased brain Ang-II levels and hypertension.

In keeping with these rat studies, our laboratory has developed a series of experimental mouse models with altered blood pressure caused by brain RAS intervention. Given the species-specific digestion of angiotensinogen by renin (that is, human angiotensinogen can only be cleaved by human renin, not by mouse renin) and the relative ubiquitous expression of other RAS components, overexpression of global human angiotensinogen and neuronal-specific or glial-specific human renin (under synapsin or GFAP promoter) allows us to restrict overexpression of angiotensin peptides

and thus RAS hyperactivity to neurons or glial cells primarily in the brain[23]. We have not detected any human renin protein in the circulation. In both models, overexpression of RAS in the brain leads to elevated sympathetic outflow. This overexpression leads to increased cardiac output, heart rate, and an increase in blood pressure[23].

In line with the animal data, human hypertensive patients display enhanced sympathetic nerve signals as revealed by low-frequency (0.1Hz) heart rate recording[99], microneurography recording[100,101] and single-unit recordings[101]. Additionally, centrally acting antihypertensive drugs such as Clonidine (alpha-2 adrenergic receptor agonist) are effective in treating primary hypertension. Admittedly however, currently available RAS inhibitors do not target the brain exclusively. Thus technical limitations complicate the analysis of the functions of the brain RAS in humans.

What are the expression patterns of RAS members in the brain? It is well acknowledged that angiotensinogen is expressed abundantly in glial cells (astrocytes) in most parts of the brain[102,103]. Interestingly, angiotensinogen is also specifically expressed in neurons in cardiovascular-control nuclei[102]. *In vitro* cell culture analysis has provided insights of angiotensinogen expression in CCF cells, a human astrocytoma cell line[104]. Unlike AGT, ACE displays relatively ubiquitous expression in the brain[103]. Thus, to generate Ang-II, renin becomes rate-limiting. Unfortunately however, due to the extremely low expression of renin in the brain, its detection had been controversial until the utilization of a renin-promoter-driven EGFP reporter in transgenic mice. Our laboratory has taken advantage of the sensitivity of EGFP to find that renin is expressed in cardiovascular-control nuclei and that its expression overlaps with the expression of AGT[102]. What is more intriguing is that Ang-II immunoreactivity appears to correlate well with the expression of AT1R in various brain regions[105].

Many angiotensin receptors (AT1a, AT1b, AT2, Mas and AT4/IRAP) have been identified in regions of the central nervous system, including the circumventricular organs as well as sites inside the blood brain barrier (BBB)[106-110]. Moreover, it has been

demonstrated recently that the prorenin/renin receptor exhibits an enriched expression in some of the cardiovascular-control areas where renin is expressed, such as the hypothalamus and brain stem[111,112] . It has been suggested that the prorenin/renin receptor catalyzes faster cleavage of angiotensinogen by recruiting higher concentration of renin and prorenin locally. Conceptually, it is attractive to hypothesize that the prorenin/renin receptor would concentrate an otherwise low amount of renin in the vicinity of AT1 receptors (Figure 3). Interestingly, Contrepas *et al.* have demonstrated that a mutation in (P)RR gene in humans leads to X-linked mental retardation due to a deletion of exon 4 in (P)RR[112,113]. They further provide evidence that the prorenin receptor may be involved in neuronal cell differentiation. It is possible that (pro)renin in the extracellular space is enriched and activated to produce extracellular angiotensin, which subsequently binds to AT1R at neuronal plasma membrane to elicit alteration in intracellular signaling transduction pathways to prepare neuronal cells for differentiation. Perhaps dysfunction in the prorenin receptor gene (PRR) hinders generation of adequate angiotensin, which would interfere with neuronal differentiation. All these taken together support the presence and function of prorenin/renin receptor in the brain.

Brain Angiotensin Peptides

Ang-II was identified in several cardiovascular control nuclei in the brain by Lind *et al.*[114-117]. Multiple lines of evidence support that Ang-II functions as a neurotransmitter within the blood brain barrier (BBB) to regulate sympathetic outflow and fluid homeostasis. First, endogenous Ang-II has been located in neurons via immunocytochemistry in rat brain[118]. Ang-II immunoactivity has also been detected in the synaptic vesicles at the axonal terminals of SFO neurons via electron microscopy[119]. Secondly, retrograde labeling revealed a neuronal pathway from SFO to PVN, which is Ang-II immunoactive[120]. Interestingly, PVN expresses AT1R, which has been verified via

autoradiography[121,122]. Third, Ang-II stimulates PVN neurons in a dose-dependent manner[123,124]. A study from our laboratory demonstrated that Ang-II specifically expressed in the SFO is responsible for water intake, as its genetic ablation in a model with brain-specific RAS hyperactivity reduces spontaneous water intake[125]. This study is supported by research from Sinnayah P. *et al.* demonstrating that genetic ablation of AGT in SFO resulted in attenuated pressor responses to infusion of renin[126]. Additionally, others found that angiotensin-induced drinking responses could be abolished via transection of SFO efferent projections[127]. In addition to regulating water intake, Ang II also acts to regulate sympathetic tone. Ang-II activates PVN neurons projecting to the RVLM and spinal cord via suppression of the NO-induced inhibitory effect of GABAnergic neurons[128,128,129]. Moreover, bilateral injection of GABA agonist into the PVN resulted in a significant decrease in renal sympathetic activity and arterial blood pressure in water-deprived rats[130]. These and other data strongly support a role of hypothalamic Ang-II in elevating sympathetic output and blood pressure[130,131]. Taken together, these data suggest there are neuronal pathways originating from the SFO to PVN to Posterior Pituitary and RVLM[132,133], among others, and that the action of Ang-II in these nuclei are critical for its physiological function in fluid homeostasis, sympathetic outflow and cardiovascular regulation. We hypothesize that local production of angiotensin via brain renin is required to mediate these effects.

Further compelling evidence supporting a crucial role of brain Ang-II is derived from a study on angiotensinogen knockout mice with brain-specific Ang-II expression. First of all, the global knockout of angiotensinogen in mice leads to postnatal lethality. In a separate transgenic mouse model, Ang-II peptide is expressed under human glial fibrillary acidic protein (GFAP) promoter, which allows glial cell-specific overexpression of Ang-II in the brain. Subsequently, the GFAP-Ang-II mice were crossed with angiotensinogen global knockouts to generate mice that only express Ang-II in the brain but not in the periphery. The offspring from the cross exhibited normal survival ratios[134].

Our laboratory showed that human renin transgenes driven by the glial-specific GFAP promoter or the neuronal-specific synapsin promoter led to robust expression of human renin in the brain and consequently a remarkable increase in drinking volume, salt preference and urinary output compared to wild-type controls[23]. As described previously, these studies were performed when human angiotensinogen was simultaneously present, required due to the species-specificity of the reaction between renin and angiotensinogen[135,136]. Notably, unlike a transgenic mouse model globally overexpressing human renin, the plasma human renin level was not detected in the glial or neuronal-specific human renin transgenic mice.

Alternative Ang-II generating pathways have been reported involving cathepsin G, tonin[137] and chymase[138]. Although there is a distinct possibility that these enzymes are truly functional in generating Ang-II, a series of aforementioned genetic data support the hypothesis that angiotensin generation in the brain is renin-dependent. It is likely that downstream Angiotensin peptides such as Ang-III[139,140] and Ang-(1-7)[19,141] also participate in central blood pressure control. Both Ang-II and Ang-III have been demonstrated to increase release of antidiuretic hormone (ADH) (Hypertension Primer, 4th Edition), while Ang-(1-7) is believed to counteract Ang-II induced pressor responses via binding to G-protein-coupled Mas receptors[142-144]. Emerging studies have suggested the function of a newly identified angiotensin peptide, Ang-(1-12), in the brain in blood pressure regulation[145,146]. Unlike other angiotensin peptides, its generation has been suggested to be renin-independent[147,148].

A Focus on Brain Renin

Renin regulates the rate-limiting step in angiotensin peptide generation, and thus it plays a critical role in blood pressure control. Renin activity was first identified in rat and dog brain based on its ability to hydrolyze angiotensinogen. Brain extracts demonstrated a similar time course and dose-dependent curve in generating Ang-II to

those of renal extracts[149]. This suggests that renin is the main enzyme that generates Ang-II in the brain - not other non-specific aspartyl proteases such as cathepsin D. Moreover, genetic studies support the idea that angiotensin synthesis in the brain is renin-dependent[23]. Another separate study has verified central production of renin via depleting its renal source in bilateral nephrectomized dogs[150]. In addition, renin-expressing cells have been identified via immunohistochemistry in rat and mouse brains[151,152]. In primary cell cultures from rat brain, renin exhibited neuronal and glial expression[153]. Neuronal expression of renin was also identified in humans, indicating the importance of brain renin across species[154]. To probe the functional relevance of brain renin to cardiovascular regulation, intracerebroventricular (ICV) injection of renin antisense oligos has been performed in spontaneously hypertensive rats (SHRs) and 2-kidney-1-clip (2K1C) rats[89,90]. In both cases, brain-specific inhibition of renin successfully decreased blood pressure. Since renin is the rate-limiting enzyme in the RAS, a primary pathway of Ang-II generation, the fact that it is present at low levels in a highly restricted manner in certain cardiovascular control nuclei suggests its profound impact on Ang-II mediated hypertension.

Conventional Secreted Renin

Renin has long been considered as an enzyme that is secreted from renal JG cells into the circulation where it cleaves angiotensinogen into the intermediate peptide Ang-I. Ang-I is then turned into Ang-II by ACE under most circumstances. Of the many organs that express renin, the kidney is the major site of production. There are two classic pathways to stimulate renal renin secretion. The first one is through renal sympathetic nerve activity (RSNA)-activated β adrenergic receptors on JG cells. The second one is via decreased sodium concentration in the renal tubular fluid, which is then detected by macula densa cells of the distal nephron that are in close proximity to JG cells. Connections and communication between macula densa and JG cells is thought to be

mediated by connexins. Alterations in the types of connexins in the kidney lead to abnormalities in blood pressure regulation via the RAS[155,156].

The canonical mouse renin gene consists of 9 exons, with its transcription and translation start site in the first exon (Figure 4). The first exon contains the coding sequences for the signal peptide (pre-segment) and first third of the pro-segment of secreted renin. Interestingly our laboratory and others have shown that secreted renin is not the only functional form of renin.

A Novel Intracellular Renin Isoform

Alternative splicing is a transcriptional process during which diverse utilization of exons occurs to give birth to completely or partially different mature messenger RNAs. This happens mostly in eukaryotes and it provides a tremendous evolutionary advantage to the organism as it allows variability of proteins that could be encoded by a single gene. However, abnormal splicing could be detrimental. It is reported that nearly 60% of human disease is caused by incorrect splicing rather than mutations directly affecting coding sequences[157]. In a particular cell type, the splicing pattern is largely determined by a combination of transcription factors expressed in that cell type. During a regular transcriptional event, the DNA sequence of a gene is transcribed by RNA polymerase into precursor message RNA (pre-mRNA), starting immediately downstream of a transcriptional promoter. The pre-mRNA is then further processed (spliced) to get rid of non-coding intronic sequences, resulting in mature mRNA. The splicing procedure is executed by the spliceosome, which consists of five RNA molecules (known as small nuclear RNAs, snRNAs) and more than 50 proteins[158]. The exon-intron borders have specific nucleotide arrangements for recognition by spliceosomes, usually GU at the 5' end and AG at the 3' end of introns. In addition to alternative splicing, different cell types use various combinations of transcriptional factors to control gene expression through a single promoter or distinct promoters for the same gene. Usage of alternative

promoters in the genome further complicates the mechanisms of gene regulation. Utilization of differential promoters can affect gene expression in the following ways. First, transcriptional patterns (expression level, cell type and time) can vary from the same gene by employing discrete promoters that respond distinctly to transcription factors. Second, the translational efficiency and turnover rate of mRNAs with different 5' UTR can vary[159]. Last but not least, alternative promoters tend to result in alternative splicing and ultimately protein isoforms at the genomic level[160].

Lee-Kirsch *et al.* first identified a discrete transcript of renin as a result of alternative splicing in the brain of mouse, rat and human[161]. Based on primer extension and 5' RACE studies, this unique isoform utilizes a novel first exon (termed exon1b) and initiates protein translation from exon 2 due to lack of an ATG in exon1b. In the human renin gene, exon1b is located upstream of the conventional first exon (namely exon1a), while in mouse it sits downstream of exon1a in intron1 (Figure 4). Interestingly, the first in-frame ATG in exon 2 is highly conserved across species, more so than the surrounding amino acids in the pro-segment and is therefore most likely an alternative translation start codon[161,162]. The resulting protein lacks the signal peptide required for secretion, and the first third of the pro-segment, thus remaining intracellular (intracellular renin). Biochemical studies in AtT-20 cells (mouse anterior pituitary adenoma cell line) transfected with this novel form of renin cDNA revealed that this form of renin remains intracellular and constitutively active, as renin activity was detected only in cell lysates, but not in culture medium[161]. This novel isoform will be referred as intracellular renin (icRen) hereafter.

Our laboratory also identified the existence of icRen in the brain of a human-renin-PAC-transgenic mouse. This 160kb PAC (P1 Artificial Chromosome) transgene harbors the human renin gene in the center, as well as its neighboring genes at each end. Thus, presumably all cis-elements which regulate renin gene expression should be present in this construct, and the normal expression pattern of renin should be

maintained. Using mice harboring this PAC160 construct, we have validated the presence of human icREN in fetal mouse brain RNA samples[162]. In the human renin PAC transgenic, icRen mRNA is the predominant renin transcript in the brain, and the protein was localized throughout the hypothalamus[163]. As indicated by non-quantitative RT-PCR, mouse brain samples and Neuro-2a cells both express approximately equal amounts of secreted and intracellular renin, whereas kidney expresses much more (>100-fold) secreted renin than intracellular renin. To distinguish the roles of secreted and intracellular renin, we have performed overexpression studies in transgenic mice with secreted or intracellular renin under a brain specific promoter. Both models exhibited elevated mean arterial blood pressure and drinking volume[22]. We hypothesize that sRen and icRen play differential roles at discrete cellular locations of the cardiovascular-control nuclei in the brain to regulate cardiovascular functions as well as electrolyte/fluid homeostasis (Figure 3).

In addition to studies from Lee-Kirsch *et al.* and our group, there have been several other studies indicating the presence and function of this icRen in rat. Clausmeyer *et al.* reported that icRen exists in adrenal gland and its expression in the heart is stimulated up to 4-fold by myocardial infarction[164,165]. Peters *et al.* observed that icRen results in an increase in aldosterone production in transgenic rats overexpressing icRen[166].

Given the structural similarity of icRen and secreted renin (here after named sRen), and because icRen is in fact a truncated c-terminal portion of sRen, it is virtually impossible to distinguish them using antibodies. In addition, renin in general is at very low levels throughout the brain, which adds another difficulty to any standard detection assay. Herein, we have taken advantage of the discrete first exons of each isoform to make genetic deletions specifically of either sRen or icRen. Genetic ablation of secreted brain renin with preservation of intracellular renin will provide evidence for possible central roles of these two isoforms in mediating blood pressure and drinking behavior.

Various Models of Renin Knockout

It is noteworthy that there have been several systemic renin knockout models generated in the past decade. Starting with a renin knockout in the inbred 129 strain, which has two copies of the renin gene (*ren1*^{d} and *ren2*^{d}) sharing 94% homology[167], *ren1*^{d} and *ren2*^{d} were separately deleted via two homologous recombination events, retaining one or the other. The *ren1*^{d} and *ren2*^{d} genes display different expression patterns but are both equally expressed in renal JG cells. Therefore, the *ren1*^{d} or *ren2*^{d} systemic knockout mice were viable. Moreover, there is no difference in blood pressure in *ren2*^{d} knockouts and *ren1*^{d} male knockouts when compared to the wild-type, suggesting functional compensation with the remaining *ren1*^{d} and *ren2*^{d} allele[168,169]. Two other groups generated systemic renin knockouts in the inbred C57BL/6[170] and in a mixed strain of C57xCBA[171]. Both models produce no renin throughout the body. These renin knockout mice exhibit postnatal lethality that has been reported to be rescued by injection of saline and mineralocorticoid shortly after birth. Complete renin null mice on a C57BL/6 background, rescued via these injections, displayed increased energy expenditure and attenuated capability to gain weight with high fat diet[172]. By contrast, studies in our laboratory demonstrate that brain-specific overexpression of Ang-II in double transgenic mice with human renin and human AGT leads to an elevated basal metabolic rate and thus a lean phenotype (unpublished data). The reason for this discrepancy is unclear but two features common to both models may be increased sympathetic outflow (measured directly in our model and indirectly in the renin knockout mice), and markedly suppressed plasma renin.

To overcome the problem of lethality and over-expression, we have performed conditional gene targeting in the inbred C57BL/6 strain, which harbors only a single copy of the renin gene (designated *ren1*^{c})[173]. The resulting mouse model carries a floxed allele of renin, which allows us to distinguish secreted renin from intracellular renin. The complementary model, (a floxed allele of intracellular renin) is also in the final stages of

production (targeted ES cells have been identified and chimeric mice are currently in breeding). Subsequently, we bred sRen-flox mice with either systemically-expressed E2A-Cre or brain-specifically-expressed Nestin/GFAP-Cre to generate whole-body and brain-specific sRen knockouts. Our goal was that characterization of this brain secreted renin knockout model will shed light on the necessity and efficacy of secreted vs. intracellular renin in Ang-II generation.

Outline of Dissertation Projects

Development of sRen-flox and sRen-null Mice

To test the hypothesis that secreted and intracellular renins play differential roles, especially in the brain, we utilized a conditional gene-targeting strategy to flox the unique first exon and surrounding regulatory sequences of each isoform. By breeding a Cre-expressing mouse line with the flox line, we were able to specifically delete one isoform while preserving the other. The first mouse model we obtained from this project was the sRen-null. This model is a result of sRen-flox crossed with E2A-Cre, a globally Cre-expressing line. This allows us to generally address the difference between sRen and icRen in the whole body.

Characterization of Systemic sRen Knockout Mice

We performed comprehensive genetic, molecular, histological and physiological characterizations on the sRen-null model. As will be introduced in subsequent chapters, we demonstrated similarities and differences between sRen and icRen using this model.

Characterization of Brain-specific sRen Knockout Mice

One of the goals of my dissertation study is to dissect the role of brain-specific renin, as distinguished from renin of other sources (e.g. circulating renin and kidney-specific renin). In addition to studying the function of brain-specific renin in general, we also investigated the discrete roles of sRen and icRen in the brain.

Establishment of and Studies on DOCA-salt Mice

Several lines of evidence from the rat model suggested that DOCA-salt-induced hypertension is mediated through the central nervous system. We hypothesize that brain renin-angiotensin system is a key player in DOCA-salt induced hypertension in mice. With the brain-specific sRen knockout model, we designed and performed a series of studies to address this hypothesis. Not only would the sRen brain KO allow us to collect information on the role of brain RAS, but also we would be able to answer the question of which renin isoform is more important in DOCA-salt induced hypertension.

Figure 1. *Cardiovascular-control Nuclei in the Mouse Brain.*

Many of the nuclei that regulate cardiovascular functions and electrolyte/fluid homeostasis are located in the circumventricular region, hypothalamus and brain stem (top figure). Depicted in the bottom figure are Subfornical Organ (SFO), Paraventricular Nucleus (PVN), Median Preoptic Nucleus (MnPO), Organum vasculosum laminae terminalis (OVLT), Area Postrema (AP), Nucleus Tractus Solitarius (NTS), Rostroventrolateral Medulla, (RVLM) and Caudalventrolateral Medulla (CVLM). The black regions are ventricles. We hypothesize that the neuronal pathway from SFO to PVN is angiotensinergic, whereas the projections from PVN to RVLM are responsive to Ang-II stimulation. (Figures adapted from The Mouse Brain in Stereotaxic Coordinates, G. Paxinos and K.B.J. Franklin, Second Edition, courtesy of Justin Grobe, Ph.D.)

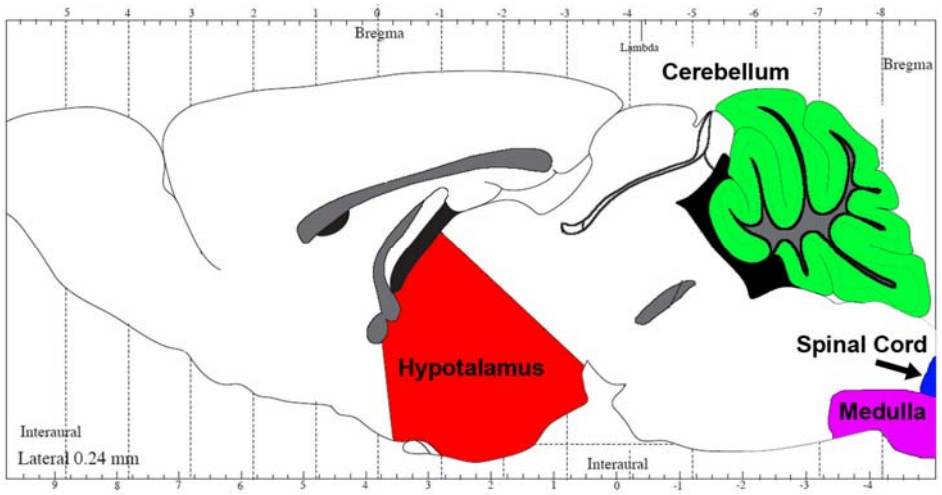
Bregma
Lambda
Cerebellum
Bregma
Hypotalamus
Spinal Cord
Medulla
Interaural
Lateral 0.24 mm
Interaural

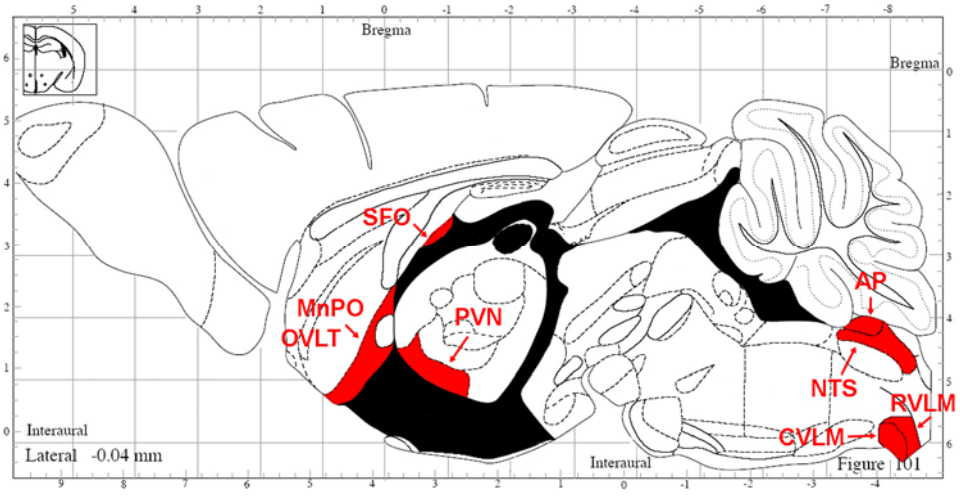
Bregma
Bregma
SFO
MnPO
OVLT
PVN
AP
NTS
RVLM
CVLM
Interaural
Lateral -0.04 mm
Interaural

Figure 101

Figure 2. *Renin-Angiotensin System (RAS).*

Renin is the first and the rate-limiting enzyme in RAS. As depicted in this schematic, angiotensinogen is processed by renin into Ang-I, which is further cleaved either by ACE, ACE2 or chymase into downstream peptides. The RAS is becoming more complex as more enzymes, peptides and receptors are unmasked.

From Grobe,J.L., Xu,D. & Sigmund,C.D. An intracellular renin-angiotensin system in neurons: fact, hypothesis, or fantasy. *Physiology. (Bethesda.)* **23**, 187-193 (2008).

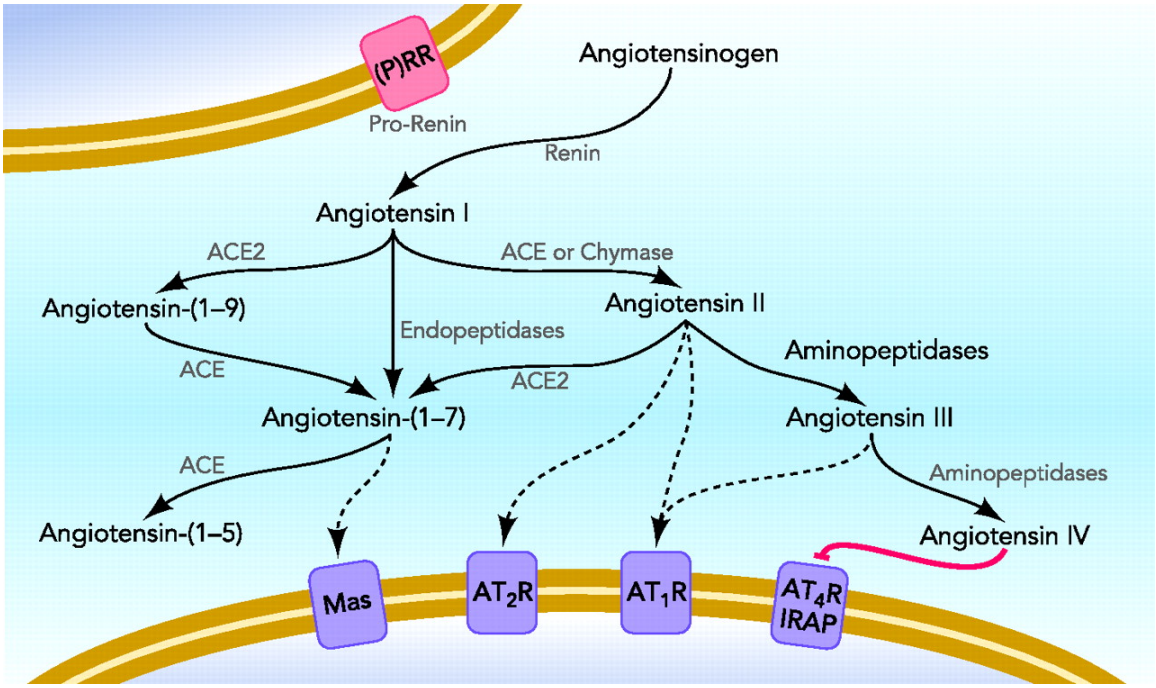

Ang-I (Ang 1-10)	**H-Asp-Arg-Val-Tyr-Ile-His-Pro-Phe-His-Leu-OH**
Ang-(1-9)	**H-Asp-Arg-Val-Tyr-Ile-His-Pro-Phe-His-OH**
Ang-II (Ang 1-8)	**H-Asp-Arg-Val-Tyr-Ile-His-Pro-Phe-OH**
Ang-III (Ang 2-8)	**H-Arg-Val-Tyr-Ile-His-Pro-Phe-OH**
Ang-IV (Ang 3-8)	**H-Val-Tyr-Ile-His-Pro-Phe-OH**
Ang-(1-7)	**H-Asp-Arg-Val-Tyr-Ile-His-Pro-OH**
Ang-(1-5)	**H-Asp-Arg-Val-Tyr-Ile-OH**
Ang-(1-12) mouse & rat	**H-Asp-Arg-Val-Tyr-Ile-His-Pro-Phe-His-Leu-Leu-Tyr-OH**
Ang-(1-12) human	**H-Asp-Arg-Val-Tyr-Ile-His-Pro-Phe-His-Leu-Val-Ile-OH**

Figure 3 *Function of sRen vs. icRen and Neuronal Synthesis of Intracellular Ang.*

Given that both sRen and icRen have been demonstrated to be expressed in the brain, we hypothesize that they play distinct roles in angiotensin generation and thus regulation of blood pressure through the CNS. sRen is most likely secreted from neuronal cells into the extracellular space, where it cleaves glial-secreted angiotensinogen (AGT) into angiotensin in the extracellular spaces in the brain. Final angiotensin peptides could potentially bind to AT1R on neuronal cell membrane. Alternatively, icRen could be synthesized and retained in the cytoplasm of neurons. It then generates angiotensin intracellularly using AGT of neuronal origin or AGT taken up from the interstitium. Subsequently, neuronal angiotensin could act as a neurotransmitter to elicit activity of downstream neurons and thus regulate cardiovascular functions.

From Grobe,J.L., Xu,D. & Sigmund,C.D. An intracellular renin-angiotensin system in neurons: fact, hypothesis, or fantasy. *Physiology. (Bethesda.)* **23**, 187-193 (2008).

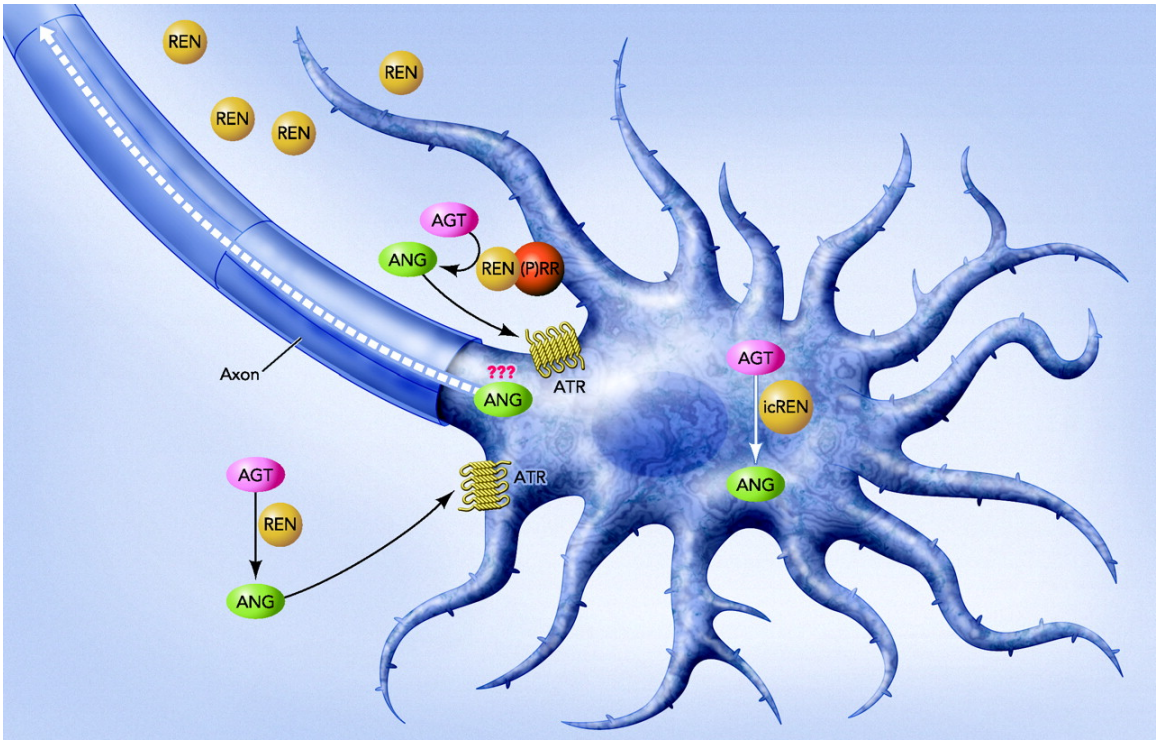
REN
REN
REN
REN
AGT
ANG
REN
(P)RR
Axon
???
ATR
ANG
AGT
icREN
ANG
AGT
REN
ANG
ATR

Figure 4 *Schematic of Mouse Renin Gene and Alternative Splicing.*

The mouse renin gene is conventionally composed of nine exons. As mentioned previously, our laboratory and others have identified an alternative splicing event in mouse, rat and human. In the case of the mouse gene, the novel exon1 (named exon1b) is located in the classic intron1. The alternative splicing occurs from exon1b directly to exon2, skipping the classic exon1 (named exon1a from here on). As a result, a transcript that lacks the conventional protein translation start codon is expressed. Presumably, this novel transcript then utilizes the first in-frame ATG in exon2 to initiate protein translation. Notably, this first ATG in exon2 is evolutionarily conserved. The resulting protein lacks the signal peptide and the first third of the pro-segment in classic preprorenin, thus remaining intracellular and constitutively active.

From Grobe,J.L., Xu,D. & Sigmund,C.D. An intracellular renin-angiotensin system in neurons: fact, hypothesis, or fantasy. *Physiology. (Bethesda.)* **23**, 187-193 (2008).

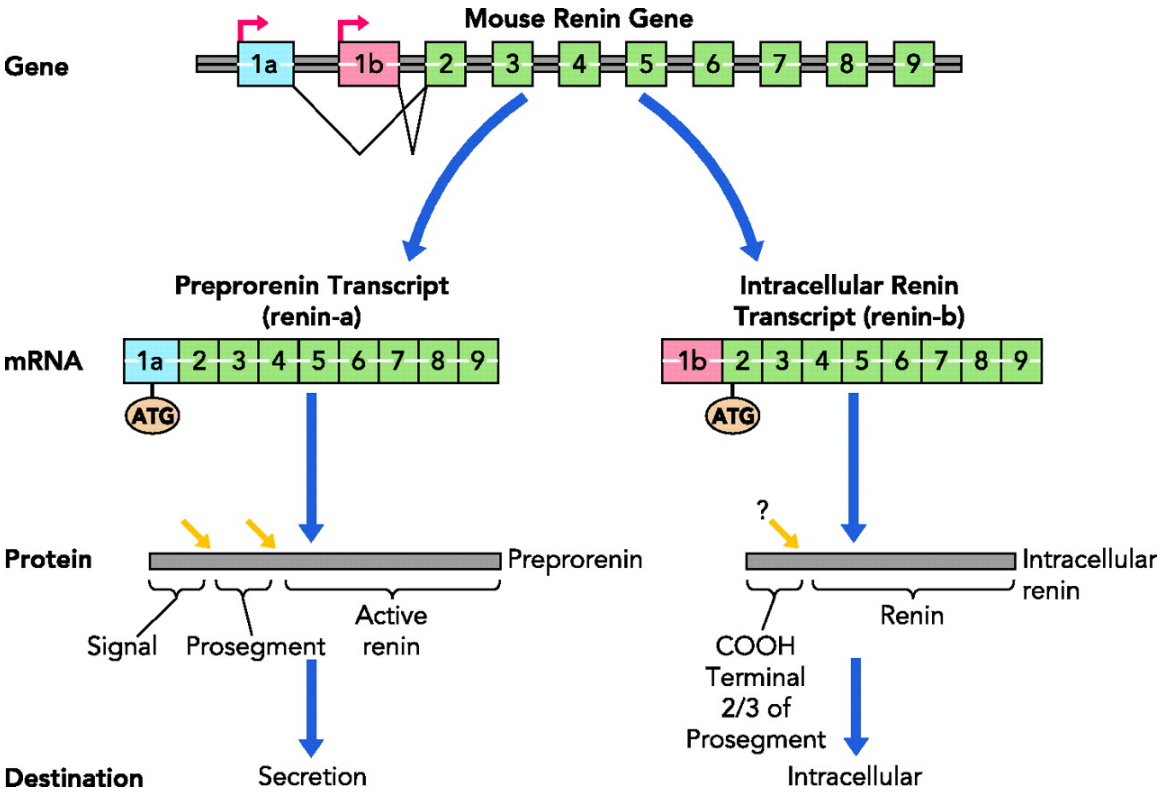
Mouse Renin Gene
Gene
1a
1b
2
3
4
5
6
7
8
9
Preprorenin Transcript
(renin-a)
Intracellular Renin
Transcript (renin-b)
mRNA
ATG
ATG
?
Protein
Preprorenin
Intracellular
renin
Signal
Prosegment
Active
renin
Renin
COOH
Terminal
2/3 of
Prosegment
Destination
Secretion
Intracellular

CHAPTER 2

DEVELOPMENT OF SREN-FLOX, SREN GLOBAL AND BRAIN-SPECIFIC KNOCKOUT MICE

Introduction

To address the hypothesis that sRen and icRen play differential roles in the regulation of blood pressure through the central nervous system, we took advantage of the Cre-LoxP system to establish both sRen and icRen specific knockout mice. This chapter will mainly focus on the development of sRen knockout models, and some early work on the icRen knockout development. We first generated sRen-flox using embryonic stem cells from the C57B6/JL background to avoid the second copy of the renin gene (*Ren2*) that is present in the 129 mouse strain, the strain that is more commonly used for gene targeting. Subsequently, sRen-flox was bred with E2A-Cre, Nestin-Cre or GFAP-Cre transgenic mice to give rise to global, neuronal and glial sRen knockouts, respectively. The analyses of these models are forthcoming in subsequent chapters.

Gene Targeting of the Mouse Renin Locus

Construction of pGHIJKL (Exon1a-sRen Knockout)

Exon1a along with the flanking regions(+/– 500bp) was PCR amplified from BAC RP23-41A16 which originated from a C57BL/6J mouse chromosome 1 BAC using primers G and H as indicated in Table 1. This PCR fragment was cloned into the SacI/PstI site of pBYLoxPa (Figure 5), resulting in the vector pBYLoxPa-GH. Subsequently the downstream homologous arm was PCR amplified with the I/J primer set and then cloned into the SalI/XhoI site of this pBYLoxPa-GH. The new intermediate construct is thus named pBYLoxPa-GHIJ. Simultaneously, pBY49a (Figure 6) was modified by adding a BamHI-SfiI-SfiI'-EcoRI linker to replace the old BamHI/EcoRI site, resulting in the new pBY49a-SfiI vector. The GHIJ fragment bearing one LoxP site in pBYLoxPa-GHIJ was

subcloned into pBY49a-SfiI. This generated the second intermediate construct pBY49a-GHIJ. The upstream homologous arm KL was then PCR cloned into the NotI/HpaI site of pBY49a-GHIJ to complete the targeting construct pGHIJKL (Figure 7).

Construction of pABCDEF (Exon1b-icRen Knockout)

Exon1b along with flanking regions (+/– 500bp) was PCR amplified from BAC RP23-41A16 originating from a C57BL/6J mouse chromosome 1 BAC clone using primers A and B as indicated in Table 2. Then this PCR fragment was cloned into the SacII/XbaI site of pBYLoxPa, resulting in pBYLoxPa-AB. Subsequently, the downstream homologous arm was PCR amplified with the C/D primer set and then cloned into the SalI/XhoI site of pBYLoxPa-AB. The new intermediate construct is thus named pBYLoxPa-ABCD. The ABCD fragment bearing one LoxP site in pBYLoxPa-ABCD was subcloned into pBY49a-SfiI, the modified plasmid described above. That makes the second intermediate construct pBY49a-ABCD. The upstream homologous arm EF was PCR cloned into the NotI/HpaI site of pBY49a-ABCD to complete the targeting construct pABCDEF (Figure 8).

Construction of pABCDEF-Mut

pABCDEF-Mut is a plasmid with the first in-frame ATG->GCG mutation in Exon2 for Exon1b Knock-out. The QuikChange® XL Site-Directed Mutagenesis Kit from Stratagene was used to carry out mutagenesis in pBYLoxPa-ABCD (~7kb). Primers used for mutagenesis are listed in Table 3. This MutpBYLoxPa-ABCD was digested and sequenced to verify the mutation. The ABCD fragment with the mutation was subcloned into pBY49a-SfiI. The EF homologous arm from pABCDEF was then subcloned into the NotI/HpaI site of Mut pBY49a-ABCD to complete the third targeting construct MutpABCDEF. This site-directed mutation is located at nucleotides 5817-5819 in MutpABCDEF.

Submission of Targeting Constructs for ES Cell Electroporation

All final targeting plasmids were sequenced with primers covering five cloning junctions as well as the mutation site before each submission of targeting plasmids for gene targeting (Table 4). For the first submission of plasmids, the upstream/downstream homologous arms and floxed regions were PCR amplified and sequenced. No unwanted mutations were found in any exon sequenced.

Targeting plasmid (100ug) was linearized with 40ul of NotI (10u/ul) for 2 hours. An aliquot was run on a 1% gel to verify complete digestion. Then the reaction tube was submitted directly to 1) the Gene Targeting Facility at University of Iowa and 2) InGenious Targeting Laboratory, inc. (iTL) to perform electroporations on ES cells.

Construction of Control Plasmids pABCDE'F and pGHIJK'2L

pABCDE'F and pGHIJK'2L as indicted in Figure 9 and Figure 10, respectively, were cloned on the basis of pBY49a-ABCD and pBY49a-GHIJ. Briefly, additional 5' genomic DNA upstream of EF was PCR cloned along with EF into the NotI/HpaI site of pBY49a-ABCD utilizing primers E' and F. While additional 5' genomic sequence upstream of KL was PCR cloned along with KL into the NotI/HpaI site of pBY49a-GHIJ utilizing primers K'2 and L. Sequences of primers E' and K'2 are listed in Table 5. These constructs were developed to provide a control for eventual screening of recombinant ES cells. These control plasmids carry the portion of the upstream homology that contains the upstream PCR primer that is not present in the targeting construct.

ES Cell Screening

Targeting plasmids were electroporated into SCR mouse embryonic stem cells. SCR cells are derived from a tyrosinase mutant line C57BL/6J-Tyr(c-2J) with white coat color. The transfected ES cells were then subjected to positive selection by neomycin and negative selection by tyrosine kinase. To verify *bona fide* site-specific homologous recombination and to exclude random insertions, the PCR-based first screening

employed a variety of primers (Table 6). For icRen knockouts, we took additional steps to confirm genotypes of each clone candidate. The primers used in the additional steps are listed in Table 7.

Genomic DNA Extraction from ES Clones

To carry out PCR screening, genomic DNA was extracted from ES clones. First, the plate with ES clones was thawed at room temperature. PBS (25ul) was added to each well to resuspend the pellets. An equal volume of 2x cell lysis buffer containing 0.5mg/ml Proteinase K and 0.2mg/ml RNase A was added into each well. Proteinase K and RNase A were added into lysis buffer right before use. Subsequently, the plate was sealed well with Parafilm between the lid and the bottom, and was incubated at 55^{o}C with moderate shaking overnight. On the second day, DNA was precipitated with 50ul of isopropanol at -20^{o}C overnight. The precipitation step could be reduced to 2 hr if starting amounts of ES cells were in excess. On the third day, the plate was centrifuged at 2400 rpm for 10 min at room temperature. The supernatant was discarded and the pellets were washed 3 times with cold 70% ethanol. The pellets were air-dried for 20 min and resuspended in 30ul of ddH_2O.

<u>PCR Screening Conditions</u>

sRen Knockout Initial ES Cell Screening

We first performed an initial PCR screen to identify site-specific homologous recombinants for sRen KO. The forward primer X and the reverse primer Z (see tables for primer sequences from here on) were used in this assay. Unless otherwise indicated, all PCRs from hereon were carried out in 10ul reactions with hot-start amplification. The amount of template used in this assay ranged from 20-100ng. Platinum Taq (Invitrogen) was used as the polymerase. This assay was optimized with an annealing temperature of

51.5 ^{O}C and an extension time of 1.5 minutes. A representative PCR Gel is depicted in Figure 11.

sRen Knockout ES Cell Control PCR

An internal control PCR was also used to verify the quality of genomic DNA from each ES clone. This reaction amplifies a downstream region of the *Ren1^{C}* locus, extending from exon4 to exon5. The forward primer P and the reverse primer Q were utilized in this assay. Other reaction parameters were the same as sRen ES screening.

Additional Quality Control and Optimization

The control plasmid pGHIJK'2L was mixed with wild-type C57 genomic DNA at a 1:1 molar ratio as a positive control (3.3pg plasmid/1ug gDNA). A total of 50ng of mixed DNA was used in each 10ul reaction. It was demonstrated in preliminary experiments that linearized control plasmid with genomic DNA or circular control plasmid mix with genomic DNA does not differ from each other with regard to PCR efficiency. Pure genomic DNA and ddH_2O were used as negative controls. The reagents in experimental, positive control and negative control reactions were aliquots from the same master mix. All reactions were completed at the same time in the same PCR block.

For the initial screen of icRen knockouts ES cells, there were quite a few technical problems during the early stage of this procedure. The problem was eventually circumvented by changing PCR conditions such as pH and Mg^{2+} concentration. After trying a variety of commercially available buffers and the PCR Optimization Kit from Invitrogen, it has been shown that a 5x buffer made by myself works the best (pH=9.06, 300 mM Tris. HCl 75mM $(NH_4)_2SO_4$). (See Figure 12 and Figure 13) The locations of all PCR Primers used for the icRen screen are listed in Figure 14.

icRen Knockout Initial ES Cell Screening

The forward primer Y was used in this reaction. The reverse primer X was switched to Neo1R during optimization. Neo1R also locates in the Neomycin cassette (Table 7). This PCR is capable of amplifying genomic DNA template varying from as low as 10ng up to 200ng. Platinum Taq and 5x PCR Buffer (pH=9.06) were used in this assay. Other reagents were of standard concentrations. Instead of having 35 identical PCR cycles, the first 10 PCR cycles used an annealing temperature of 50 ^{o}C, whereas the annealing temperature for the last 25 cycles was set to 53 ^{o}C. A representative PCR gel is indicated in Figure 15.

icRen PCRs to Verify 5' LoxP and 3' LoxP

After this initial PCR, a series of PCRs were carried out to confirm ES candidate clones. We first examined the integrity of 5' LoxP and 3' LoxP sites. We used the forward primer "tailscreen 1bF2" and the reverse primer "tailscreen 1a/1b R4" to amplify 5' LoxP and its surrounding regions. A representative gel is shown in Figure 16. As for the 3' LoxP screening, we used the forward primer "tailscreen 3'LoxPF1" and the reverse primer "tailscreen 3'LoxPR1". The amplicon sizes are around 300-400 bp as demonstrated in Figure 17. Both amplifications use the same PCR program and recipe (except for primers). Platinum Taq and 5x PCR Buffer (pH=9.06) were employed in these assays. The annealing temperature was 50 ^{o}C. Either of the PCR reactions could also be used for subsequent germ-line screening.

icRen Mutation Test PCR

After confirming both LoxP sites, we proceeded to identify the existence of the ATG->GCG mutation using the forward primer "Mut-test-F" and the reverse primer "Mut-test-R". In this particular assay, we utilized Hi-Fidelity Platinum Taq (Invitrogen), its 10x HF Buffer and 50mM $MgSO_4$ at standard concentrations. The first 10 repeated

PCR cycles had an annealing temperature of 50 ^{o}C, whereas the subsequent 25 cycles had an anneling temperature of 53 ^{o}C. A representative gel is shown in Figure 18.

icRen Internal Control PCR

We employed a similar approach as we used for the sRen screening to control for the quality of genomic DNA from each ES clone. The forward primer M and the reverse primer N were used to amplify a genomic region in the downstream homologous arm as shown in Figure 9. We used an annealing temperature of 51.5 ^{o}C and an extension time of 1.5 minutes.

icRen 3' End Homology and Junction PCR

At the last step of PCR screening, the 3' homologous region and the region downstream of it in the genome were checked to make sure the junction of these two regions was correct. The forward primer "pABCDEF-Final 3" and the reverse primer "Exon5R1" were used in this reaction. Hi-Fidelity Platinum Taq was again used with its standard buffer and reagents. The annealing temperature was 52^{o}C and the extension time was 6 minutes. A representative gel is demonstrated in Figure 19.

After PCR screenings, Southern blotting was performed to further confirm the genotypes of ES candidate clones.

Southern Blot

A. Genomic DNA extraction from cell pellets in 1.5 ml centrifuge tubes

First, the size of the pellet was estimated. Then 3-5 times more volume of PBS was added to resuspend the pellets. An equal amount of 2x cell lysis buffer was added (Proteinase K and RNase A were added as described previously). The tube was sealed well and incubated at 55 ^{o}C in a water bath overnight. The next day, 1/10 volume of 3M NaAc and 2 volumes of 100% ETOH were added into each tube. DNA was pelleted via centrifugation at 13000rpm for 15 minutes. Subsequently, the DNA was washed twice

with ice-cold 70% ethanol. After each wash, centrifugation was performed at 13000rpm for 5 minutes. Once the pellet was air-dried, it was resuspended with ddH_2O for at least 2 hours at room temperature.

B. Generation of Southern Probes

For exon1a knock-outs, primers F2-18 (5'-CAGCTGTTTCATGGGGG-3') and R460-480 (5'-CTTCCAGCTGACCCCCTCCTA-3') were used to clone the probe template into TOPO PCR2.1(Invitrogen). Prior to radio-labeling the probe, the template was liberated from the plasmid backbone with EcoRI and gel-purified. Subsequently the probe was labeled using the Rediprime II Random Primer Labeling System from GE Healthcare. For exon1b knock-outs, primers F8-25 (5'-TGCCAGCCAGGGTCAGGT-3') and R540-557 (5'-GGCAGGCATGGGGGTGTG-3') were used to clone the probe template into TOPO PCR2.1.

(3) Running a Southern Gel

Genomic DNA (15ug) was digested in a 300ul reaction with SpeI overnight at 37 ^{o}C. The next day the DNA was precipitated with NaoAC and 100% ETOH at -20 ^{o}C for 2 hours and centrifuged down at 13,000 rpm for 30 minutes. Subsequently the pellet was washed with 70% ETOH and air-dried before resuspension. Then the DNA was dissolved in ddH_2O overnight to allow complete resuspension. The DNA was re-quantified right before loading onto the gel. Gel electrophoresis was performed at low voltage (25-45 volts) overnight.

C. Blotting

The DNA was transferred from the agarose gel to a nitrocellulose membrane in 20x SSC buffer overnight or for a minimum of 8 hours. The next day the membrane was removed from the gel and UV cross-linked for 12 seconds.

D. Hybridization

The nitrocellulose membrane was rolled up with a piece of mesh cloth of similar size and placed into a hybridization tube. Fifteen milliliters of pre-heated pre-hybridization buffer with fresh Salmon Sperm DNA was put into the same tube and pre-

hybridized at 65 ^{o}C for 2hours or overnight. Denatured radioactive probe was added into the hybridization buffer along with fresh Salmon Sperm DNA. The hybridization was carried out overnight.

E. Washing and Making a Radiograph

The membrane was washed with 6x SSC for 5 minutes, followed by a 10- minute and 5-minute wash with 2x SSC. Subsequently, the membrane was covered with plastic wrap and exposed to a phosphor screen for 3-5 hours. The phosphor screen was then exposed using a phosphor imager. Long-term exposure of the membrane was carried out using films.

A schematic of the Southern design for sRen is shown in Figure 20. This strategy was employed to confirm the genotype of targeted ES cells as well as germ-line-transmitted founder mice. A representative Southern Blot for sRen KO founder is demonstrated in Figure 21.

Generation of Chimeras

Confirmed ES clones were then injected into the blastocysts of pseudo-pregnant mothers to give birth to chimeras. The fathers of chimeras were C57BL/6J wild-type mice. Shown in Figure 22 are representative pictures of a chimera, which has 5-10% white patches on the black coat-color background.

<u>sRen Knockout Breeding and offspring Screening</u>

Screening of Germline-transmitted Progeny

PCR primers (Table 8) from the upstream homologous arm and the Neo cassette were used to identify germline transmitted offspring from FV115 chimeras bearing the targeted exon1a allele (see Figure 23 for schematic design). We used the forward primer “F1-tailscreen1a” and the reverse primer “R4-tailscreen1a /b” in this assay. Platinum Taq and 5x PCR buffer (pH=9.06) were again employed. The optimized annealing

temperature was 50 ^{o}C. A representative gel is shown in Figure 23. The expected band size is 530bp.

Generation of Systemic sRen Knockout

FV115 line founder mice harboring the floxed exon-1a allele along with the neomycin cassette were bred with mice expressing FLpase in the early embryo (driven by CMV-IE enhancer/Chicken β-actin promoter). These deletes the neo gene which was inserted during recombination. The resulting mice containing the floxed exon-1a allele (lacking the neomycin gene) were then bred with E2A-Cre transgenic mice (C57BL/6J background) from Dr. Baoli Yang's laboratory. The cre-recombinase is turned on during an early embryonic stage in order to generate a systemic knockout of secreted renin. This deletes all the intervening DNA between the loxP sites to generate a null allele. We retained mice carrying the floxed allele as the new founders to be used for tissue-specific knockouts.

Screening of sRen Floxed Littermates without Neo

To screen for floxed alleles lacking Neo, as indicated in Figure 24, the primer sets (Forward: pGHIJKL Final Primer2, Reverse: 5R49a-GHIJ, Table 9) were anchored to the upstream homologous arm and the floxed exon (1a or 1b) of the mouse renin gene. Platinum Taq and 5x PCR buffer (pH=9.06) were used in this assay. A touchdown PCR program with its annealing temperature declining from 65 ^{o}C to 50 ^{o}C was utilized to give more specificity of the reaction. The amplicon originating from the wild-type allele is expected to be shorter than the one from the targeted allele. A representative PCR is shown in Figure 24. This PCR for sRen is also known as screen #2.

Screen of Heterozygous and Homozygous Knock-outs (Screen #4)

In this screen, the forward primer "pGHIJKL Final Primer2" is located in the upstream homologous region, while the reverse primer "Exon1aFloxedout-R1" is

located in the downstream homologous region (Figure 25). This would allow the amplification of a wild-type band of 1227 bp and a null band of 337 bp (Figure 25). See Table 10 for primer sequences. Platinum Taq and 5x PCR buffer (pH=9.06) were used in this reaction. We optimized the annealing temperature to 56.5 ^{o}C and the extension time to 1.5 minutes.

Confirmation of sRen Null by Southern Blots

(1) Genomic DNA Extraction from Mouse Tissue

Tissue was cut into small pieces (roughly 0.3mm x 0.3mm x 0.3mm) prior to homogenization. Homogenization was performed in 15 ml falcon tubes or 1.5 ml tubes with 1.2 ml digestion buffer per 100mg tissue (100mM NaCl, 10mM pH8 Tirsh-HCl, 25mM EDTA, 0.5% SDS, 0.1 mg/ml proteinase K-added freshly). A Dounce homogenizer was used. Subsequently the samples were transferred into 1.5ml tubes and incubated at 50^{o}C overnight in tightly-capped tubes with slow rotation. The following day, RNase A was added to a final concentration of 100ug/ml and incubated with samples at 37 ^{o}C for 2 hours. Next, an equal volume of Pheno/Chloroform/Isoamyl Alcohol (PCI) was added and rotated with the samples for 20 minutes at room temperature. Phase separation was performed by centrifugation at 3000 rpm for 5 minutes. Following that, the upper aqueous phase was pipetted out and transferred into a fresh tube. Another equal volume of PCI was added to it. Samples were rotated again for 20 minutes and centrifuged at 3000 rpm for 5 minutes. The extraction of the aqueous phase was repeated again with 24:1 Chloroform/Isoamyl Alcohol (CIA). After transfer of the aqueous phase to a new tube, an equal volume of isopropanol was layered on top of it. The genomic DNA was precipitated for 5 minutes and spun down at 13000 rpm for 10 minutes. Subsequently, the DNA pellet was washed in 70% ethanol and centrifuged for 5 minutes. Genomic DNA was dried at room temperature for 10-15 minutes and resuspended in ddH_2O overnight.

(2) Southern Blot of sRen Systemic Knockouts (WT band VS. null band)

We examined both the 5' end and 3' ends of the targeted region using a 5' probe and a 3' probe in two separate experiments. The schematic for the Southern design is depicted in Figure 26. The 5' Probe was named Ex1a-2 (Exon1a KO-Probe2). The primers used to amplify this probe from the BAC genomic sequence are as follows: Forward: TCTATAGTTTGACTCTGACACGTTACTA, Reverse: CTGGAAGAAGGACTGTTGTGAC. Whereas the 3' Probe named "Intron4Exon5" was amplified with the forward primer AAATCAGTGCGAGCCCTTCC and the reverse primer AGAACACTTCCTCCTTTAGCAC from the BAC genomic sequence.

Generation of Brain-specific sRen knockouts

FV115 floxed mice were bred with either Nestin-Cre or GFAP-Cre mice in order to generate neuronal/glial specific sRen KOs. This takes two breeding steps. In the first generation, F/F x Cre+ scheme was established to obtain F/+, Cre+. In the second step, F/+, Cre+ mice were crossed with F/F to get F/F,Cre+ mice. F/F Cre- littermates were used as controls.

icRen Knockout Germline Screening

For exon1b knockout screening, initially PCR primers Tailscreen 1bF2 and Tailscreen 1a/1b R4 (Table 11) were employed to identify germline-transmitted offspring from positive ES clone-derived chimeras. The expected amplicon size was 424 bp. However, we did not have any success with respect to this line. Germline screening of this gene targeting project has been extremely challenging. So, we have adapted another set of primers (forward: tailscreen3'LoxPF1, reverse: tailscreen3'LoxPR1, Table 11) for germline screening. This set of primers is identical to the ones we used to confirm 3' end LoxP sites in ES cells. The advantage of this newer set is that we will have a band from WT allele independent of the band we would get from a targeted allele. In this assay, both a band from WT and a band from targeted will identify germline

transmitted samples. I have screened hundreds of littermates from chimeras. The germline screen for this line is still in progress.

A similar Southern blotting strategy will be used for exon1b (icRen) targeted allele similar to the one we employed in the Southern Blot for exon1a (sRen) targeting allele (Figure 27).

Figure 5. *Starting plasmid pBYloxPa.*

This plasmid was obtained from the Gene Targeting Facility at the University of Iowa. This plasmid consists of two Multiple Cloning Sites (MCS), with one upstream of a LoxP sequence and the other one downstream of the same LoxP, which is demonstrated as a red triangle. This plasmid contains an Ampicillin-resistant gene and serves as a parent plasmid for subsequent cloning steps.

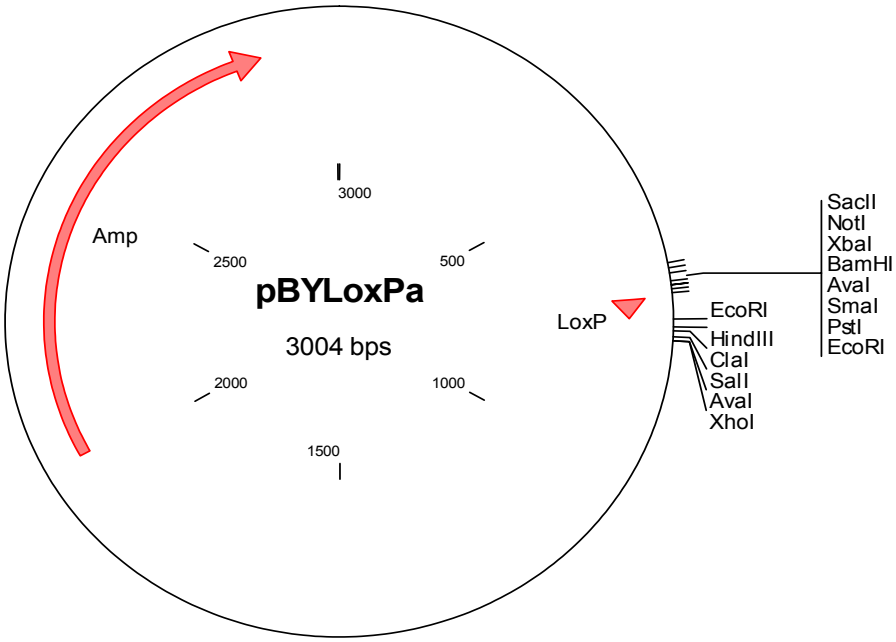
pBYLoxPa
3004 bps
3000
500
1000
1500
2000
2500
Amp
LoxP
SacII
NotI
XbaI
BamHI
AvaI
SmaI
PstI
EcoRI
EcoRI
HindIII
ClaI
SalI
AvaI
XhoI

Figure 6. *Starting plasmid pBY49a.*

This is a second parent plasmid that was also from the Gene Targeting Facility. This plasmid contains a LoxP (shown as a red triangle) as well as two FRT sites (indicated as blue boxes). This plasmid is also ampicillin-resistant. In addition, it includes a neomycin resistant gene and a thymidine kinase gene as selective markers, both driven by the phosphoglycerate kinase (PGK) promoter for robust expression in eukaryotic cells. There is one MCS located upstream of the LoxP site. The other MCS is located downstream of the 5' FRT sequence.

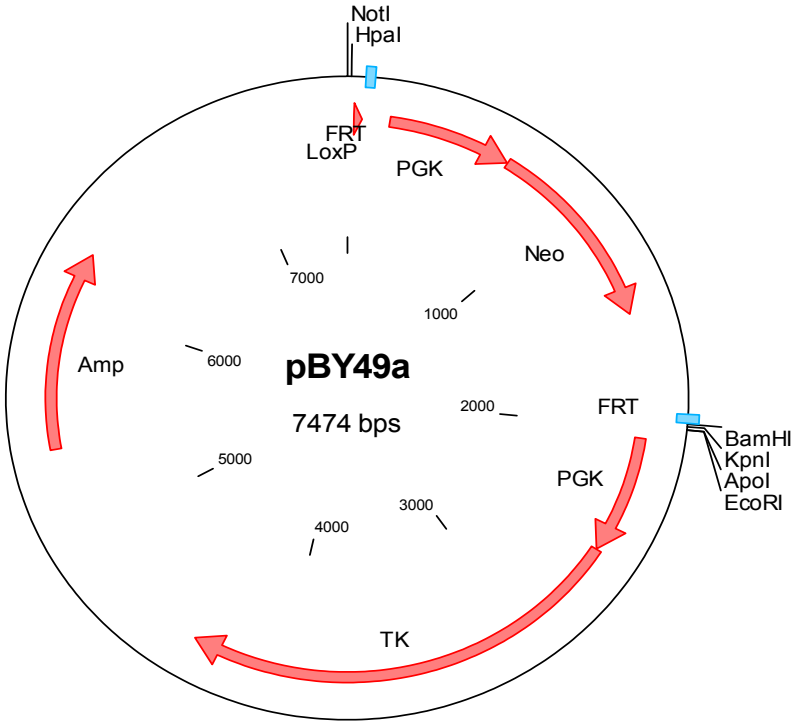
NotI
HpaI
FRT
LoxP
PGK
Neo
7000
1000
Amp
6000
pBY49a
7474 bps
2000
FRT
BamHI
KpnI
ApoI
EcoRI
5000
PGK
3000
4000
TK

Figure 7. *Final Plasmid pGHIJKL.*

In this final targeting construct, exon1a (specific for sRen) is cloned along with its flanking genomic sequences. They are depicted as one entire fragment GH in blue. Upstream of GH is the neomycin cassette that is flanked by two FRT sites to facilitate removal of neomycin by FLpase in the future. The entire neomycin cassette, two FRT sites and GH fragment are all flanked by two LoxP sites shown as triangles. The floxed region could thus be removed by Cre recombinase in the future. The KL fragment in yellow is the upstream homologous arm, while the IJ fragment in red serves as the downstream homologous region.

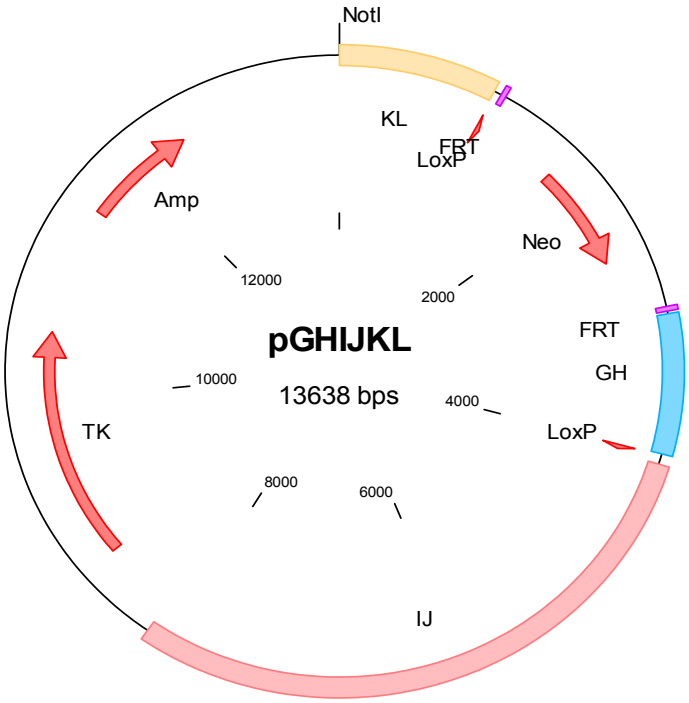
NotI
KL
FRT
LoxP
Amp
Neo
12000
2000
pGHIJKL
13638 bps
FRT
GH
10000
4000
TK
LoxP
8000
6000
IJ

Figure 8. *Final Plasmid pABCDEF.*

This targeting construct is structurally similar to the other targeting plasmid pGHIJKL shown in Figure 7. In this plasmid, EF in yellow is the upstream homologous arm, while CD in red is the downstream homologous region. The AB fragment in blue is the region of interested we plan to remove from the genome. AB contains exon1b (specific for icRen) as well as its flanking regions.

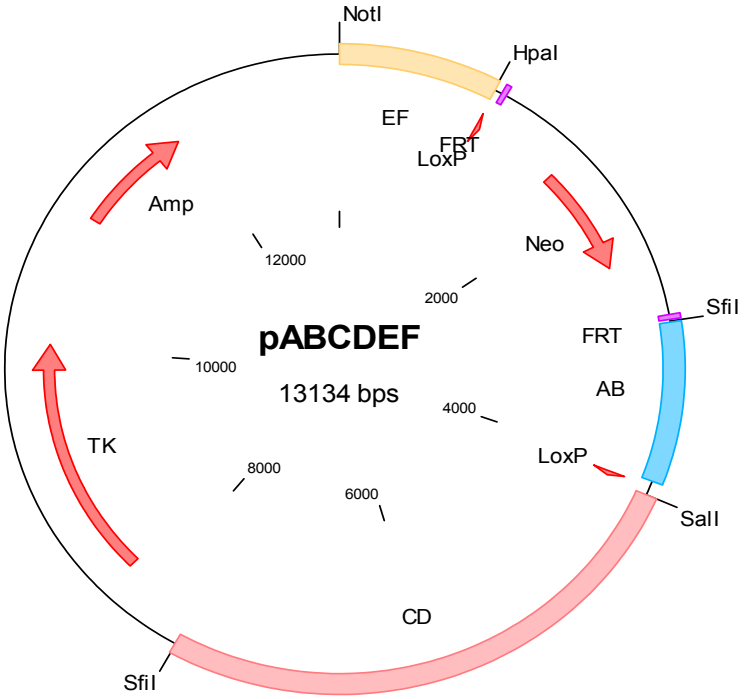
NotI
HpaI
EF
FRT
LoxP
Amp
Neo
12000
2000
SfiI
pABCDEF
FRT
10000
13134 bps
AB
4000
TK
LoxP
8000
6000
SalI
CD
SfiI

Figure 9. *Control Plasmid pABCDE'F.*

This plasmid is largely similar to the plasmid pABCDEF, except for the upstream region (lavender) of the EF fragment. The upstream region expands from the NotI site to the 5' end of EF. This upstream region was cloned from the upstream genomic sequence to the 5' end of EF from the BAC. This region would serve as an anchor site for the primer Y and thus allow PCR amplification with the primers Y and Neo1R. Therefore, this plasmid acts as a positive control in the ES screening for icRen knockouts.

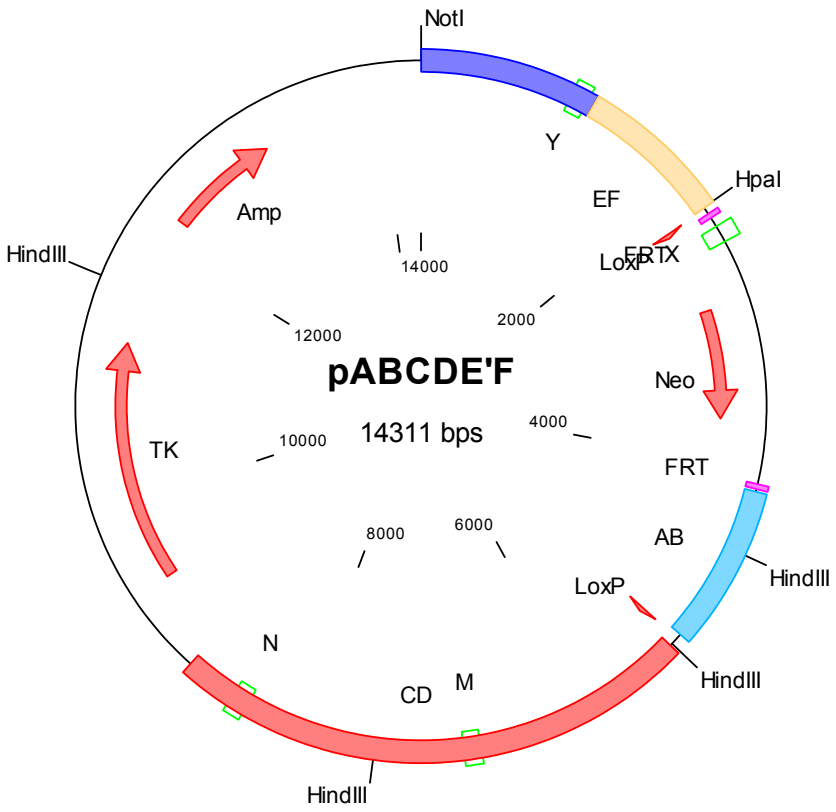
NotI
Y
EF
HpaI
LoxP
ERTX
Amp
HindIII
14000
2000
12000
pABCDE'F
14311 bps
Neo
4000
TK
10000
FRT
8000
6000
AB
HindIII
LoxP
N
HindIII
CD
M
HindIII

Figure 10. *Control Plasmid pGHIJK'2L.*

This vector is structurally similar to the other control plasmid pABCDE'F. In this case, the upstream genomic region (lavender) to the 5' end of fragment KL was cloned from the BAC and then placed to the upstream of KL in the vector. This would allow amplification with the primers Z and Neo1R (or X). Thus, the plasmid could serve as a positive control in the ES screen for sRen knockouts.

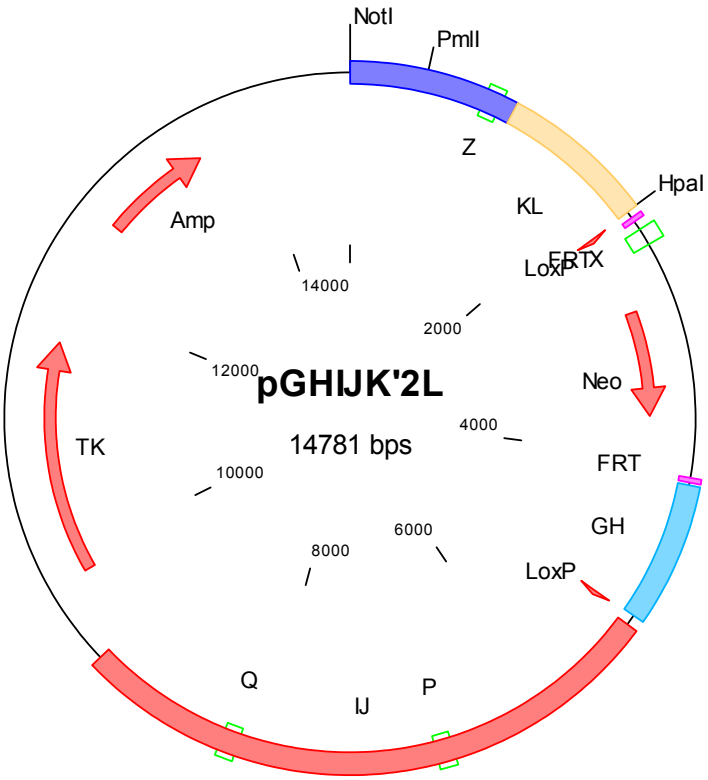
NotI
PmlI
Z
HpaI
KL
FRTX
LoxP
Amp
14000
2000
12000
pGHIJK'2L
Neo
4000
14781 bps
TK
FRT
10000
6000
GH
8000
LoxP
Q
P
IJ

Figure 11. *Representative Gel of sRen Initial Screen PCR.*

In this PCR, the reverse primer Neo1R were used to replace the reverse primer X, thus the amplicon size was 2.1Kb instead of 1.5 Kb. Both Z/X and Z/Neo1R primer pairs worked with similar efficiency in the sRen knockout screening. Neo1R was more frequently used for later icRen screenings. We have identified three positive clones (FV115, 213 and 225) as shown this PCR.

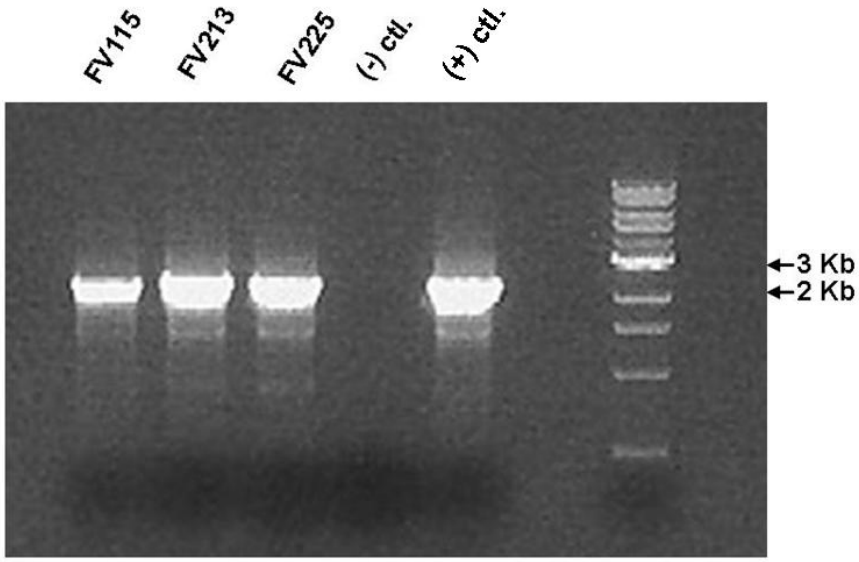
FV115
FV213
FV225
(-) ctl.
(+) ctl.
3 Kb
2 Kb

Figure 12. *Optimization for Best PH and Mg Concentration*

This figure is an optimization PCR showing that pH=9.06, with $MgCl_2$ concentration at 1.0-1.5mM are optimal with most specific and robust amplification. For every three lanes from left to right, the templates are ddH_2O, 30ng of mixed DNA (gDNA: control plasmid = 1:1) and 1ng pure control plasmid, respectively. All subsequent icRen knockout ES screening PCRs were performed at pH 9.06 with 1.5mM of $MgCl_2$.

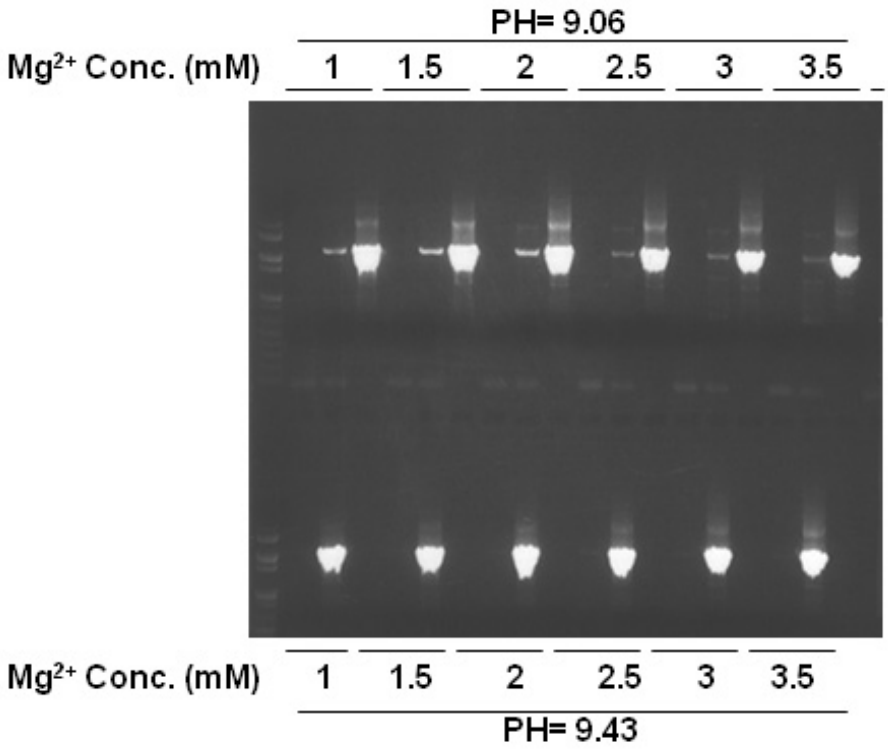
PH= 9.06
Mg2+ Conc. (mM)
1
1.5
2
2.5
3
3.5
Mg2+ Conc. (mM)
1
1.5
2
2.5
3
3.5
PH= 9.43

Figure 13. *Optimization for Best Template Amount and Annealing Temperature*

The gel below indicates that the PCR reaction for icRen initial ES screening is sensitive enough to amplify a 2 kb fragment from 10ng of genomic DNA at a broad range of annealing temperatures from 49.5 ^{o}C to 58.2 ^{o}C.

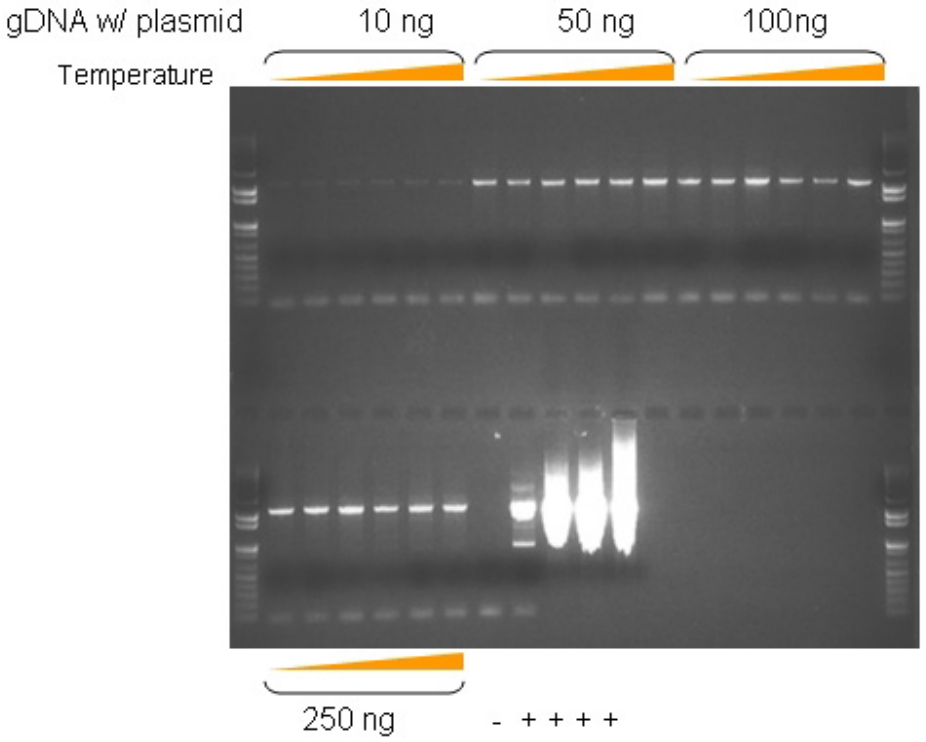
gDNA w/ plasmid
10 ng
50 ng
100ng
Temperature
250 ng
- + + + +

Figure 14. *Schematic of PCR Primers in Exon1b (icRen) Gene Targeting Screen.*

The top row shows mouse renin locus in the genome. It is composed of nine conventional exons (blue boxes), an alternative first exon (exon1b in yellow box), its classic proximal promoter (blue arrow), the potential alternative promoter for icRen transcription (yellow arrow), and an enhancer (red arrow) upstream of the promoters and exons. The second row demonstrates corresponding regions of the *mRen1*^{c} cloned into the targeting plasmid. This row is also part of the linearized plasmid pABCDEF (Figure 8). The star in CD fragment indicates the ATG->GCG mutation designed to potentially abolish the initiation of icRen translation. The blue box named “Ex V” in the third row represents exon 5 after homologous recombination.

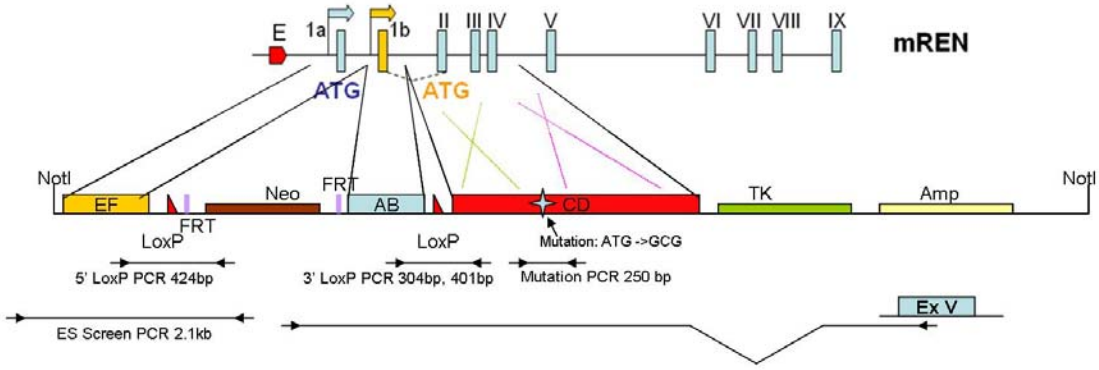
E
1a
1b
II
III IV
V
VI
VII
VIII
IX
mREN
ATG
ATG
NotI
EF
FRT
Neo
FRT
AB
CD
TK
Amp
NotI
LoxP
LoxP
Mutation: ATG ->GCG
5' LoxP PCR 424bp
3' LoxP PCR 304bp, 401bp
Mutation PCR 250 bp
Ex V
ES Screen PCR 2.1kb

Figure 15. *Representative Gel of icRen Initial Screening.*

This PCR screening was carried out using the forward primer Y and the reverse primer Neo1R. This primer set will generate a product of 2.1 kb (Figure 14). Clones D1, D3 and D10 were originally identified as positive candidates by this method. Given that this PCR only examines the 5' end site-specific homologous recombination, all three clones in this gel turned out to be false positive, as they did not pass subsequent PCR screens. A series of positive and negative controls were employed in this reaction as well.

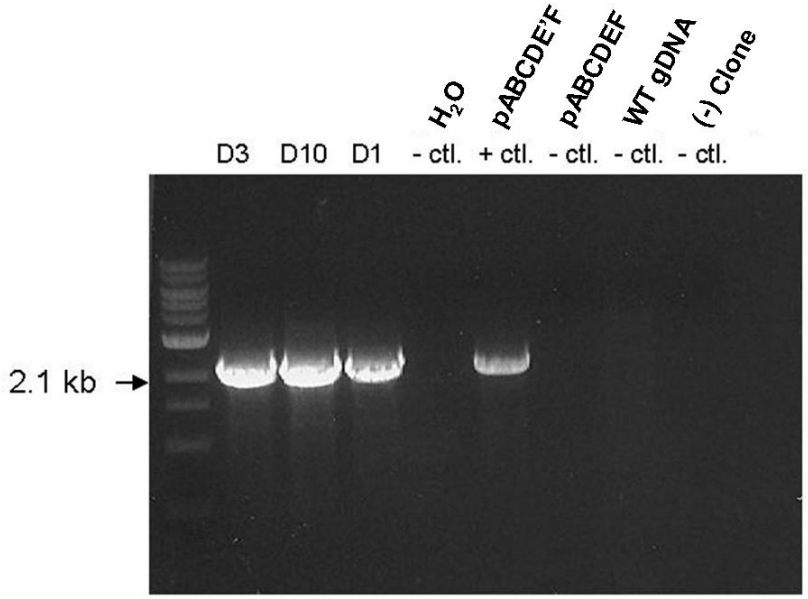
H2O
pABCDE'F
pABCDEF
WT gDNA
(-) Clone
D3
D10
D1
- ctl.
+ ctl.
- ctl.
- ctl.
- ctl.
2.1 kb

Figure 16. *Representative Gel of icRen 5' LoxP PCR.*

In this PCR, the same three clones (D1, D3 and D10) were examined. As indicated below, they all have intact 5' LoxP sites. The expected amplicon runs at 424 bp.

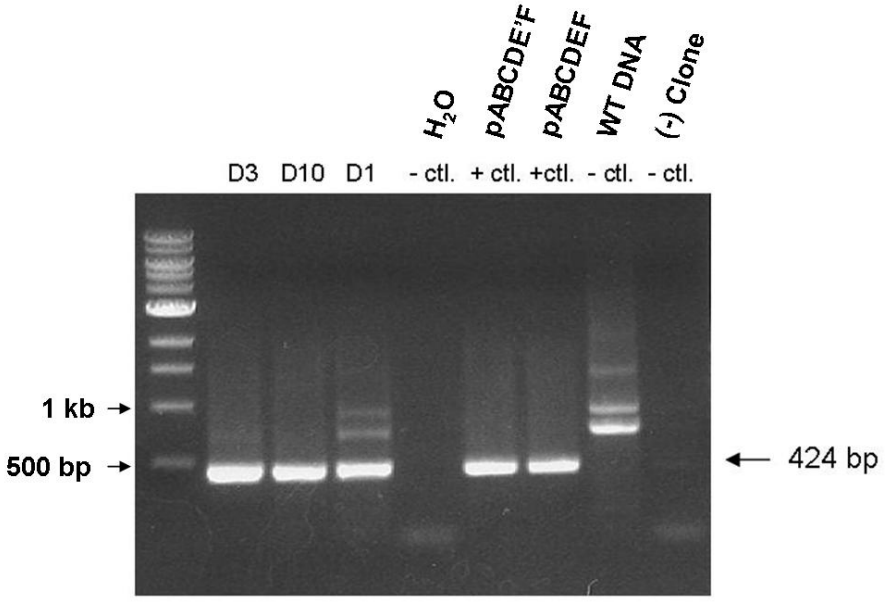
H2O
pABCDE'F
pABCDEF
WT DNA
(-) Clone
D3
D10
D1
- ctl.
+ ctl.
+ctl.
- ctl.
- ctl.
1 kb
500 bp
424 bp

Figure 17.*Representative Gel of icRen 3' LoxP PCR*

The examination of 3' LoxP sites in clones D1, D3 and D10 indicated that only two (D1 and D10) out of three clone preserved the intact 3' LoxP site, as only D1 and D10 were able to generate the top band of 401 bp. The 401-bp band represents the targeted allele, whereas the bottom 304-bp band is a product of the wild type allele.

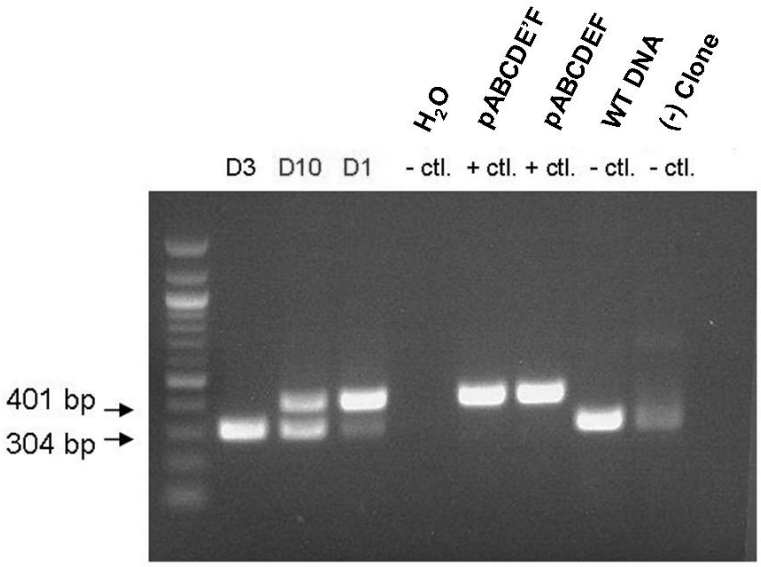
H2O
pABCDE'F
pABCDEF
WT DNA
(-) Clone
D3
D10
D1
- ctl.
+ ctl.
+ ctl.
- ctl.
- ctl.
401 bp
304 bp

Figure 18. *Representative Gel of icRen Mutation Test PCR*

This PCR approach give a band around 250 bp from both the targeted allele and the wild type allele. In order to identify the mutation, PCR products were isolated and purified from this gel and sequenced.

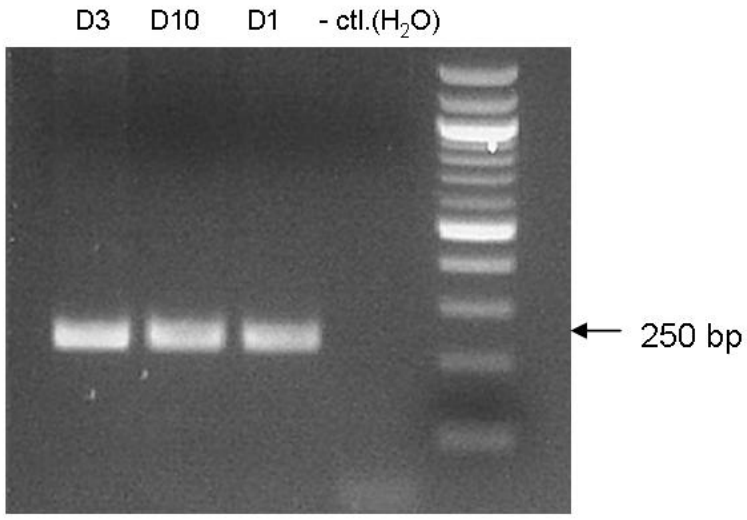
D3
D10
D1
- ctl.(H_2O)
250 bp

Figure 19. *Representative Gel of icRen 3' End Confirmation PCR.*

This PCR assay gives a product of 5.5 Kb across the 3' end homologous region and the downstream region (exon 5) to the 3' homologous arm as depicted in Figure 14. The primers used were 'pABCDEF-Final 3" and "Exon5R1". Some of the false positive ES clones only generated a non-specific band around 3 kb, not the band at 5.5 kb.

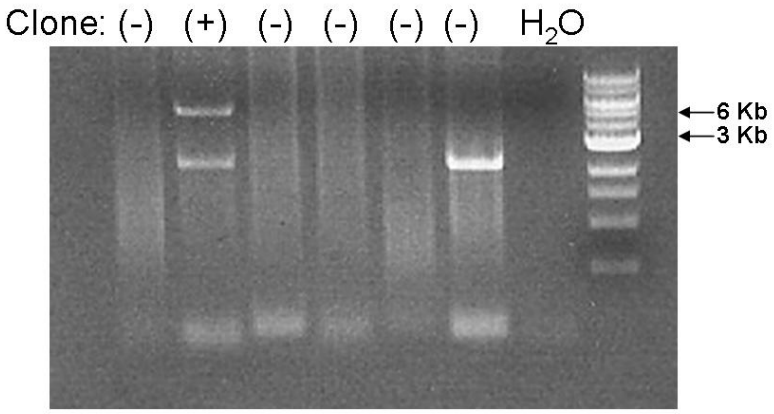
Clone: (-) (+) (-) (-) (-) (-) H_2O
6 Kb
3 Kb

Figure 20. *Schematic of sRen Southern in Founder Mice.*

The first row in this figure demonstrates the wild type allele of *mRen1*^{c}. The black and gray boxes are exons. Two SpeI sites are separately located upstream of and at the downstream region of this gene. The black arrow represents the Southern probe used in this assay. The second row indicates part of the targeting plasmid pGHIJKL. The third row shows the genomic composition after homologous recombination. As a result, an additional SpeI site was introduced upstream of exon1a. By using SpeI digestion of genomic DNA and this Southern probe, we were able to detect a target allele-specific band of 3.15 kb.

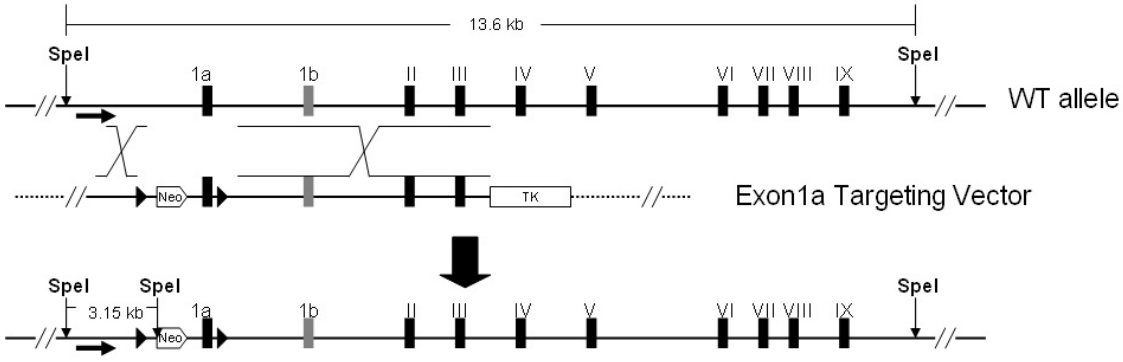
13.6 kb
SpeI
SpeI
1a
1b
II
III
IV
V
VI
VII
VIII
IX
WT allele
Neo
TK
Exon1a Targeting Vector
SpeI
SpeI
3.15 kb
SpeI
Neo

Figure 21. *Southern Blot Verifying sRen Knockout Founders.*

A typical Southern blot using genomic DNA from a germline-transmitted founder and control animals is shown in this figure. The wild type band is at 13.6 kb, whereas the targeted allele-specific band is at 3.15 kb. The 1kb Quick-Load ladder (New England Biolabs) was used. The first lane is C57 wild type control. The second line is genomic DNA from a negative littermate, while the third lane is the germline-transmitted positive littermate. The last lane is the linearized positive control plasmid pGHIJK'L.

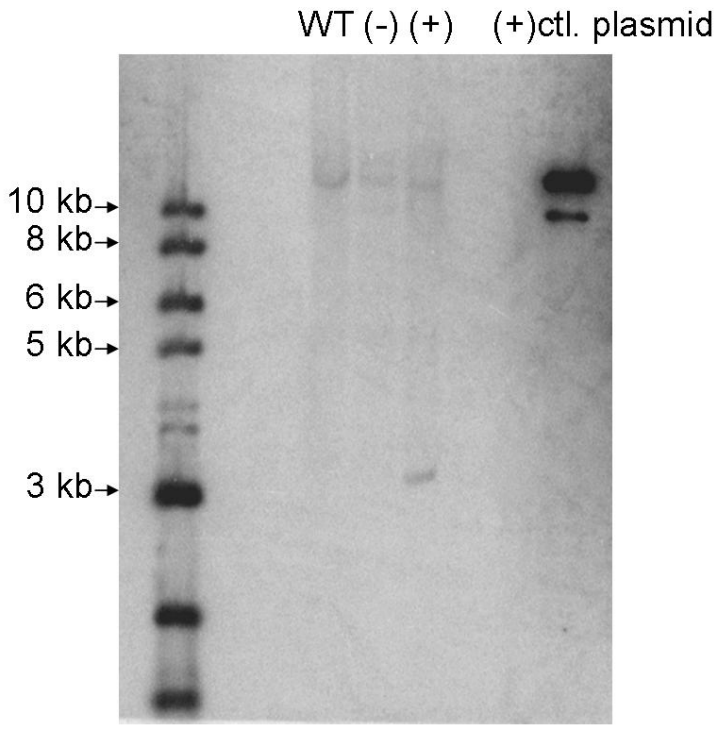
WT (-) (+)
(+)ctl. plasmid
10 kb
8 kb
6 kb
5 kb
3 kb

Figure 22. *Representative Pictures of Gene-targeted Chimeras.*

These two pictures demonstrate a chimeric mouse with white patches on its flank and abdomen on a predominantly black coat color. The white coat color was a result of a tyrosinase mutation in the ES cells from C57B6L/J genetic background. After the targeted ES cells with this tyrosinase mutation were injected into the inner layer of wild type C57B6L/J blastocyst, the mosaic blastocyst developed into an intact embryo in the pseudo-pregnant mother and later an adult mouse. Therefore the white cells were derived from the injected ES cells. Presumably, there is a better chance of targeted ES cells developing into germ cells in a mouse with higher percentage of chimerism (white patches).

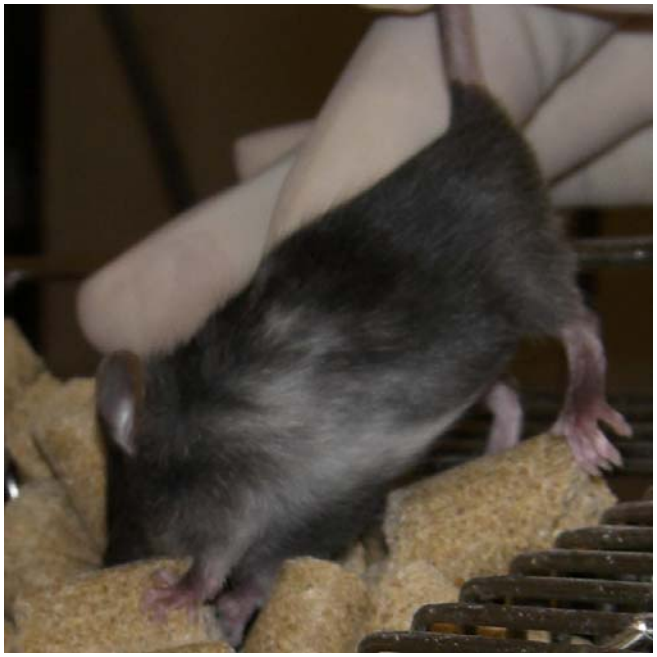

Figure 23. *Germline Screening of sRen or icRen Knockouts.*

The cartoon shows the schematic design of germline screening and location of the forward and reverse primers. In this design, only germline transmitted progeny will give a positive band of the correct size. A representative gel of the sRen knockout germline screening is also shown in this figure. In this gel, the expected band is around 500 bp. Two arrows on the top of the gel indicate two germline-transmitted offspring (6198/1 and 6198/3) from a sRen-flox chimera (FV115/2). Negative (ddH_2O) and positive controls (targeting plasmid) are located at the bottom part of the gel.

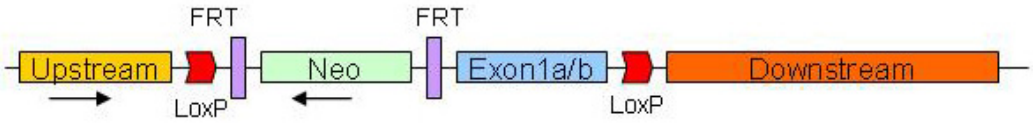
FRT
FRT
Upstream
Neo
Exon1a/b
Downstream
LoxP
LoxP

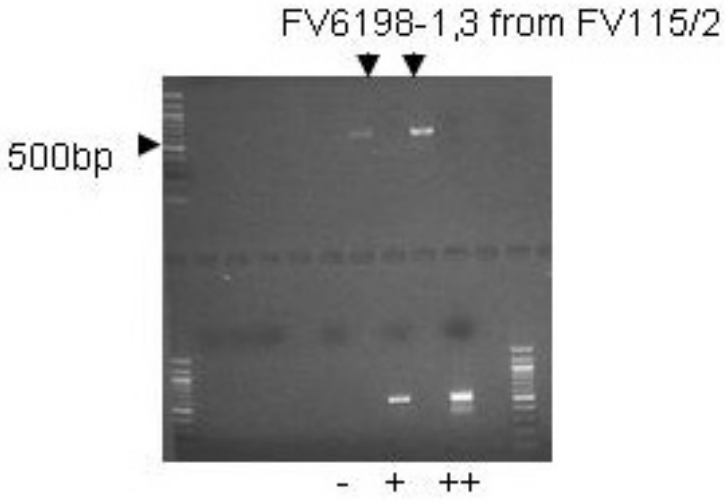
FV6198-1,3 from FV115/2
500bp
-
+
++

Figure 24. *Screening for Floxed Allele in sRen or icRen.*

As depicted in this schematic, a forward primer anchors to the upstream homologous region and reverse primer locates in the floxed region were used. This primer combination will generate a wild type band of smaller size than the band from the targeted allele. An example of a PCR screening for sRen floxed allele is shown as follow (Also Known as Screen #2). The expected WT band size is 312bp, whereas the expected targeted band size is 485bp.

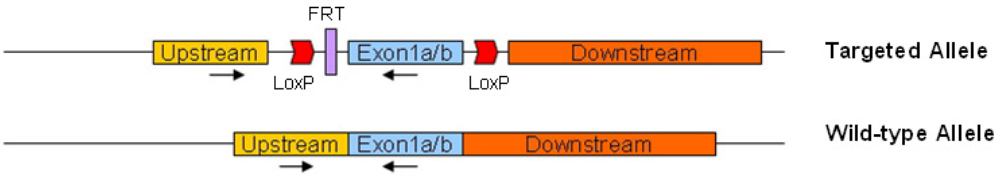
FRT
Upstream
Exon1a/b
Downstream
LoxP
LoxP
Targeted Allele
Upstream
Exon1a/b
Downstream
Wild-type Allele

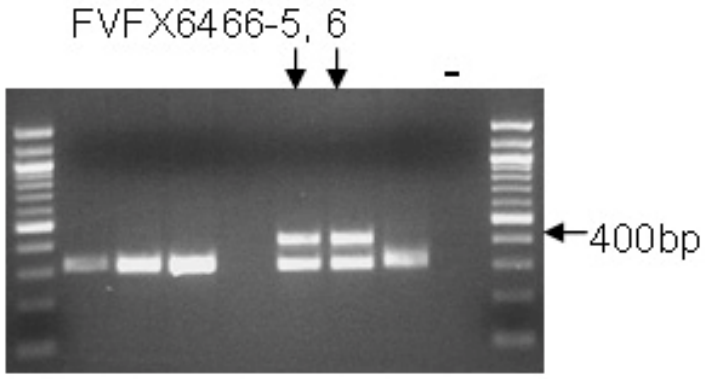
FVFX6466-5, 6
-
400bp

Figure 25. *Screening for sRen Homozygous and Heterozygous Knockout.*

In this assay, the forward primer is designed in the upstream homologous region, whereas the reverse primer anchors to the downstream homologous arm. Because the blue region (exon1a/1b and its neighboring sequences) are much larger than the LoxP site (red arrow) and its linker regions, the wild type band is bigger than the null band. A representative genotyping PCR with three sRen heterozygous knockouts is shown in this figure.

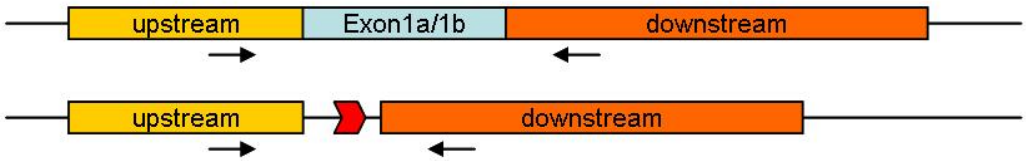
upstream
Exon1a/1b
downstream
upstream
downstream

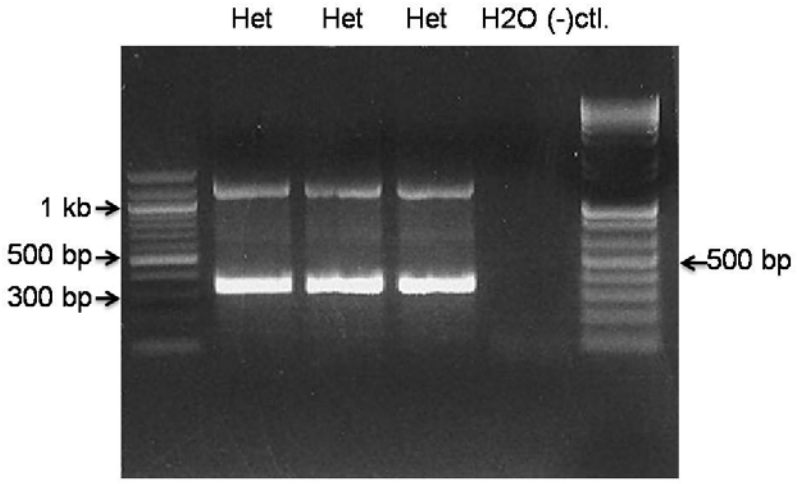
Het
Het
Het
H2O (-)ctl.
1 kb
500 bp
300 bp
500 bp

Figure 26. *Schematic of Southern Design to Confirm sRen Null.*

The null allele was generated after Cre-induced recombination. In the last row, the two hatched boxes at each end of the targeted locus are the 5’ Southern probe and the 3’ Southern probe. For the 5’ end Southern blot, HindIII digestion generates a null band of 8248 bp due to the introduction of an exogenous HindIII site in the LoxP linker region. Likewise, the 3’ end Southern generates a null band of 6592 bp with EcoRI digestion thanks to the exogenous EcoRI site in the LoxP region.

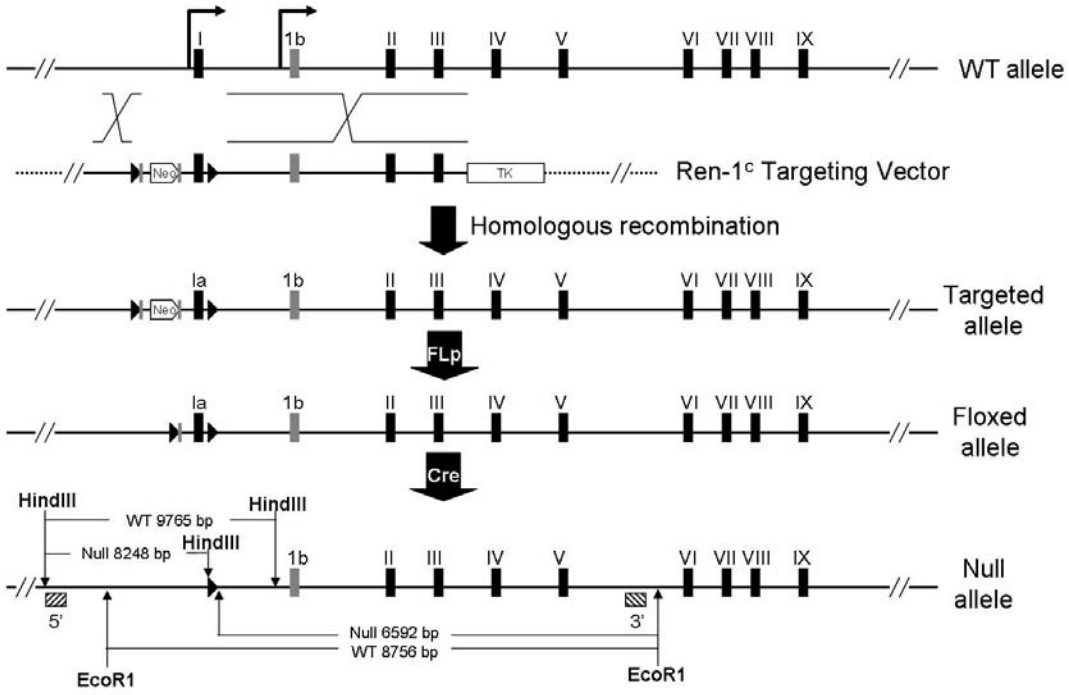
I
1b
II
III
IV
V
VI
VII
VIII
IX
WT allele
Neo
TK
Ren-1c Targeting Vector
Homologous recombination
Ia
Targeted allele
FLp
Floxed allele
Cre
HindIII
WT 9765 bp
Null 8248 bp
Null allele
5'
3'
Null 6592 bp
WT 8756 bp
EcoR1

Figure 27. *Schematic of icRen Southern in Germline-transmitted Founder Mice.*

SpeI digestion will be employed in this Southern design. When a 5’ Southern probe is used, this design will produce a 4.3 kb targeted band due to the insertion of an exogenous SpeI site in the Neo cassette, where as the wild type band will be 13.6 kb. When a 3’ Southern probe is used, this design allows the generation of an 8.7 kb targeted band and a 13.6 wild type band. The horizontal black arrows at each end of the gene indicate the locations of a 5’-end and 3’-end Southern probes.

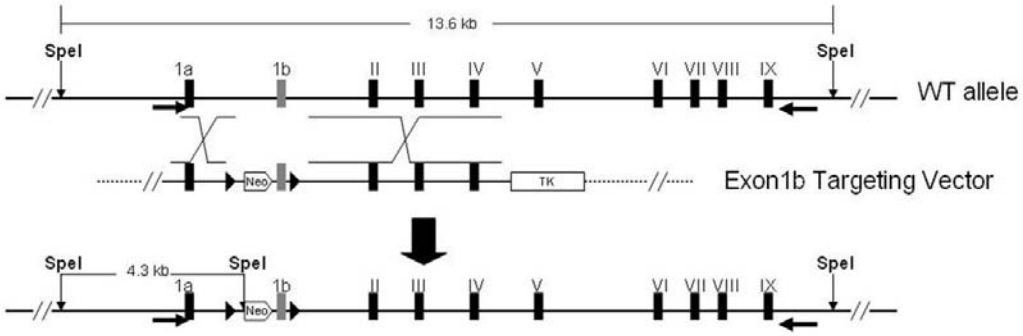
13.6 kb
SpeI
SpeI
1a
1b
II
III
IV
V
VI
VII
VIII
IX
WT allele
Neo
TK
Exon1b Targeting Vector
SpeI
4.3 kb
SpeI
SpeI
1a
1b
Neo

Table 1. *Primers to Clone Targeting Vector pGHIJKL*

Primer G	5’-ATCGCAGAGCTCGGCCATGCAGGCCTTGGGGGAGATTAGATAAAGC-3’
Primer H	5’-ATCGCACTGCAGTCCAGCTACAGATGAACTC-3’
Primer I	5’-ATCGCAGTCGACGACCTCAAGTCTGTCCTCTGTG-3’
Primer J	5’-ATCGCACTCGAGGCCTCAGTGGCCATCTTATGTGCTCGTGCTTCTG-3’
Primer K	5’-ATCGCAGCGGCCGCGGGCTTTCCTGTGCTCATC-3’
Primer L	5’-ATCGCAGTTAACAAGGCCTCCCAGCATTTC-3’

Table 2. *Primers to Clone Targeting Vector pABCDEF*

Primer A	5’-ATCGCACCGCGGCCATGCAGGCCTGGGGTAATCACAGCAGAG-3’
Primer B	5’-ATCGCATCTAGATTGAGAAGAAAGCCCATTG-3’
Primer C	5’-ATCGCAGTCGACGCCGTTGCCTTACATAC-3’
Primer D	5’-ATCGCACTCGAGGCCTCAGTGGCCAGAACAGGCTTAGACACT-3’
Primer E	5’-ATCGCAGCGGCCGCGAAGGGGGAGAAGGAGAGC-3’
Primer F	5’-ATCGCAGTTAACAGGTTTATCCCCACAA-3’

Table 3. *Primers to Clone Targeting Vector pABCDEF-Mut*

Forward	5’-GAATCCCGCTCAAGAAA**GCG**CCTTCTGTCCGGGAAATCCTGG-3’
Reverse	5’-CCAGGATTTCCCGGACAGAAGG**CGC**TTTCTTGAGCGGGATTC-3’

Table 4. *Primers to Sequence Cloning Junctions, LoxP, FRT and Mutation Sites*

pABCDEF-final1	5’- CTTTATGCTTCCGGCTCGTATGTT-3’
pABCDEF-final2	5’- CTGTAGCTGGAAGACCTCAA-3’
Final3	5’- AGTACTGTGGTTTCCTTTTGTGT-3’
pABCDEF-final4	5’- TGTGCTCCCTGCTCTGTGTAAAGT-3’
pABCDEF-final5	5’- AGGTTAGGAGTACTGAGATTAGG-3’
pGHIJKL-final1	5’- CTTTATGCTTCCGGCTCGTATGTT-3’
pGHIJKL-final2	5’- CCCATGCCTGCCACCACTCTGC-3’
pGHIJKL-final4	5’- GTAGGCCAAAGGAGTAACAT-3’
pGHIJKL-final5	5’- TCAGAAGCACGAGCACATAAGA-3’

Table 5. *Primers to Clone Control Plasmids pABCDE'F and pGHIJK'2L*

E'	5'-ATATGCGGCCGCCAGTCTCTAGTTCTTCTTG-3'
K'2	5'-ATATGCGGCCGCAGCAGAGGCTTTAGTTCC-3'

Table 6. *Primers Used in Initial PCR Screens for Both sRen and icRen Lines*

Primer X	5’-GCTACCGGTGGATGAGGAATGTGT-3’
Primer Y	5’-GGTGAGTCTAGATGAAAGGAGGTA-3’
Primer Z	5’-AGCCAGCAGAAAAGCACTCA-3’
Primer M	5’-CAGAATAAGTGACTCCAAGAAACC-3’
Primer N	5’-CTCTCCCTGATCCGTAGTGG-3’
Primer P	5’-GAGAGGAATAGAAGGGGGTTTTTA-3’
Primer Q	5’-CCACGGGGGAGGTAAGATT-3’

Note: The positions of all these primers are indicated in the control plasmid maps. For screenings of the icRen line, more primers were used as listed in Table 7.

Table 7. *Primers Used to Confirm Genotypes of icRen ES Clones*

Neo1R	5’-AGCCATGATGGATACTTTCTCG-3’
tailscreen 1bF2	5’-CCCTTTGGCTTTGGCGAGAG-3’
tailscreen 1a/1b R4	5’-AGGCCACTTGTGTAGCGCCAA-3’
tailscreen 3’LoxPF1	5’- TTCTGTGCTCCCTGCTCTGTGTAA -3’
tailscreen 3’LoxPR1	5’- TCTCACCAAGGATCCCAGCCAATG -3’
Mut-test-F	5’- AGCACTGCACGACTCTTCTG -3’
Mut-test-R	5’- AGAGAAAAGGAGATAGCAGATGAG -3’
pABCDEF-Final 3	5’-AGTACTGTGGTTTCCTTTTGTGT-3’
Exon5R1	5’- AGAACACTTCCTCCTTTAGCAC-3’

Table 8. *Primers Used to Screen Germline Transmission of sRen KOs*

F1-tailscreen1a	5’-ACAGCACAGTTCCTCATTAGAC-3’
R4-tailscreen1a /b	5’-AGGCCACTTGTGTAGCGCCAA-3’

Table 9. *Primers Used to Screen Floxed Allele of sRen KOs (Screen #2)*

pGHIJKL Final Primer2	5’-CCCATGCCTGCCACCACTCTGC-3’
5R49a-GHIJ	5’- CCTCCTTTCATCTAGACTCACCAT -3’

Table 10. *Primers Used to Screen Homozygous sRen KOs (Screen #4)*

pGHIJKL Final Primer2	5’-CCCATGCCTGCCACCACTCTGC-3’
Exon1aFloxedout-R1	5’-CCCCACAGAGGACAGACTTGAGGT-3’

Table 11. *Primers Used in icRen Germline Screen*

Tailscreen 1bF2	5’-CCCTTTGGCTTTGGCGAGAG-3’
Tailscreen 1a/1b R4	5’- AGGCCACTTGTGTAGCGCCAA-3’
tailscreen 3’LoxPF1	5’- TTCTGTGCTCCCTGCTCTGTGTAA -3’
tailscreen 3’LoxPR1	5’- TCTCACCAAGGATCCCAGCCAATG -3’

CHAPTER 3

CHARACTERIZATION OF SREN GLOBAL KNOCKOUTS

Abstract

The primary product of the renin gene is preprorenin. A signal peptide sorts renin to the secretory pathway in juxtaglomerular cells where it is released into the circulation to initiate the renin-angiotensin system cascade. In the brain, transcription of renin occurs from an alternative promoter encoding an mRNA starting with a new first exon (exon-1b). Exon-1b initiating transcripts skip over the classical first exon (exon-1a) containing the initiation codon for preprorenin. Exon-1b transcripts are predicted to use a highly conserved initiation codon within exon-2, producing renin which should remain intracellular due to the lack of the signal peptide. To dissect the roles of secreted and intracellular renin, we took advantage of the unique organization of the renin locus to generate a secreted renin-specific knockout which preserves intracellular renin expression. Expression of secreted renin mRNA was completely ablated in the brain and kidney, whereas intracellular renin mRNA expression was preserved in fetal and adult brain. We noted a developmental shift from the expression of secreted renin mRNA in the fetal brain to intracellular renin mRNA in the adult brain. Homozygous secreted renin knockout mice exhibited very poor survival at weaning. The survivors exhibited renal lesions, low hematocrit, an inability to generate concentrated urine, decreased arterial pressure and impaired aortic contraction. These results suggest that 1) preservation of intracellular renin expression in the brain is not sufficient to compensate for a loss of secreted renin, and 2) secreted renin plays a pivotal role in renal development and function, survival, and the regulation of arterial pressure.

Introduction

Renin is the first and rate limiting enzyme in the renin-angiotensin system (RAS). Renin processes angiotensinogen (AGT) into Ang-I, which is further proteolytically

cleaved by angiotensin converting enzyme (ACE) into Ang-II. In the canonical pathway, Ang-II derived from the circulation binds to AT1 and AT2 receptors in target tissues to exert its function to regulate cardiovascular and water/electrolyte homeostasis. In addition to Ang-II, ample evidence now supports the hypothesis that alternative angiotensin peptides, such as Ang-(1-7), may act as effector peptides in cardiovascular regulation.[60,174] The relative contribution of Ang-II and Ang-(1-7) remains a source of debate and has added significant complexity to the RAS. A second level of complexity stems from the wealth of data showing that many, if not all components of the RAS are expressed in many tissues. The concept that tissue-specific RAS pathways exist in tissues, including the kidney, brain, heart, vasculature, and adrenal gland, resulting in local production and action of angiotensin peptides continues to gain experimental support.[75] In the kidney, local Ang-II is thought to regulate blood flow and sodium reabsorption, whereas in the brain it stimulates thirst and sympathetic activity. The fact that antihypertensive agents targeting the RAS are effective in hypertensive patients with normal or even low plasma renin activity has contributed to the argument that tissue RAS are physiologically relevant and important.

The classical renin protein is composed of a signal peptide that leads to its secretion and release into the systemic circulation, a pro-segment that protects the active site of the enzyme from interacting with angiotensinogen, and mature active renin. The canonical site of renin synthesis, storage and release is the juxtaglomerular (JG) cells of the kidney. It is thought that other sites of renin synthesis release primarily prorenin. The first exon of renin (termed exon-1a) transcribed in renal JG cells encodes the initiation codon for translation. We and others identified an alternative isoform of renin mRNA in the brain of mouse, rat and human.[161,162] This isoform is derived from a different transcription start site and transcribes a unique first exon (termed exon-1b). Transcripts initiating at exon-1b skip over exon-1a and splice directly to exon-2, which contains an evolutionarily conserved in-frame ATG which may act as an alternative

translation initiation codon.[22] Exon-1b transcripts are predicted to encode a truncated form of renin that lacks 1) the signal peptide, and thus remains intracellular, and 2) the first third of the pro-segment, and thus is constitutively active. Previous studies have shown that this form of renin, which we have termed intracellular renin (icRen), is enzymatically active and functional both *in vitro* and *in vivo*.[22,161,166] We hypothesize that these two renin isoforms play differential roles in cardiovascular regulation and fluid homeostasis. Functional studies examining the importance of renin in the brain have been very challenging because the level of renin protein is extremely low. Moreover, because there are no unique amino acids in icRen (the sequence of icRen is a subset of secreted renin, sRen) there is no easy way to differentiate the products. We therefore employed a unique gene targeting strategy to generate knockouts (both null and conditional) of one isoform, while retaining expression of the other. Herein we report that we have established a null model of sRen with the preservation of icRen expression.

Methods

Generation of sRen Knockout Mice

Gene targeting was performed in mouse ES cells derived from a tyrosinase mutant line of C57BL/6J-Tyr(c-2J). Germ-line transmission was screened in the offspring from the chimeras bred with C57BL/6J. Details of vector construction are in the Supplemental Methods[175]. All experimental procedures on mice were approved by the University of Iowa Animal Care and Use Committee and were conducted in accordance with the National Institutes of Health (NIH) Guide for the Care and Use of Laboratory Animals.

Gene Expression

RNA was extracted from mouse tissues using TriReagent (Invitrogen). Mouse renin mRNA was measured with an RNase protection assay as previously described.[162]

Specific primers were used to amplify the sRen and icRen mRNA. The forward primer for sRen and icRen mRNA anchors to exon-1a and exon-1b, respectively. A common reverse primer located in exon-3 was used for both. A primer set in exon-4 and exon-5 was utilized to detect total renin mRNA. Taqman probes were used for realtime-PCRs for sRen and total renin mRNA. Cyber green with Takara Taq polymerase was employed to measure icRen mRNA. Primers sequences are listed in Table 12.

Renal Histology and Function

Kidneys were harvested and incubated in Pen-Fix for 3 days, paraffin-embedded and subjected to H&E staining. Following a 2-day acclimation period, urine was collected for 24 hours in metabolism cages designed for mice (Nalgene). Urine osmolarity was determined by freezing-point analysis (Fiske 2400). Urine sodium and potassium were determined by flame photometry (Instrumentation Laboratory 943). Animals were killed by CO_2 asphyxiation, decapitated, and blood was transferred into three 75 mm heparin-coated capillary tubes for hematocrit. Tubes were centrifuged at 12,600 x g for 3 minutes (BD Triac) before reading. Remaining blood (400 µL) was collected into 50 µL of 0.5 M EDTA, mixed, and placed on ice for 5 minutes. Plasma was stored at -80°C until analysis. Plasma aldosterone was determined by ELISA (Cayman Chemical, #10004377) using the manufacturer's instructions.

Cardiovascular Studies

Under ketamine and xylazine anesthesia (85.5 mg/kg: 12.5 mg/kg), by means of an anterior neck incision, left common carotid artery was implanted with a radiotelemetry catheter (PA-C10, Data Sciences International). The radiotelemeter transmitter was kept subcutaneously into the right flank. After 10 days of recovery, direct arterial pressure and heart rate were recorded continuously during 10 days (sampling every 5 minutes with 10 seconds intervals). After the day/night recordings, the sampling frequency was increased to 2000 Hz and a two hour recording was made

for analysis of the spontaneous baroreflex using the sequence method.[176] The sympathetic and parasympathetic (vagal) effects to the heart were assessed by autonomic blockade with propranolol (5 mg/kg) and methyl-atropine (2 mg/kg), respectively. The intrinsic heart rate was calculated after simultaneous β-adrenergic and muscarinic blockade. Aortic function was measured *ex vivo*. Aortas were dissected and incubated in an organ bath while constrictor or dilator agents were added into the chamber at increasing doses as described.[177]

Statistical Analysis

All comparisons were between gender and age-matched wild-type and knockout mice. Data are plotted as mean±SEM and were analyzed with ANOVA. $P<0.05$ is considered statistically significant.

Results

We employed a unique gene targeting approach to preserve expression of icRen while deleting sRen. In order to accomplish this, it was necessary to retain the common portions of the gene encoding renin (exons 2-9). Therefore we specifically ablated exon-1a of mouse renin gene along with the classical promoter while preserving exon-1b as well as its discrete transcriptional regulatory elements in the genome of C57BL/6J (Figure 28). The use of C57BL/6 ES cells allowed us to work in a genetic background containing only a single allele of the renin gene (*Ren-1*^{c}). Recall that the 129 strain carries two alleles of renin (*Ren-2* and *Ren-1*^{d}). The introduction of Cre-LoxP system confers this model the capability to cripple sRen expression in specific tissues or cell types. ES cell clones were screened via PCR genotyping, and chimeric mice were generated from ES clone FV115. Founder mice harboring the floxed exon-1a allele along with the neomycin cassette were bred with mice expressing FLPase in the early embryo. The resulting mice containing the floxed exon-1a allele (lacking the neomycin gene) were then bred with E2A-Cre mice expressing Cre-recombinase in the early embryo to

generate a null allele of sRen. A series of PCR assays were sequentially performed to verify the fidelity of gene targeting, to screen for germline transmission, the floxed allele, and ultimately the null allele (data not shown). Southern blotting using probes outside the homology arms in the targeting construct confirmed the generation and transmission of the sRen null allele in +/- and -/- mice (Figure 29).

Intercrosses of +/- mice were performed to obtain -/- homozygotes. An analysis of the first 105 offspring from these crosses at 3 weeks of age revealed significant pre-weaning lethality as only 2 -/- mice (out of 26 expected) survived to 3 weeks of age (Figure 30A). On the contrary, live sRen-/- mice were obtained at birth, and an analysis of fetuses collected at prenatal day 18.5 revealed a normal ratio of +/+, +/- and -/- offspring (Figure 30B). This implicates a defect in survival between birth and weaning. Although kidneys from sRen-/- newborns appeared structurally normal (Figure 31A-D), kidneys from surviving adult sRen-/- mice exhibited severe renal atrophy (Figure 31F,H) compared with sRen+/+ controls (Figure 31E,G). Consistent with other models of RAS gene deficiency, sRen-/- mice exhibited a significantly reduced hematocrit (Figure 30C).[178] Also consistent with previous models, sRen-/- mice exhibited increased urine output and an inability to generate a concentrated urine (Table 13).[179] Probably as a compensatory mechanism, plasma aldosterone was elevated by 35% (Table 13). We conclude that secreted renin is required for survival and its loss causes severe defects in the structure and function of the kidney after birth.

We next sought to obtain evidence for the preservation of icRen mRNA expression in the sRen- null mice. We used primer sets capable of individually detecting sRen vs icRen mRNA, and total renin (sRen + icRen mRNA). There was a marked reduction in total renin mRNA in the kidney and brain from 18.5 day gestation fetuses from sRen-/- as compared with +/+ and +/- littermates (Figure 32A). This was attributed to a loss of sRen mRNA as there was clear preservation of icRen mRNA in sRen-/- mice. These data were confirmed by real time Q-PCR (Figure 32B). It is notable that at this

stage of fetal development, renin mRNA in the brain is mainly attributable to sRen mRNA as the decrease in total renin mRNA completely paralleled the decrease in sRen mRNA in sRen-/- mice. On the contrary, icRen mRNA was preserved and even increased in the brain of sRen-/- fetuses (Figure 32B). Similar results for total renin and sRen mRNA were observed in the kidney, consistent with the highly predominant transcription from the classical promoter in renal JG cells.

In adult survivors, total renin mRNA was completely ablated in the submandibular gland and kidney of sRen-/- mice (Figure 33A). As expected, there was no expression of renin mRNA in the liver. Q-PCR revealed that the levels of sRen mRNA were completely ablated, whereas the levels of icRen mRNA were increased in the brain of adult sRen-/- mice (Figure 33B). Interestingly, however, there was no apparent change in the level of total renin mRNA in the brain from adult sRen-/- mice suggesting a developmental shift in utilization of renin mRNA isoforms. Our data suggests that during late embryonic development, sRen mRNA is the major isoform expressed in the brain, whereas in adults, icRen mRNA is the predominant form expressed in the brain.

We next measured mean arterial blood pressure and heart rate via radiotelemetry. sRen null mice which survived to adulthood displayed a normal circadian rhythm (Figure 34A), but exhibited a significant decrease in mean arterial blood pressure compared to age and gender matched wild-type littermates during both the daytime and nighttime hours (Figure 34B). Baseline heart rate was unchanged in both groups (Figure 34C). Baroreflex function in sRen-/- was essentially normal except there was a decrease in the number of baroreflex sequences (Table 14). This may reflect a decrease in the blood pressure variability. The autonomic regulation of heart rate was also normal in sRen-/- although there was a trend toward an increase in the vagal tone to the heart as observed after muscarinic blockade with methyl-atropine. The intrinsic heart rate was similar in both groups.

Aorta from sRen-/- mice exhibited normal responses to acetylcholine and nitroprusside after pre-constriction with $PGF_{2\alpha}$, and exhibited normal contractile responses to $PGF_{2\alpha}$, phenylephrine and KCl (Figure 35 A-D, F). However, an impaired constrictor response to 5-HT was noted in the aorta from sRen-/- mice (Figure 35E).

Discussion

This is the first study designed to examine the differential roles, if any, of sRen and icRen in the regulation of cardiovascular function. The long term goal of this project is test the provocative hypothesis that the unique expression of icRen in the brain plays a role in blood pressure and water and electrolyte homeostasis[35]. As a first step toward this goal, we used a novel gene targeting strategy to fully ablate sRen while preserving icRen mRNA. The novel findings from our study are that complete loss of sRen, even with preservation of icRen, causes lethality, and in adult survivors, severe renal abnormalities, anemia, an inability to concentrate urine, and hypotension. This suggests that sRen is an essential component required during early neonatal life and is a critical regulator of arterial pressure in adults. Our data also suggests that preservation of icRen is not sufficient to rescue defects caused by loss of sRen.

RAS Deficiency, Lethality and Renal Defects

The increased lethality and renal structural abnormalities observed in adult sRen null mice is consistent with other models of RAS gene ablation including renin null mutants lacking the entire renin gene.[170,172,179,180] That the mice in the present study are born in normal numbers, exhibit normal renal histology at birth, but then succumb within a few weeks is also consistent with other RAS deficiencies. Similarly, anemia has been reported in mice lacking ACE.[178] This implies that Ang II generated in the extracellular spaces in tissues or in the systemic circulation is required for continued development of the kidney after birth and is a major regulator of arterial pressure in adults. Mice lacking sRen were impaired in their ability to generate concentrated urine

although their total sodium and potassium excretion was essentially normal. The modest elevation in aldosterone is likely a consequence of these renal defects. Although icRen mRNA is the predominant form of renin mRNA in the brain of adult mice, it represents only a very small fraction (estimated at less than 1%) of the total renin mRNA in the kidney. Consequently, it is not surprising that preservation of this small fraction of icRen mRNA in the kidney was insufficient to rescue the defects caused by loss of sRen. Indeed, it remains unclear what minimum level of renal renin is required to retain viability and renal structure and function and whether this renin needs to be secreted.

Complementation studies have been used to identify the important sites of RAS expression in order to rescue defects observed in RAS knockout mice. For example, we previously reported that the human renin and human angiotensinogen genes could fully complement lethality and renal defects in angiotensinogen deficient mice.[181] Because the transgenes were expressed in many tissues and plasma Ang II was elevated, it provided a proof-of-principle that genetic means could be used to replace endogenous Ang II with transgenic Ang II. Other genetic data from our laboratory showing that exclusive targeting of renal angiotensinogen and renal Ang II is insufficient to rescue lethality in angiotensinogen deficient mice implicated the importance of circulating Ang II for the maintenance of renal structure.[158] This is supported by complementation studies form other investigators where over-expression of RAS components in adipose tissue or liver resulted in Ang II release in the circulation which rescued renal defects.[182,183] More contradictory to this hypothesis was data from Lochard *et a*l who reported that brain-specific over-production of Ang II normalized blood pressure and corrected some renal defects in angiotensinogen deficient mice.[134] The Ang II level in the brain was elevated by approximately 6-fold, and was presumably generated in the extracellular space because the construct was cleverly designed to secrete Ang II. Interestingly, the increase in brain Ang II did not translate into an increase in circulating Ang II in their transgenic mice. It should be noted however, that they did not repeat

these measurements when their transgene was bred on the angiotensinogen deficient genetic background. Consequently, the mechanism by which brain-specific Ang II improved renal structure and function remains unclear. In our study, preservation, or even an increase in icRen expression in the brain was clearly ineffective at preventing renal abnormalities.

Evidence for an Intracellular Renin in the Brain

Our data showing preservation of icRen mRNA expression in the sRen null mice provides additional support for the concept that an independent renin mRNA is transcribed at the renin locus. The increase in icRen mRNA in the brain of sRen null mice, and the developmental shift in the expression from sRen in the fetal brain to icRen in the adult brain suggest that independent regulatory elements and a novel promoter mediate expression of icRen mRNA. This conclusion is strengthened when one considers that the ablation of sRen was generated by deletion of exon-1a and 500 bp of surrounding DNA including the classical renin promoter. Sequence analysis of the region directly upstream of mouse exon-1b reveals the absence of a classical TATA-box but the presence of a potential CCAAT box at approximately -50. A promoter prediction program also identified a potential promoter sequence approximately 700 bp upstream of exon-1b (within intron 1 of the renin locus).[184] The same algorithm predicted a promoter upstream of exon 1a, but did not identify a promoter in the second intron. Understanding the transcriptional elements and physiological signals regulating expression of icRen will require additional investigation. It may be important to consider whether the low levels of icRen mRNA in the brain reflect the activity of a very weak promoter or are due to other factors. For example, Mercure *et al.* previously showed that whereas truncation of the renin pro-segment resulted in increased renin activity, it also caused a marked decrease in secretion and expression of renin.[185] Therefore it is

unclear if the very truncation which eliminates the signal peptide and part of the pro-segment also causes decreased expression.

Lee-Kirsch first identified transcripts initiating at exon-1b in the brain of mouse, rat and human.[161] AtT-20 cells transfected with exon-1b cDNAs resulted in renin activity in cell lysates, but not medium, and *in vitro* translated icRen was not processed in microsomal membranes. These results were consistent with the production of active prorenin and retention of the protein intracellularly. We then identified the presence of the exon-1b mRNA in the brain of transgenic mice carrying a highly regulated genomic construct encoding the human renin gene and followed up by validating its presence in human fetal brain RNA.[162] The exon-1b form of renin mRNA was the predominant form in the brain of these mice and the protein was localized throughout the hypothalamus.[163] The hypertension in double transgenic mice carrying this highly regulated human renin gene was reduced after intracerebroventricular losartan, providing indirect evidence supporting the function of icRen. More direct evidence for the function of icRen is derived from studies specifically over-expressing this form of the protein. We reported that brain-specific expression of either sRen or icRen in transgenic mice resulted in a similar increase in blood pressure.[22] Peters et al reported that expression of icRen in transgenic rats is retained in the cytoplasm and results in increased aldosterone production[166]. Clausmeyer reported the presence of icRen mRNA in the adrenal gland, and its synthesis in the heart was stimulated after myocardial infarction.[164,165] Therefore, icRen may not be exclusive to the brain.

Perspectives

There are many lingering questions surrounding the intracellular RAS concept (reviewed in [35]). Is icRen localized in a cellular compartment where it can generate angiotensin peptides? What happens to these peptides if and once they are generated? Of obvious importance would be to determine if this occurs in neurons, and if so, what

the function of intracellular Ang II is in neurons. Although our data clearly suggest that icRen cannot substitute for loss of sRen, it does not rule out a physiological function for icRen. By taking advantage of the fact that sRen and icRen mRNAs are derived from independent transcription start sites, we have generated the first of a series of models designed to dissect the physiological significance of sRen and icRen. Unfortunately, because the sRen and icRen proteins are essentially identical in sequence (icRen is a subset of secreted prorenin), antibodies specific to each isoform cannot be generated. This coupled with the low level of renin expression in the brain has hampered studies addressing its function. Consequently, the generation of the complementary model described herein, that is, ablation of icRen with preservation of sRen, should provide a unique experimental platform from which to assess the function of this protein. As icRen is the primary isoform of renin mRNA expressed in the adult brain and its expression is largely, but not exclusively brain-specific, an icRen null should function as a brain-specific renin knockout. The generation of this model is currently in progress.

Figure 28. *Generation of sRen Knock-out Mouse Model.*

Cre-LoxP strategy was used to target exon-1a of mouse *Ren-1*^{c} gene using the targeting vector shown. Homologous recombinant founder mice containing the targeted allele were bred with FLpase transgenics to generate the floxed allele. The null allele was obtained by breeding with E2A-Cre transgenic mice. The frt (gray rectangle) and loxP (black triangles) sites are indicated. Exon 1b is shaded black and gray. The final null allele is shown along with the expected sizes from *EcoR*1 and *Hin*dIII digestion and use of the 5' and 3' probes (crosshatched boxes). The restriction site indicated in bold are those present in genomic DNA whereas those in italics are unique to the null allele and engineered at the loxP site.

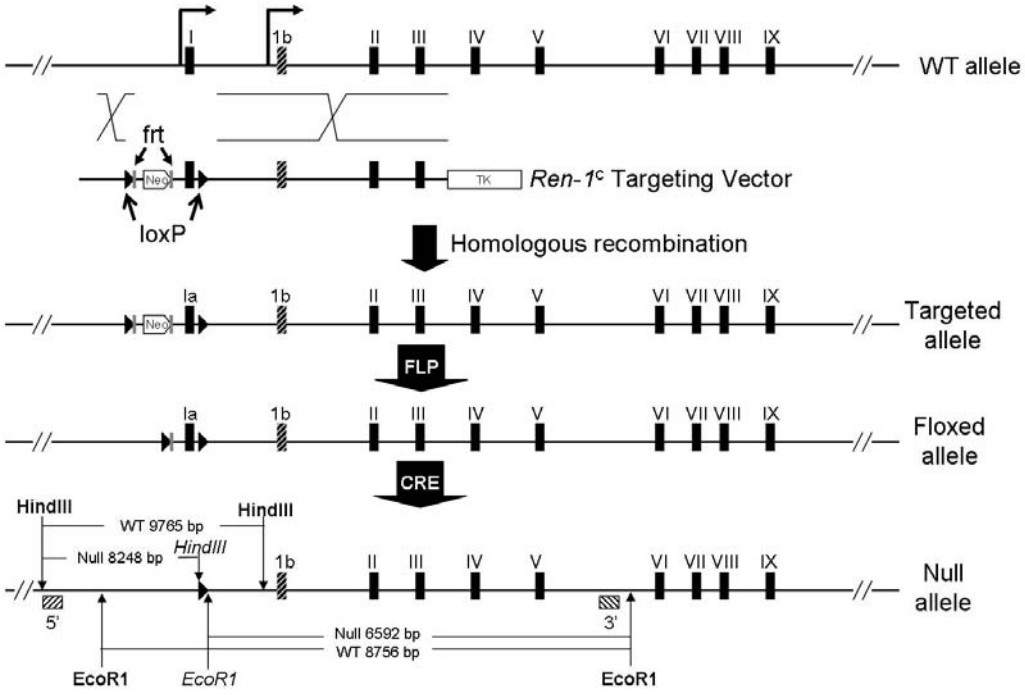
I
1b
II
III
IV
V
VI
VII
VIII
IX
WT allele
frt
Neo
TK
Ren-1c Targeting Vector
loxP
Homologous recombination
Ia
Targeted allele
FLP
Floxed allele
CRE
HindIII
WT 9765 bp
Null 8248 bp
HindIII
HindIII
5'
3'
Null 6592 bp
WT 8756 bp
EcoR1
EcoR1
EcoR1
Null allele

Figure 29. *Southern Blotting of Null and Littermate Controls.*

5’ and 3’ Southern probes were employed to confirm correct targeting of *Ren-1*^{c} exon1a. *Hin*dIII digestion produces a 9765 bp wildtype (WT) band and an 8248 bp null band with the 5’ probe. *Eco*RI digestion generates an 8756 bp WT band and a 6592 bp null band using the 3’ probe. The positions of the probes were shown in Figure 28.

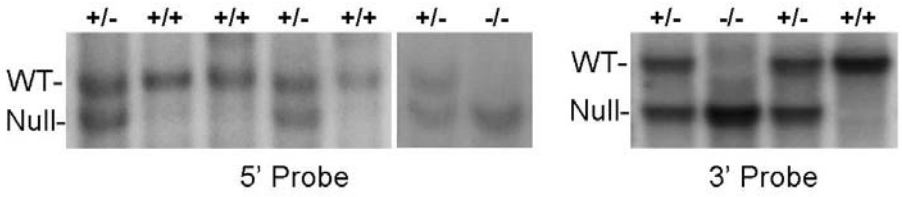
+/-
+/+
+/+
+/-
+/+
+/-
-/-
WT-
Null-
5' Probe
+/-
-/-
+/-
+/+
WT-
Null-
3' Probe

Figure 30. *Genetics.*

A-B. Genotype frequencies of 3 week old (A) and 18.5 gd fetal (B) offspring of +/- X +/- crosses. *, $P<0.05$ by χ^2. C. Hematocrit of mice with the indicated genotypes. *, $P<0.05$ vs +/+.

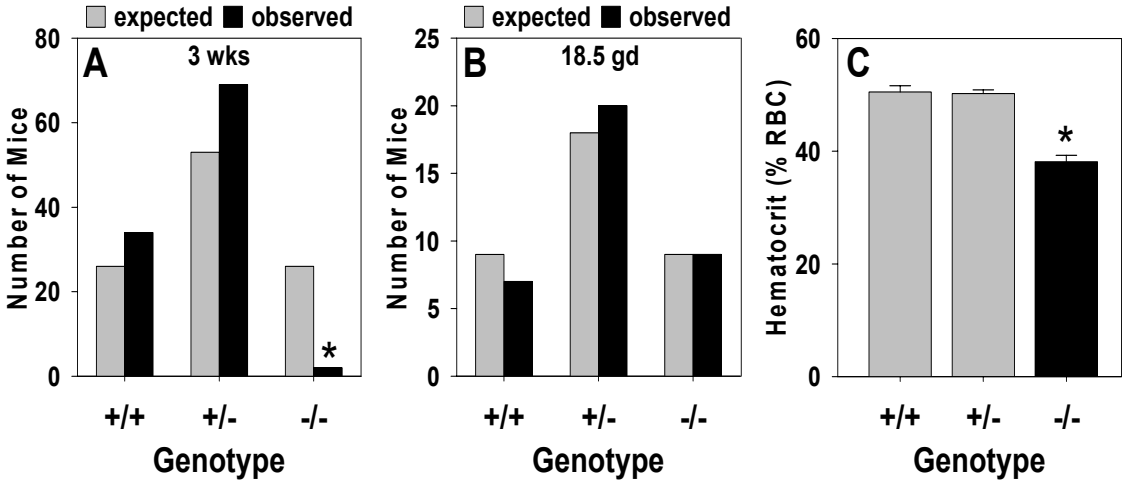
expected
observed
A
3 wks
Number of Mice
80
60
40
20
0
*
+/+
+/-
-/-
Genotype
B
18.5 gd
25
20
15
10
5
C
Hematocrit (% RBC)
60
40

Figure 31. *Renal Histology*.

A-D. Saggital and coronal sections through kidney from newborn sRen+/- (A, C) and sRen-/- (B, D) mice. Images were photographed through 4X lens (A-B) and 10X lens (C-D). E-H. Cross-section (E, F) and hematoxylin and eosin staining (G, H) of sRen+/+ (E, G) and sRen-/- (F, H) kidney from surviving adult mice.

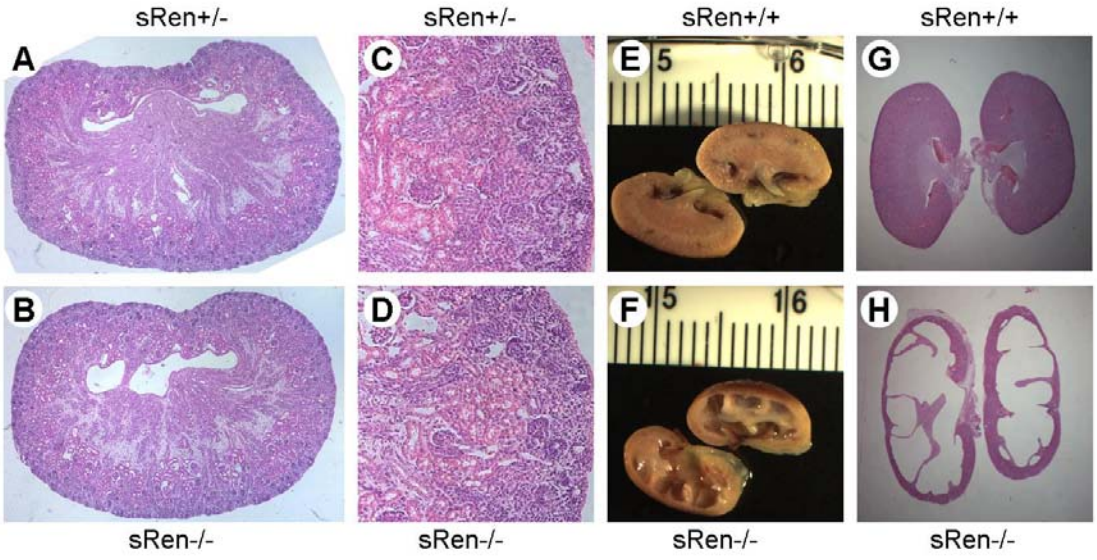
sRen+/-
sRen+/-
sRen+/+
sRen+/+
A
C
E
G
B
D
F
H
sRen-/-
sRen-/-
sRen-/-
sRen-/-

Figure 32. *Expression Profile of Renin Isoforms in Fetuses.*

A. RT-PCR of the indicated renin isoform mRNAs and GAPDH in brain (Brn) and kidney (Kid) of 18.5 gd fetuses genotypes as indicated. +/- reflects presence or absence of reverse transcriptase (RT) in the reaction. B. Realtime Q-PCR assays on ren-ex1a, ren-ex1b and total renin mRNA in the brain (left) and kidney (right) as indicated. +/+, gray bars; -/-, black bars. *, $P<0.05$. N=4 for all samples except N=3 for ren-ex1b in brain.

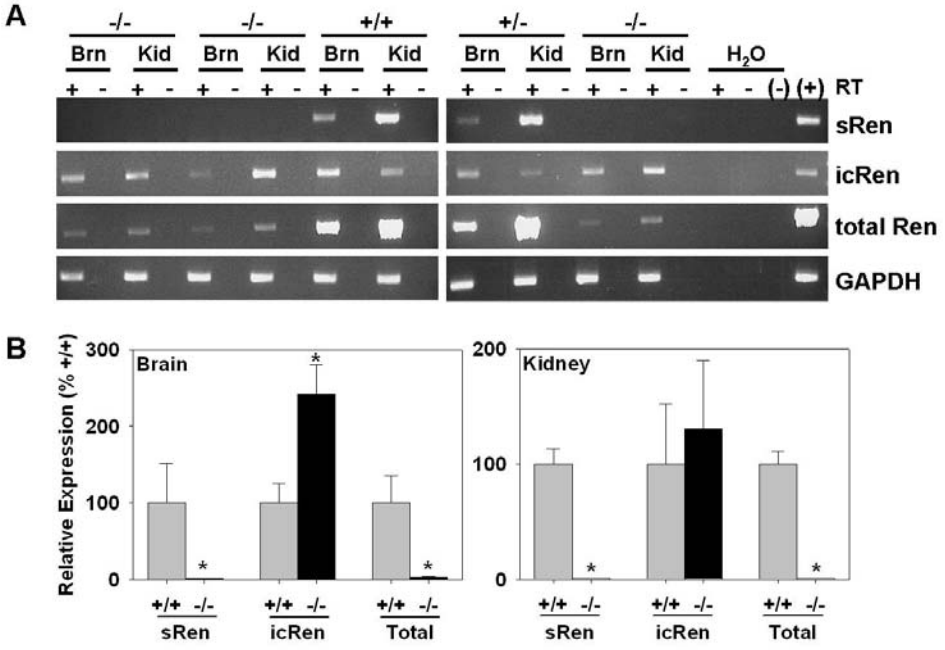
A
-/-
-/-
+/+
+/-
-/-
Brn
Kid
Brn
Kid
Brn
Kid
Brn
Kid
Brn
Kid
H2O
+ - + - + - + - + - + - + - + - + - + - (-) (+) RT
sRen
icRen
total Ren
GAPDH
B
Relative Expression (% +/+)
300
200
100
0
Brain
*
*
*
+/+ -/-
sRen
+/+ -/-
icRen
+/+ -/-
Total
200
100
0
Kidney
*
*
*
+/+ -/-
sRen
+/+ -/-
icRen
+/+ -/-
Total

Figure 33. *Renin Expression Levels in Adults.*

A. RNase protection assay of submandibular gland (SMG) liver and kidney RNA from adult mice of the indicated genotypes. The renin and cyclophilin mRNA protected products are shown. B. Realtime Q-PCR assays on ren-ex1a, ren-ex1b and total renin mRNA in the brain as indicated. +/+, gray bars; -/-, black bars. *, $P<0.05$. The sample number is indicated for each bar.

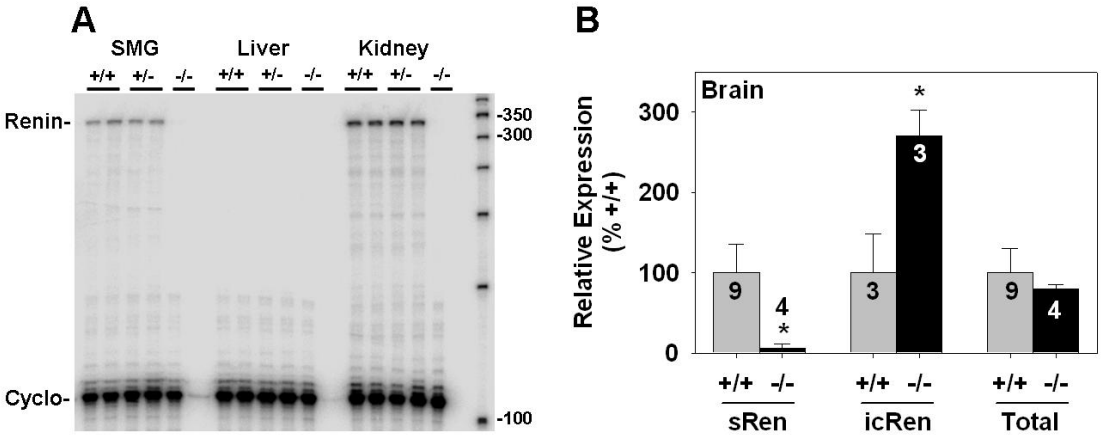
A
SMG
Liver
Kidney
+/+ +/- -/- +/+ +/- -/- +/+ +/- -/-
Renin-
Cyclo-
-350
-300
-100
B
Brain
Relative Expression (% +/+)
300
200
100
0
9
4
*
3
*
3
9
4
+/+ -/-
+/+ -/-
+/+ -/-
sRen
icRen
Total

Figure 34. *Blood Pressure, Heart Rate and Aortic Function*

A. Hourly MAP over a 48-hr period of +/+ (gray) and -/- (black). B-C. Summary of 10-days of blood pressure (B) and heart rate recording (C) of +/+ and -/- split into day and night time periods. *, $P<0.05$. N=5 for +/+ and 4 for -/-.

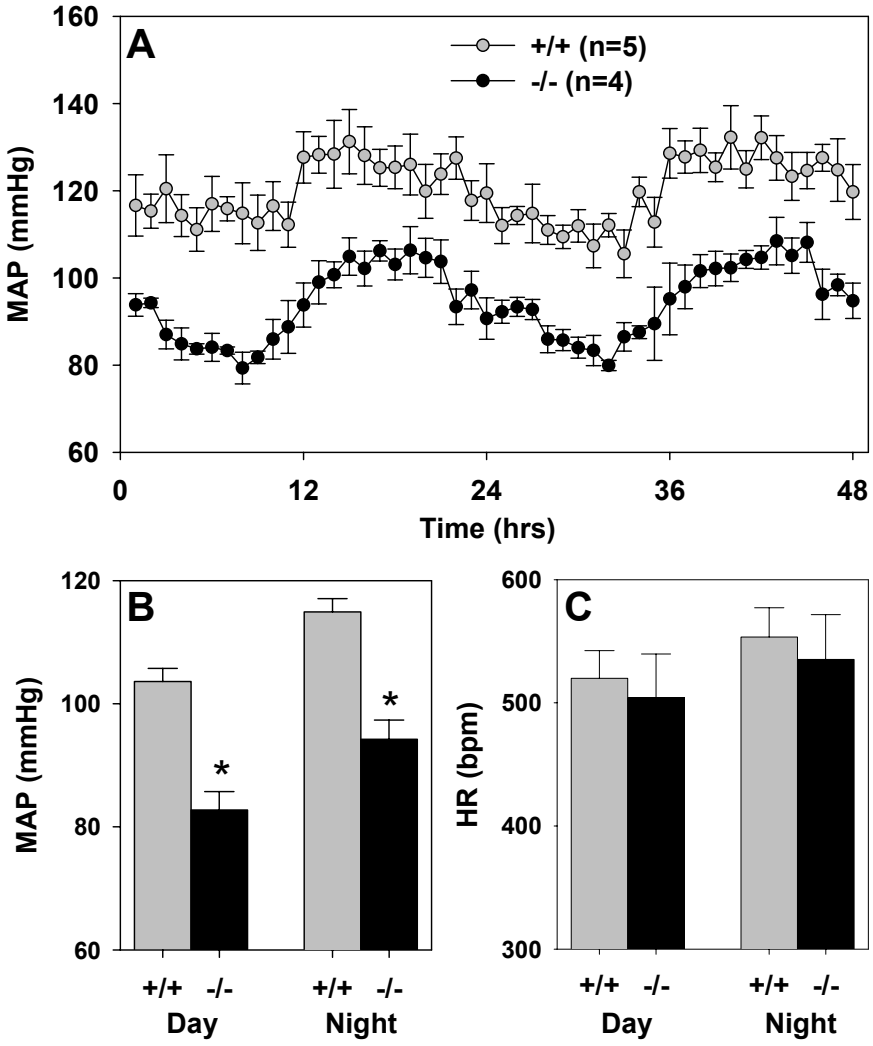
A
+/+ (n=5)
-/- (n=4)
MAP (mmHg)
160
140
120
100
80
60
0
12
24
36
48
Time (hrs)
B
MAP (mmHg)
120
100
80
60
*
*
+/+
-/-
+/+
-/-
Day
Night
C
HR (bpm)
600
500
400
300
+/+
-/-
+/+
-/-
Day
Night

Figure 35. *Aortic Vascular Functions.*

Thoracic aorta form homozygous sRen knockouts and littermates were incubated *ex vivo* to examine their vascular responses to different vasodilators and vasoconstrictors. A. Vasodilation response to acetylcholine. B. Vasodilation upon sodium nitroprusside stimulation. C. Vasoconstriction upon prostaglandin factor 2 alpha treatment. D. Contractile response to phenylephrine. E. Contractile response of aorta to 5-HT (serotonin). sRen knockouts demonstrated blunted vasoconstriction to 5-HT. F. Vasoconstriction to KCl stimulation.

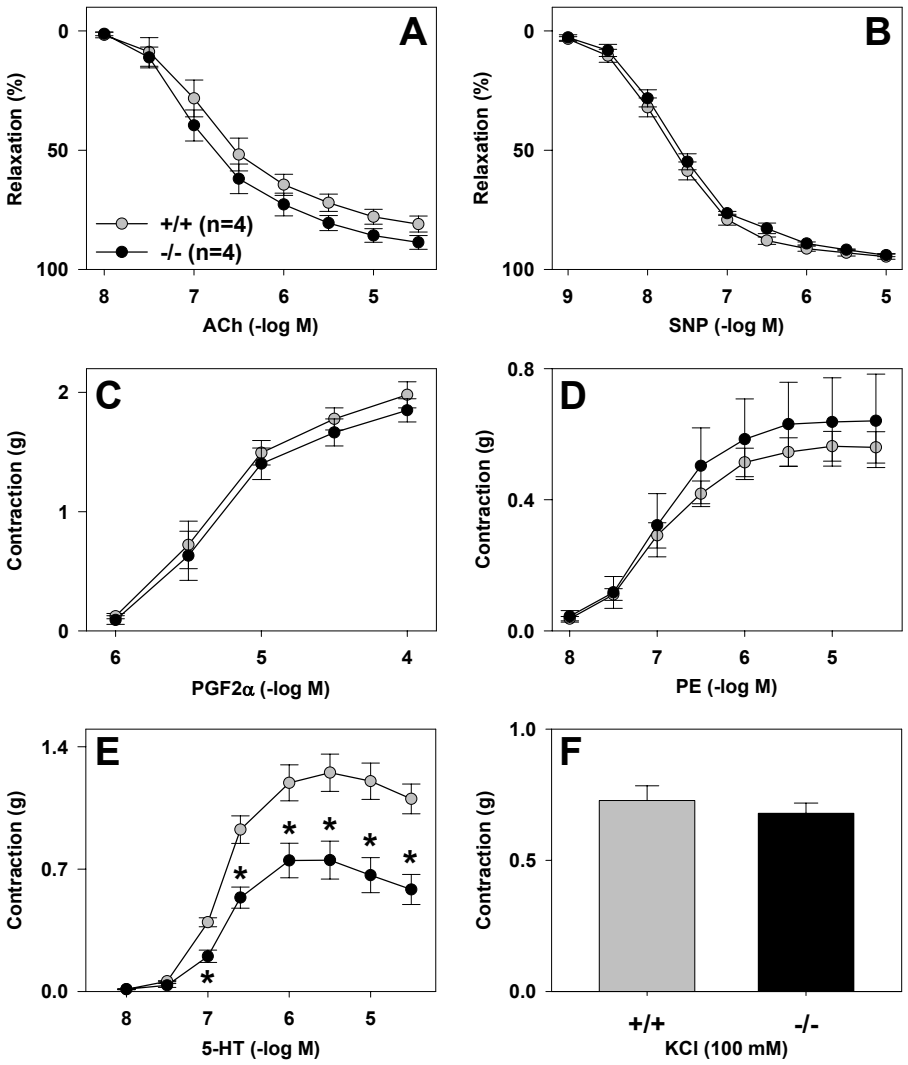
A
Relaxation (%)
0
50
100
+/+ (n=4)
-/- (n=4)
8
7
6
5
ACh (-log M)
B
Relaxation (%)
0
50
100
9
8
7
6
5
SNP (-log M)
C
Contraction (g)
0
1
2
6
5
4
PGF2α (-log M)
D
Contraction (g)
0.0
0.4
0.8
8
7
6
5
PE (-log M)
E
Contraction (g)
0.0
0.7
1.4
8
7
6
5
5-HT (-log M)
F
Contraction (g)
0.0
0.5
1.0
+/+
-/-
KCl (100 mM)

Table 12. *Oligonucleotides and Primers.*

RT-PCR Primers		
sRen Forward:	5'-ACCTTCAGTCTCCCAACACGCACC-3'	
sRen Reverse:	5'-GGGAGGTAAGATTGGTCAAGGAAGG-3'	
icRen Forward:	5'-TTTGATGAGAGGATACGCATAGCACTTC-3'	
icRen Reverse:	5'-GGGAGGTAAGATTGGTCAAGGAAGG-3'	
Total Ren Forward:	5'-GTCCGACTTCACCATCCACTAC-3'	
Total Ren Reverse:	5'-AGAACACTTCCTCCTTTAGCAC-3'	
Q-PCR Primers and Probes		
sRen Forward:	5'-GCACCTTCAGTCTCCCAACAC-3'	
sRen Reverse:	5'-TCCCGGACAGAAGGCATTTTC-3'	
sRen Probe:	5'-CCTTTGAACGAATCCC-3'	
icRen Forward:	5'-CCGGCTGCTTTGAAGATTTGAT-3'	(CYBER)
icRen Reverse:	5'-ATGCCAATCTCGCCGTAGTA-3'	(CYBER)
Total Ren:		
Assay ID-Mm02342888_Gh (Applied Biosystems)		
Probe Sequence:	TCACGATGAAGGGGGTGTCTGTGGG	

Table 13. *Plasma Aldosterone and Renal Function in sRen-/- and sRen+/+ Mice.*

Genotype	PAC *(pg / mL)*	UOsm *(mOsm / kg)*	UOsm *(mOsm / d)*	UV *(mL / d)*	U_{Na} *(mM)*	U_K *(mM)*	U_{Na} *(mEq / d)*	U_K *(mEq / d)*
+/+ (n=3)	694±70	3295±496	4.4±0.6	1.4±0.3	359±18	231±57	0.5±0.1	0.4±0.1
-/- (n=4)	933±51*	634±117*	5.0±0.5	9.0±2*	85±17*	62±12*	0.7±0.1	0.5±0.1

Note: PAC, Plasma aldosterone concentration; Uosm, Urine osmolality; UV, Urine volume; U_{Na}, Urinary sodium; U_K, Urinary potassium. sRen homozygous knockouts exhibited increased plasma aldosterone and urinary volume, as well as decreased urinary osmolality, urinary sodium concentration and urinary potassium concentration.

Table 14. *Cardiovascular Parameters in Ren-ex1a-/- and +/+ Mice.*

	No. Sequences	**Gain**	**BEI**	**iHR** (bpm)	**ΔHR Atropine** (bpm)	**ΔHR Propranolol** (bpm)
+/+ (n=4)	278±31	2.9±0.2	0.08±0.01	477±4	+62±18	-57±37
-/- (n=4)	154±15	3.5±0.3	0.06±0.01	470±40	+132±26	-48±18
P Value	0.011	0.093	0.28	0.87	0.069	0.82

Note: The sequence method was employed to measure baseline baroreflex. The number of sequences indicates the total number of effective spontaneous baroreflex. BEI, baroreflex effective index, equals number of sequences divided by number of ramps. BEI implicates the frequency of spontaneous baroreflex; Gain equals the change in heart rate divided by the change blood pressure. Gain indicates the average degree of spontaneous baroreflexes. iHR, intrinsic heart rate. ΔHR-Atropine is an indication of vagal tone on heart rate control, whereas ΔHR-Propranolol is a presentation of sympathetic drive on heart rate control.

CHAPTER 4

NEURON- AND GLIAL-SPECIFIC ABLATION OF SECRETED RENIN IS INSUFFICIENT TO ALTER BASELINE BLOOD PRESSURE AND METABOLISM

Abstract

Brain renin is known as a regulator of cardiovascular function and fluid homeostasis. We reported previously that there is a developmental shift in the utilization of renin isoforms in mouse brain[175]. Secreted renin (sRen) is the major form in the brain during the embryonic stage, whereas intracellular renin (icRen) is the predominant form in the adult brain. In order to investigate the functions of sRen versus icRen specifically in the brain, we have established neuronal-specific and glial-specific knockout models of sRen. Herein we report that cell type-specific depletion of sRen, with preservation of icRen, in the brain does not affect baseline physiological parameters in blood pressure regulation, hydromineral balance, or basal metabolic rate.

Introduction

The existence and function of an intrinsic brain renin-angiotensin system (RAS) have been suggested by a wealth of studies[20,149,150]. The brain RAS is suggested to be involved in cardiovascular regulation[123], fluid/electrolyte homeostasis[186,187], cognitive function[113] and metabolism[188,189]. Angiotensinogen expression has been found in the rat brain[190-193] as well as in cultured human astrocytes[194]. In addition, brain-specific overexpression of angiotensinogen in transgenic mice results in increased blood pressure, whereas depletion of angiotensinogen transgene in the brain reduces blood pressure [23,195,196]. Moreover, angiotensin-converting enzyme (ACE)[197] and angiotensin receptors[198] have been identified in the brain at relatively high levels. Despite a huge body of literature supporting the existence of a functional brain RAS, we still do not fully understand where and how angiotensin is generated, and where and how it exerts its functions as a neurotransmitter in order to regulate blood pressure.

Renin activity was initially identified in rat[35] and dog[150] brains based on its ability to hydrolyze AGT into Ang-II. The brain extracts displayed a similar time course and dose-dependency as renal extracts in generating Ang-II[149] *in vitro*. As renin is the main enzyme in the kidney known to generate angiotensin peptides, this suggested that renin is the main enzyme that generates Ang-II in the brain. It suggests but, does not formally rule out the possibility that other non-specific aspartyl proteases (*e.g.* cathepsin D) also participate in angiotensin generation. A separate study has verified that the presence of brain renin is independent of its renal source, by diminishing renal renin by bilateral nephrectomy[199]. In this study, Ganten *et al.* observed that angiotensin was still present in the brain well after nephrectomy. In addition, renin-expressing cells have been identified via immunohistochemistry in rat and mouse brains[151,152], and primary cultures of neuronal and glial cells from rat brains express renin[153]. Neuronal expression of renin was also identified in humans, indicating the conservation of renin expression in the brain across species[154]. Perhaps the strongest evidence is that intracerebroventricular (ICV) injection of renin antisense oligos targeting renin mRNA in spontaneous hypertensive rats (SHRs)[90] and 2-kidney-1-clip (2K1C) rats[89] causes a decrease in blood pressure.

Our laboratory has previously documented synthesis of endogenous renin mRNA in the brain using RT-PCR and Q-PCR[175]. Moreover, transgenic studies have provided further insights with regard to expression of renin in the brain. Lavoie J. *et al.* demonstrated co-localization of angiotensinogen and renin expressing cells using reporter genes in transgenic mouse brain[102]. In addition, brain-specific overexpression of human renin and AGT transgene leads to elevated blood pressure in transgenic mice[23,195]. We have also employed a P1 artificial chromosome (PAC) carrying the human renin gene along with its regulatory elements and neighboring genes as an entire transgene in mouse[200]. This model allowed us to identify an alternative splicing isoform of renin in the brain[162], which has been shown to be functional in cleaving

angiotensinogen *in vitro*[161] and to increase blood pressure *in vivo*[22]. There has also been emerging evidence of renin/prorenin receptor expression in the brain[201-203]. Although its function remains controversial, it is tempting to speculate that since renin is expressed in a very restricted manner within selected brain regions[204], the presence of a prorenin receptor might contribute to the local concentration of renin, thus increasing the efficiency of angiotensinogen activation near specific cell types. This is particularly interesting to our study, because we hypothesize that sRen and icRen play differential roles in cardiovascular regulation, potentially at discrete cellular locations. It would be possible that sRen is enriched by prorenin receptors to hydrolyze angiotensinogen in areas of the body (including brain) where sRen is not locally synthesized. Prorenin receptor has also been found localized in the cell where it may have access to icRen.

There is increasing evidence that the brain RAS may be involved in the regulation of metabolism. Studies from Porter *et al.* have identified that chronic ICV infusion of Ang-II suppressed body weight gain in young rats[188] and adult rats[189], likely through increased sympathetic stimulation of adipose tissue. In addition, the DOCA-salt induced hypertensive rats have demonstrated hyperactivity of central RAS[21,205]. Interestingly, in our preliminary studies with DOCA-salt treated mice, we have noticed a significant drop in perigenital white adipose tissue. It has also been demonstrated that pharmacological ACE inhibition[206] or AT1R blockade[207] is able to interfere with metabolism. Additionally, global knockout of total renin[172], ACE[208], AGT[182], AT1R[209] results in decreased body weight and adipose deposition, whereas AT2R[210] and MAS[211] receptor depletion resulted in morphological changes in adipose pad composition and size, respectively. Since DOCA-salt and the abovementioned RAS inhibition/knockout models all exhibit suppressed activity of the peripheral RAS, one convergent hypothesis is that the lean phenotype of all of these models could be an effect of reduced peripheral RAS activity. Therefore, sRen brain-specific knockouts may serve as a useful model to determine the contribution of the central RAS on peripheral adipogenesis and/or energy expenditure.

As introduced previously, brain angiotensins have been shown to participate in cardiovascular control. The mechanism of angiotensin generation, however, remains unclear. The discovery of an intracellular renin (icRen) in the brain has promoted a novel hypothesis for the mechanism of brain angiotensin production. Our laboratory and others have identified an alternative splicing isoform of renin initiated from a discrete exon 1 (named exon 1b). This transcript subsequently is translated into a truncated renin protein that lacks the signal peptide and first third of the pro-segment, thus remaining intracellular and constitutively active, as has been confirmed in a cell line[161]. We learned in Chapter 3 that both sRen and icRen are expressed in the brain endogenously[175], and employ discrete regulatory elements for transcription. We hypothesize that sRen acts in the extracellular space between neuronal and glial cells to hydrolyze angiotensinogen secreted from glial cells, whereas icRen is responsible for cleaving intracellular angiotensinogen in neurons and then generating angiotensin to be used as a neurotransmitter. We have discovered a developmental shift in the utilization of renin isoforms in the brain. sRen is the predominant isoform in fetal mouse brain, while icRen is the main form in adult mouse brain. It is possible that angiotensins generated by sRen are involved in early brain development and cognitive functions[113], whereas angiotensins produced by icRen are associated with cardiovascular regulation in adults. Recall, prorenin receptor mutants cause mental retardation. Studies from sRen global knockouts also indicated that sRen is the major form in the kidney, whereas icRen is expressed at minimal levels in the periphery. Therefore, we speculate that icRen exerts its function mainly in adult brain, and is critical to mediate cardiovascular output and fluid/electrolyte homeostasis. To address the hypothesis that sRen and icRen generate angiotensin in different parts of the brain (extracelluar vs intracellular), and thus exert distinct functions in regulation of cardiovascular parameters and fluid homeostasis, we crossed the sRen-flox mouse line with mice expressing neuronal and glial-specific Cre recombinases (Nestin-Cre and GFAP-Cre, respectively) to generate

neuronal or glial-specific sRen knockouts. These mice exhibit preserved expression of icRen. As discussed in Chapter 2 and as detailed in Appendix 1, we have generated ES cells specifically targeting icRen. Future experiments will be designed to directly test the physiological significance of icRen.

Materials and Methods

Generation of brain knockouts.

Brain-specific knockouts of renin were generated by crossing sRen-flox with Nestin-Cre and GFAP-Cre lines to establish neuronal and glial-specific knockout mice, respectively. Nestin-Cre and GFAP-Cre transgenic mice were obtained from Jackson Laboratory (stock numbers 003771 and 004600, respectively) and have been documented for their capability to target neuronal and glial cells, respectively[212,213]. Detailed information about the sRen-flox line is described in Chapter 3. For either line, we first crossed Cre+ with homozygous sRen flox (F/F) to give birth to F/+, Cre+. (Figure 36) Subsequently, F/+, Cre+ animals were bred to F/F to generate F/F Cre+ (brain KO) and F/F Cre- (littermate wild-type control). All animals used in this study are on C57BL/6J background. Unless otherwise mentioned, all the mice are provided with standard chow and water *ad libitum*. All animal experimental procedures are proved by the University of Iowa Animal Care and Use Committee and were performed under the guidelines of NIH Guide for Care and Use of Laboratory Animals.

PCRs and gene expression.

Primers specifically detecting flox and null alleles of sRen were used to characterize brain-specific deletions of sRen (Forward: 5'-CCCATGCCTGCCACCACTCTGC-3', Reverse: 5'-CCCCACAGAGGACAGACTTGAGGT-3'). RNA was harvested from brains (E18.5 and 2-3 month-old) and kidneys from adults as previously described. sRen and GAPDH primers and probes were used as indicated previously[175].

Tissue immunohistology.

Brains from the Nestin-Cre x ROSA mice were harvested and stained for β-galactosidase and/or immunofluorescence staining against NeuN/GFAP. For β-gal staining, sections were incubated overnight at 37^{o}C in potassium ferricyande/ferrocyanide solution (with bromo-4-chloro-3-indolyl –β-D-galactoside in diemthylformamide at 1mg/ml). After 3 washes in PBS, sections were incubated for 2 hours at room temperature in biotinylated mouse anti–NeuN antibody (Chemicon/Millipore, 1:500, in PBS plus 0.1% Triton-X). Following another 3 washes in PBS, the sections were incubated in avidin-HRP (Vector Laboratories) for 30 minutes, washed 3 times in PBS, and placed in a solution containing 0.03% 3,3' diaminobenzidine (DAB) in acetate buffer and 0.001% hydrogen peroxide. After appearance of reaction product (2-5 minutes), the sections were washed in tap water (pH6.8) and mounted on slides. For double immunofluorescence staining, sections were incubated in 4% normal horse serum for 30 minutes, followed by incubation with a mouse anti-β gal antibody (Abcam, 1:1000, in PBS plus 0.1% Triton-X) overnight at 4^{o}C. Following 3 washes in PBS, sections were incubated with a biotinylated goat anti-mouse antibody (1:200) for 2 hours, washed again in PBS for another 3 times, then incubated for 60 minutes in avidin Texas Red (Vector; 1:60), which allowed labeling of β-gal with red fluorescence. After 3 washes in PBS, sections were subjected to either NeuN staining or GFAP staining. The NeuN group was incubated in biotinylated mouse anti-NeuN (1:500) for 2 hours, washed 3 times in PBS, and incubated with avidin-Fluorescein (Vector; 1:50) for 30 minutes. The GFAP group was incubated in rabbit anti-GFAP (Abcam; 1:1000) for 2 hours, washed 3 times in PBS, and incubated with biotinylated goat anti-rabbit antibody (Vector Laboratories;1:100) for 60 minutes, washed again, then incubated with avidin AMCA (Vector; 1:50) for 30 minutes.

Kidneys from neuronal- or glial-specific sRen knockouts (F/F Cre+ vs. F/F Cre-) were removed and fixed in Bouin's buffer overnight. Subsequently, immunostaining was

carried out on 5 μm paraffin-imbedded kidney sections for renin (rabbit anti mouse, polyclonal, 1:500) and α-SMA (monoclonal anti- α-SMA-specific antibody isotype Ig2a, 1:10,000, Sigma) using a Vectastain ABC kit (Vector Laboratories)[214].

Blood pressure and heart rate.

Blood pressure was recorded via radiotelemetry as described previously[175]. Briefly, brain-specific knockouts and littermate controls were subjected to implantation of radiotelemetry catheters (TA11PA-C10, DSI™) into the left common carotid artery following ketamine and xylazine anesthesia, and animals were allowed 10 days of recovery before recording for another consecutive 10 days.

Metabolic measurements.

Oxygen consumption was utilized as a surrogate marker for basal metabolic rate. O_2 intake and CO_2 output were measured with instruments from Ametek/AEI (model S-3A/II for O_2 and model for CD-31 CO_2). Metabolic rate at thermoneutrality (30^{o}C) was recorded as mL of O_2 consumed per minute per 100g body weight. Respiratory quotient (RQ) was calculated as the ratio of CO_2 produced to O_2 consumed. A RQ value close to 1.0 indicates a higher utilization of carbohydrates, whereas a RQ near 0.7 means more utilization of fats.

In metabolic cage studies, experimental and control littermates were single-housed in specialized cages equipped with individual burettes for saline (0.9% NaCl) and tap water, for 4 days and 3 nights. Standard powdered food (NIH-31 modified 6% diet from Teklab) was supplied in each cage. Feces and urine were collected in separate cups. Total fluid intake is calculated as a sum of saline intake and water intake. Saline preference is calculated as the ratio of saline consumed to total fluid intake. Total daily salt intake is calculated with the following equation.

Total Na^+ Intake (mEq) = 0.135 x Food Intake (g) + 0.15 x Saline Intake (ml)

Tissue mass and body weight.

Brown adipose and perigenital white adipose tissues were extracted from 16 to 20-week-old female mice from the GFAP-Cre x sRen-flox line. From the same mice, hearts were extracted and normalized to body weight. For the Nestin-Cre x sRen-flox line, tissues were harvested from 20 to 25-week-old male mice.

Statistic analysis.

All the analyses and comparisons are between gender and age-matched sRen Flox/Flox, Cre+ and Flox/Flox, Cre- mice unless otherwise indicated. Data were analyzed by ANOVA and plotted as Mean± SEM. P value of less than 0.05 is considered significant.

Results

We previously reported that endogenous renin promoter activity *in vivo* was primarily detected in neurons as indicated by reporter genes[102,204]. In addition, overexpression of human renin and human angiotensinogen in neurons leads to elevated blood pressure[23]. Since the function of mouse sRen in neurons remains unclear, we generated a neuron-specific deletion of sRen by breeding sRen-flox mice to mice expressing Cre-recombinase under the control of the neuron-specific Nestin promoter. There is also evidence for glial renin function, as human renin was able to elicit an increase in blood pressure when over-expressed in glial cells where human angiotensinogen is also present[195]. As the endogenous level of renin is quite low in the brain, there is uncertainty as to the relative importance of sRen in neurons and glial cells. Indeed, our previous studies suggest that angiotensin derived from neurons and glial cells may serve different functions[215]. Therefore in addition to generating a neuron-specific deletion strain, we also generated a glial-specific deletion of sRen by breeding the sRen-flox mice with GFAP-Cre mice expressing Cre recombinase primarily in glial cells.

Tissue Specificity of Nestin-Cre and GFAP-Cre in Vivo

Although transgenic Nestin-Cre and GFAP-Cre mice were engineered to target specific tissue and cell types, we recognized that there are different Nestin-Cre lines in use and they may have slightly different expression patterns[216-218]. In order to confirm the tissue /cell type specificity of Nestin-Cre and GFAP-Cre in our hands, we first performed DNA analyses of sRen genomic sequences to detect the flox allele prior to, and null allele after, Cre-induced recombination. Figure 37 shows PCR amplification of genomic DNA from tissues isolated from F/F Cre+ and F/F Cre- (for both Nestin and GFAP lines). We employed primers that detect either the flox or null allele in the top and middle gels, and an assay which only detects the intact flox allele in the bottom gel. The latter assay was necessary because we noticed that the null allele was amplified more efficiently than the flox allele (due to size differences). A null band of lower molecular weight in any of the tissues examined would indicate Cre activity. As expected, we were able to detect the null allele only in F/F Cre+ animals but not in F/F Cre- animals for both lines. We next examined if Nestin-Cre or GFAP-Cre induces recombination in the kidney vs brain (Figure 37 Top). For the GFAP line, a null band was only detected in brain, not in kidneys of F/F Cre+ (n=3). As for the Nestin line, we detected a null band in both brain and kidney of F/F Cre+ (n=4). Given the sensitivity of PCR, an amplification of a null band from kidney suggests some Cre activity in this particular tissue. However, it does not necessarily mean that the major synthesis site of sRen, which is juxtaglomerular (JG) cells, exhibit Cre activity. However, we should point out that activity of the Nestin promoter has been previously reported in kidney[219]. This will be tested below. We next screened genomic DNA from a number of other tissues. We found that the GFAP-cre was active in both brain and brown adipose tissue, but not kidney, white adipose or heart (Figure 37 Middle). However, activity of Nestin-cre was detected in all tissues, although the ratio of null to flox allele in Figure 37 (Middle) clearly shows greater efficiency in the brain than other tissues. We then performed an assay which only

detects the floxed allele (Figure 37 Bottom). The floxed allele was still detected in all tissues screened suggesting that although cre-activity could be detected, that only a portion of the floxed alleles were actually converted to null alleles by cre-recombinase.

In order to confirm the cell-type specificity of Nestin-Cre and GFAP-Cre in the brain via immunohistochemistry, we also crossed both Cre transgenic lines with the ROSA26 reporter mouse (Figure 38). In the ROSA26 transgene, a floxed stop codon is located between the promoter of the transgene and a lacZ coding sequence. Upon Cre-induced recombination, the stop codon will be removed, and the LacZ gene will be expressed. Therefore, if a cell exhibits Cre activity, the lacZ gene will be turned on, and β-galactosidase will be expressed. We expected to observe β-gal staining primarily in neurons of Nestin-Cre+ ROSA+ animals and β-gal activity mainly in glial cells of GFAP-Cre+ ROSA+ mouse brain. We observed clear β-gal staining co-localized with NeuN (neuronal marker), but not with GFAP (glial marker, data not shown) in the Nestin-Cre+ ROSA+ mouse brain. There is no β-gal staining in Nestin-Cre- ROSA+ controls. Thus we conclude that the Nestin-Cre transgenic line we used in this study is mainly active in neurons in the brain. We are in the process of examining GFAP-Cre cell-specificity using similar approaches to those applied to the Nestin-Cre line.

Brain-Specific Deletion Caused by Nestin-Cre and GFAP-Cre

Unlike sRen global knockout mice (Chapter 3) which exhibited impaired survival after weaning, we did not detect any loss of survival in either neuronal- or glial-specific knockouts (F/F Cre+). This suggests that renal renin is probably not significantly impaired in these mice; otherwise the brain-specific sRen knockout would likely be lethal. As previously mentioned, however, Nestin-Cre exhibited a certain degree of activity in the kidney. In order to ensure that sRen expression in JG cells is not influenced, we proceeded to compare renin mRNA and protein levels in the kidney between F/F Cre+ and F/F Cre- animals (Figures 39 and 40). We first performed RT-PCR to confirm the

preservation of renal sRen. We extracted mRNA from adult kidneys of F/F Cre+ mice from both Cre lines. sRen mRNA levels in F/F Cre+ are comparable to those in F/F Cre- littermate controls, suggesting that both Cre lines do not have an impact on renal renin expression (Figure 39). Additionally, we carried out immunohistochemistry assays in kidneys from F/F Cre+ and F/F Cre- animals from both Cre lines. Using a mouse renin specific antibody, we observed renin protein expression in both F/F Cre+ and F/F Cre- kidneys at similar levels as demonstrated in Figure 40A-B.

Blood Pressure and Heart Rate

It has been suggested by previous studies that renin of neuronal or glial sources may play an important role in cardiovascular regulation, as overexpression of human renin and human angiotensinogen in either neuronal or glial cells in the brain leads to increased blood pressure[23,195]. In order to probe the role of brain sRen in cardiovascular regulation, we recorded blood pressure and heart rate over 10 days using radiotelemetry. For both neuronal- and glial-specific knockout lines, sRen deletion in F/F Cre+ (3-month old) had minimal effect on blood pressure and heart rate (Figures 41 and 42). Since global depletion of sRen leads to hypotension[175], we conclude that loss of either neuronal or glial sRen in the brain does not affect baseline arterial blood pressure.

Oxygen Consumption and Respiratory Quotient

As previously introduced, the brain RAS may play a role in metabolic modulation. We suspect from a preliminary DOCA-salt mouse project, that increased energy expenditure in this model is probably due to hyperactivity of the brain RAS. Given that metabolism is a net effect between energy intake and expenditure, we first examined the energy expenditure of Nestin-Cre and GFAP-Cre-induced sRen knockouts by recording basal metabolic rate. If sRen in either neuronal or glial cells alone is a key player in metabolic regulation, we would expect a decreased metabolic rate upon

removal of sRen from either cell type in the brain. As depicted in Figure 43, there is no statistical significance in oxygen consumption (a surrogate marker for metabolic rate) between F/F Cre+ and F/F Cre- in both lines. Nestin-Cre-induced neuronal sRen knockouts exhibited declined respiratory quotient, but GFAP-Cre-induced glial sRen knockouts did not display this phenotype. Interestingly, there is also no difference in O_2 consumption and RQ of sRen global knockouts that survived past weaning. Given that sRen is the major form of renin in the periphery, our data so far tends to exclude the importance of sRen on basal metabolic rate.

Metabolic Cage Studies

As previously described, in addition to energy expenditure, food intake is another component of energy metabolism. In order to further confirm the role of sRen in metabolism as well as to investigate the influence of sRen deletion on electrolyte/water balance, we have subjected the brain-specific knockout mice to metabolic cage studies. In these studies we measure fluid intake, urine output, salt preference, sodium intake, food intake and fecal output. For both Nestin (neuronal-specific knockout) and GFAP (glial-specific knockout) lines (Figure 44), we did not observe any significant difference between F/F Cre+ and F/F Cre- groups in daily food intake, fecal output, water intake, saline intake, total fluid consumption, urinary output, saline (0.15M NaCl) preference and total sodium intake. Since there has been a wealth of literature supporting the role of brain RAS on electrolyte fluid homeostasis[125,220-222], our data suggests deletion of sRen in one cell type only is not sufficient to hinder sodium/water balance. On the other hand, we observed a trend of increased water and saline intake, total salt intake and urinary output in global sRen knockouts. This may be in line with the function of sRen in the kidney.

Tissue Masses

Adipose deposition serves as an indicator of metabolic balance. Excess white adipose is a consequence of increased energy input and/or decreased energy expenditure. In addition, intrascapular brown adipose tissue is a critical site for thermogenesis. To study the influence of brain sRen on adipose deposition, we examined brown and white adipose in both Nestin (neuronal-specific sRen knockout) and GFAP (glial-specific sRen knockout) lines. Interestingly, F/F Cre+ mice of the Nestin line developed more brown and white adipose after normalization for body weight (Figure 45). As suggested by other investigators (unpublished data), this could be a direct effect of the Nestin-Cre transgene. Thus, we further studied adipose deposition in littermate controls of other genotypes (F/+ Cre+, F/+ Cre-, +/+ Cre+ and +/+ Cre-). From this, we also noted a partial contribution of the Nestin-Cre transgene to increased adipose size (Figure 45). We have detected no difference between F/F Cre+ and F/F Cre- in total body mass (Cre+ n=11, Cre- n=10) and body length (Cre+ n=8, Cre- n=7) for the Nestin line. As for the GFAP line, we report no difference in adipose mass, body weight and heart weight (Cre+ n=6, Cre- n=6) between F/F Cre+ and F/F Cre-. This suggests that depletion of glial sRen alone is not enough to change adipose deposition. In contrast, global knockout of sRen displayed reduction in white adipose and body mass, suggesting that peripheral sRen is influential in the regulation of adipose deposition.

Discussion

In this report, we have demonstrated that while global knockout of sRen significantly impacts blood pressure, vascular function, renal morphology, overall survival[175], body mass, adipose composition and water/electrolyte balance, depletion of the secreted form of renin from one cell type only (either neuronal or glial) in the brain is not sufficient to interfere with these endpoints. We did not detect significant changes in most of the baseline physiological functions examined in sRen neuronal or glial

knockouts. It is possible that loss of sRen from either neuronal or glial sources could compensate for the loss of each other. Thus, loss of sRen from one cell type only is not vital for baseline functions. The metabolic study indicates either 1) removal of sRen from one cell type only is not sufficient to induce change in basal metabolic rate; there is compensation from the other cell type or even leakage from the peripheral sRen, or 2) sRen is not the major enzyme that plays critical role in central metabolic modulation; which indirectly suggests that icRen might be the critical player in this process, or 3) the brain RAS is not essential for systemic metabolism; instead the peripheral RAS has a more profound influence on metabolic rate. Notably, total renin global knockout (both sRen and icRen) adults exhibit increased metabolic rate[172], whereas our sRen brain-specific and sRen global knockout did not show altered metabolic rate. Given that the major difference between our models and the total renin knockout is the presence of icRen primary in the brain, these data together indirectly support the hypothesis that icRen in the brain may be critical to regulate metabolism. Alternatively, circulating sRen might diffuse into the central nervous system through circumventricular organs to make up for the loss of intrinsic brain sRen. Regardless of source, sRen may subsequently become enriched by prorenin receptors located on neuronal plasma membrane. Another possibility is that endogenous brain sRen is not a critical regulator of baseline cardiovascular function in adults, while it might exert its role during development (as we observed predominant mRNA expression of sRen over icRen in the brain of late stage fetuses). This would be consistent with the function of Ang-II in cell proliferation and differentiation.

In this study, we have observed decreased body masses and white adipose in sRen global knockouts. These knockouts also demonstrated trends for elevated drinking, sodium intake and urinary output. Interestingly, they do not display an altered preference for 0.15M NaCl when compared to littermate controls. This suggests that sRen global knockouts are probably losing sodium and water in similar proportions due

to severe renal damage (see Chapter 3). Since the neuronal or glial-specific sRen knockout did not exhibit these changes in water/salt intake and urinary volume, it is likely that peripheral sRen is more important for electrolyte/fluid homeostasis. Alternatively, depletion of sRen from only one cell type in the brain is not sufficient to elicit a change in these aforementioned physiological endpoints at baseline.

It has been suggested in the literature that the brain RAS is an important regulator for water intake[125] and thirst responses after dehydration[81,223]. Therefore we have performed preliminary studies to induce thirst responses first using peripheral injections of Ang-II. Intraperitoneal injection of up to 10ug Ang-II/g body mass did not elicit drinking responses in wild-type control animals. In fact, it has been documented that mice are less responsive than rats to peripheral Ang-II infusion with regard to water intake, probably due to distinct peripheral thirst control mechanisms[224]. We next carried out an overnight dehydration procedure to compare drinking responses between glial sRen knockouts and littermate controls over different time courses. There is no difference between experimental and control groups (F/F Cre+ n=8, F/F Cre- n=9), suggesting that depletion of glial sRen is not sufficient to alter thirst response mechanisms. This indirectly supports the hypothesis that icRen is probably important for drinking response through the brain, since it is the major form of renin in adult mouse brain. We are currently in the process of studying dehydration responses in the neuronal-specific sRen knockouts.

The concept of intracellular renin is relatively recent and has been controversial. Although one could argue against the physiological importance of icRen in the brain, due to its extremely low expression at the protein level, studies from our group have consistently supported the idea that icRen is present in the brain[175] and is able to elevate blood pressure when overexpressed centrally[22]. The presence of icRen in the brain and other tissues has also been validated by others. The results in the current report provide further hints that brain icRen is crucial, particularly in adulthood. On the

other hand, central sRen does not appear to be required under baseline conditions to control blood pressure and fluid homoeostasis. Additional evidence supporting the pivotal role of brain renin comes from the study in which brain overexpression of Ang-II successfully rescued lethality in angiotensinogen (AGT) knockout mice[134]. Based on the above findings, we speculate that icRen is probably the main contributor to rescue lethality caused by systemic loss of AGT, since depletion of sRen in the brain does not lead to reduced survival rate.

Several technical hurdles exist to study icRen *in vivo*. First, it is expressed much less abundantly compared to renin of kidney origin. Secondly, icRen differs from sRen by lacking of the N-terminal of preprorenin, including the signal peptide and the first third of pro-segment. This makes it difficult to distinguish the proteins by antibodies. Third, because icRen is expected to remain in the cytoplasm of cells in the brain, its inhibition requires renin inhibitors that readily penetrate both blood brain barrier and cellular boundaries. As previously documented, the general aspartyl protease inhibitor Pepstatin is ineffective when injected ICV [225]. Furthermore, the renin inhibitor Aliskiren does not readily cross the blood brain barrier, with its highest concentration observed in the liver and kidney when administrated systematically (Assessment Report for Rasilez HCT, European Medicines Agency, EMEA/CHMP/575457/2008). Even if Aliskiren can be internalized by neonatal rat ventricular myocytes (NRVM)[226], there is no literature indicating that it could be taken up by the circumventricular organs (CVOs) or neuronal cells.

For years, the function of brain renin has been difficult to dissect, mostly due to its low expression level and the presence of alternative enzymes, such as tonin[227], capable of processing angiotensinogen into angiotensin peptides in the central nervous system. In addition, effects from the kallikrein-kinin (KKS) system may also account for the central modulation of blood pressure[228]. However, studies from transgenic mice overexpressing both human renin and human angiotensinogen in the brain suggest that

renin-induced angiotensinogen cleavage in the brain is still critical for blood pressure regulation[23]. Moreover, we have demonstrated co-localization of endogenous renin and angiotensinogen promoter activities in cardiovascular control nuclei in the brain using reporter genes[102]. To address the importance of endogenous brain renin, we have taken advantage of the Cre-LoxP system to generate floxed sRen model on C57BL/6J background. Not only has this sRen flox model allowed us to investigate the role of renin in the brain in this study, it may also serve as a useful tool to study renin function in other peripheral tissues in the future.

In summary, the mice models we presented in this report provide further insight into the function of the brain RAS. To directly pinpoint the role of icRen, we are currently developing an icRen specific knockout model to compare and contrast with these sRen brain-specific knockout lines.

Figure 36. *Breeding Strategy of Neuronal- and Glial-specific Knockouts*

Nestin- or GFAP-Cre transgenic mice on the C57B6L/J background (Cre+) were crossed with homozygous sRen flox mice (F/F) in the first-generation breeding.F/+ Cre+ mice were subsequently backcrossed with F/F mice again in the second-generation breeding, to generate F/F Cre+ and F/F Cre- mice.

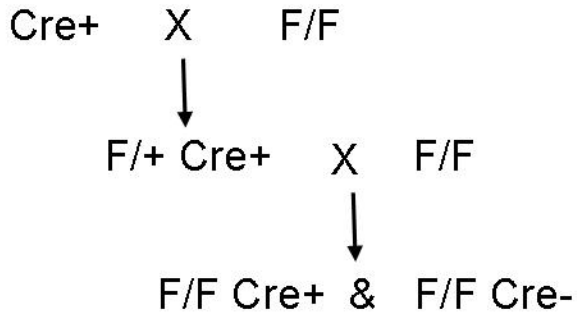
Cre+ X F/F
F/+ Cre+ X F/F
F/F Cre+ & F/F Cre-

Figure 37. *Genomic DNA Amplification to Examine Nestin-Cre and GFAP-Cre Tissue Specificity.*

Brain and kidney genomic DNA was PCR amplified to examine the activity of GFAP-Cre and Nestin-Cre. For both lines, F/F Cre+ and F/F Cre- adult animals are compared. For the top and middle panels, the same primer set was used. The top band indicates the flox allele, whereas bottom band is a result of Cre-induced recombination (null band). For the bottom panel, a different primer set was used to detect the flox band only. ddH_2O was used as a negative control with PCR reagents from the same master mix.

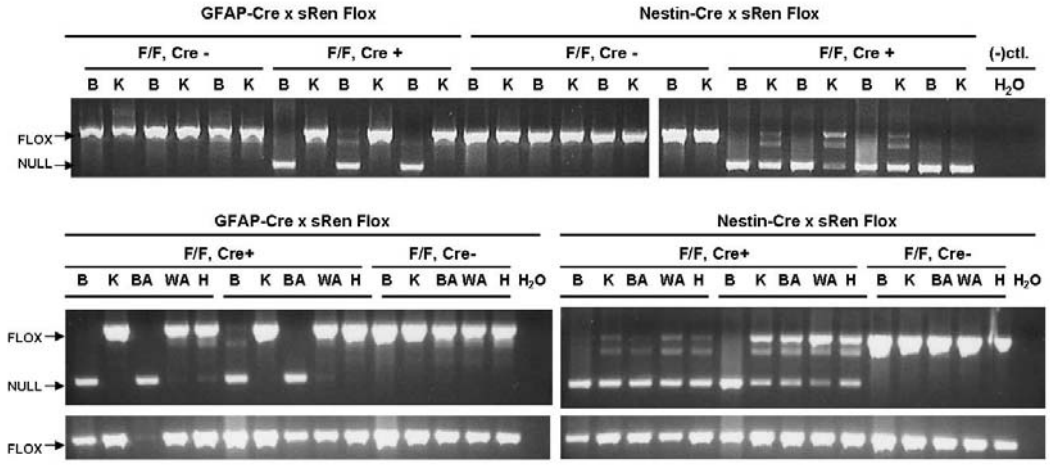
GFAP-Cre x sRen Flox
Nestin-Cre x sRen Flox
F/F, Cre -
F/F, Cre +
F/F, Cre -
F/F, Cre +
(-)ctl.
B K B K B K B K B K B K B K B K B K B K B K B K B K B K H2O
FLOX
NULL
GFAP-Cre x sRen Flox
Nestin-Cre x sRen Flox
F/F, Cre+
F/F, Cre-
F/F, Cre+
F/F, Cre-
B K BA WA H B K BA WA H B K BA WA H H2O
B K BA WA H B K BA WA H B K BA WA H H2O
FLOX
NULL
FLOX

Figure 38. *Immunohistochemistry to Test Nestin-Cre Cell-type Specificity.*

β-gal expression was examined by immunostaining in red. NeuN staining in green serves as a neuronal marker. For Nestin-Cre x ROSA, β-gal colocalizes with NeuN in Cre+, ROSA+, whereas there is no β-gal staining in Cre-, ROSA+.

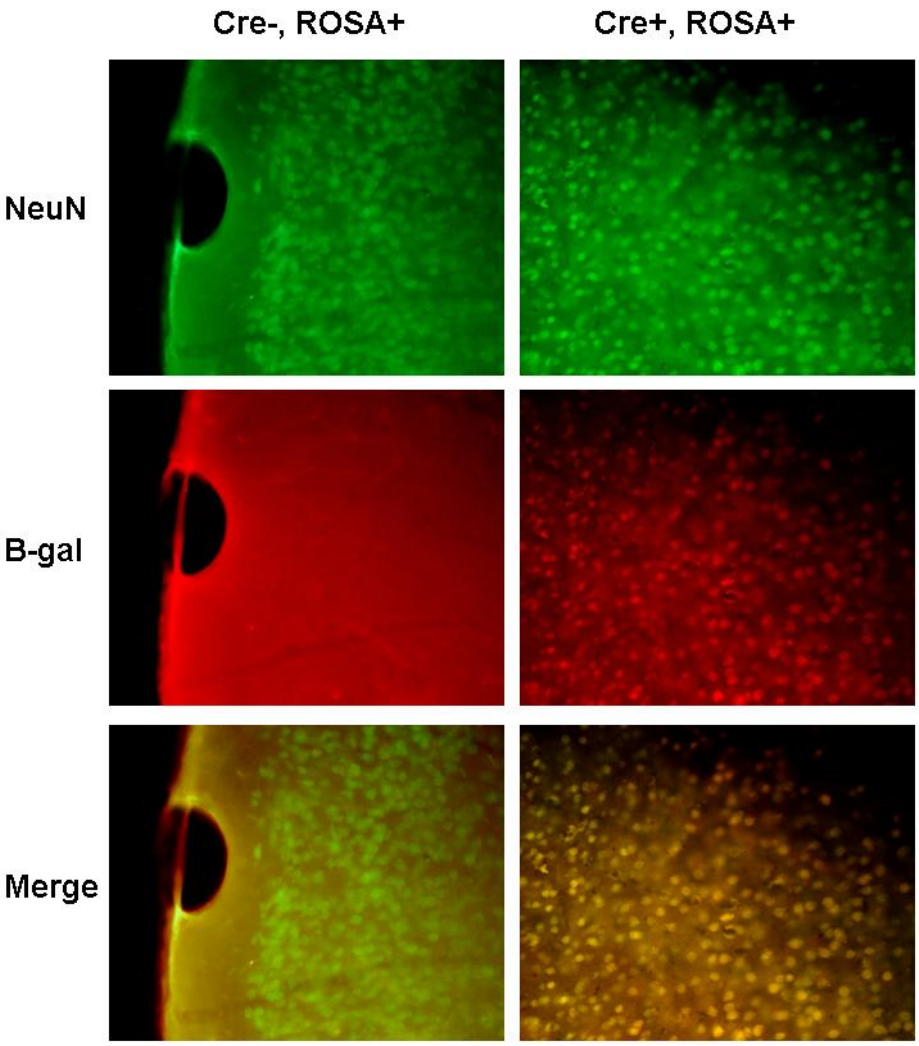
Cre-, ROSA+
Cre+, ROSA+
NeuN
B-gal
Merge

Figure 39. *RT-PCR to Examine Renal sRen Expression.*

mRNA levels of sRen were compared in kidneys of adult F/F Cre+ and F/F Cre- animals from both GFAP and Nestin lines. Renal sRen expression is not affected by neuronal (as indicated in Nestin animals) or glial-specific deletion (as displayed in GFAP samples) of sRen. GAPDH serves as an internal control.

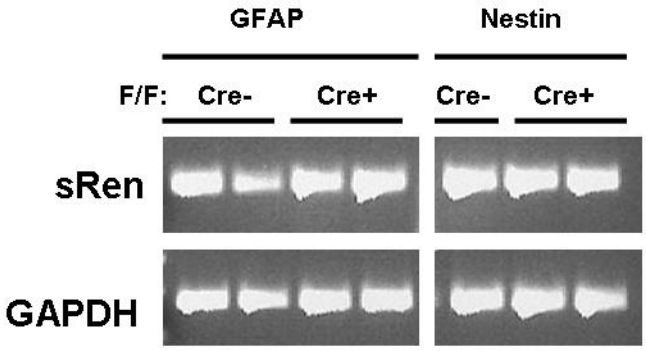
GFAP
Nestin
F/F:
Cre-
Cre+
Cre-
Cre+
sRen
GAPDH

Figure 40. *Immunohistochemistry to Study Renal sRen Levels.*

Protein levels of sRen were investigated in the kidneys of F/F Cre+ and F/F Cre- adult animals using immunohistochemistry. Brown staining represents renin immunoreactivity. Blue staining is smooth muscle actin immunoreactivity. The left collum of Figure 40A is staining from kidneys of F/F Cre- (Nestin), while the right collum of the same figure is staining from kidneys of F/F Cre+ (Nestin). For the glial-specific sRen knockouts, the left half of Figure 40B is GFAP-Cre-, while the right half is GFAP-Cre+. For both GFAP and Nestin lines, there is no difference with regard to renin protein level and expression pattern.

Figure 40A

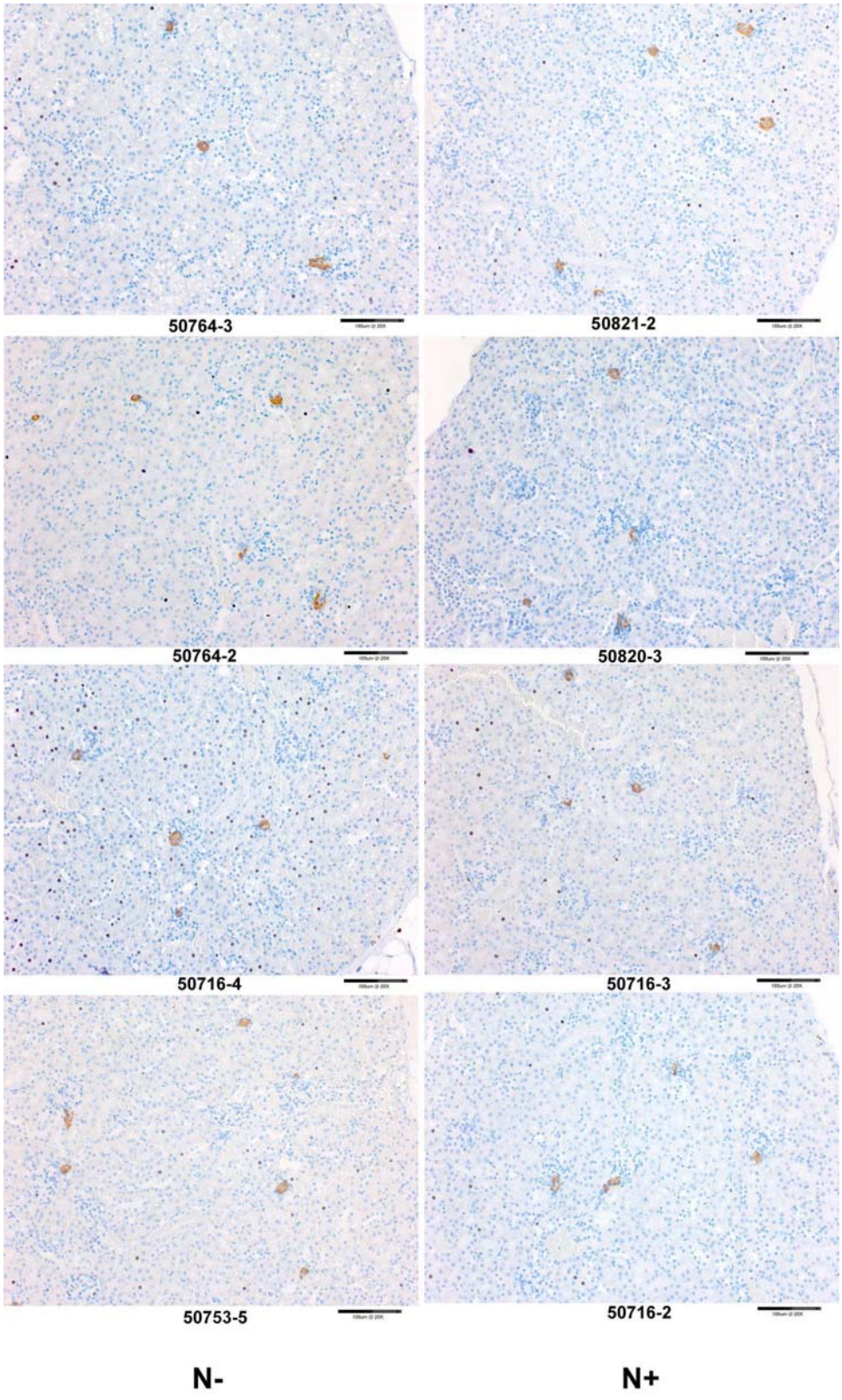
50764-3
50821-2
50764-2
50820-3
50716-4
50716-3
50753-5
50716-2
N-
N+

Figure 40B (Figure 40 Continued)

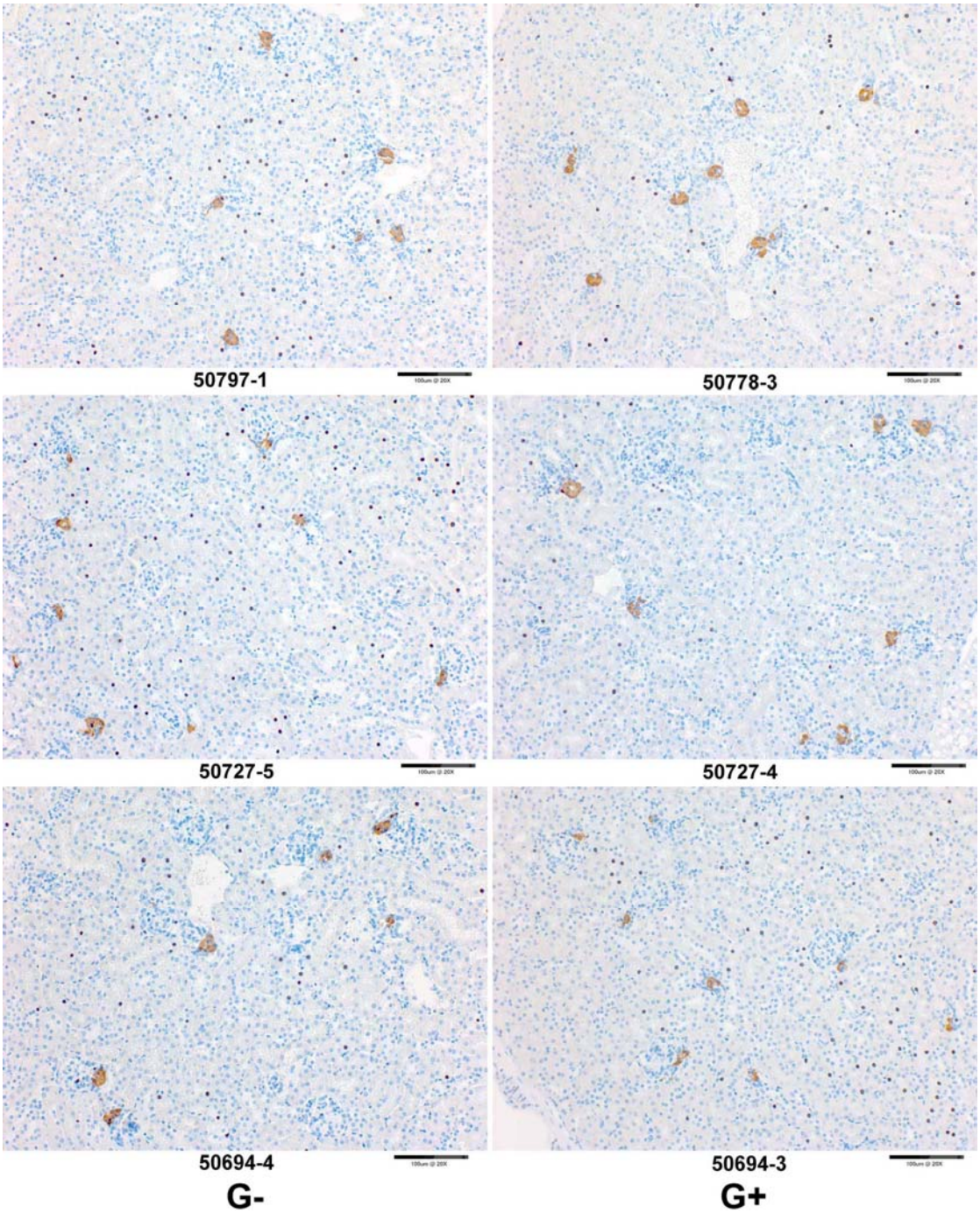

Figure 41. *24hr-Tracking of Averaged MAP Over 10 days.*

Mean arterial blood pressure was recorded using radiotelemetry in Nestin-Cre- or GFAP-Cre-induced sRen knockouts (2~3-month-old). The open bar in X axis represents day time (6am-6pm), while the black bar indicates night time (6pm-6am). Knockouts and controls from both lines exhibited normal circadian rhythm (lower blood pressure during the day and higher blood pressure during the night). There is no difference in mean arterial blood pressure between the knockouts and the controls at each time point.

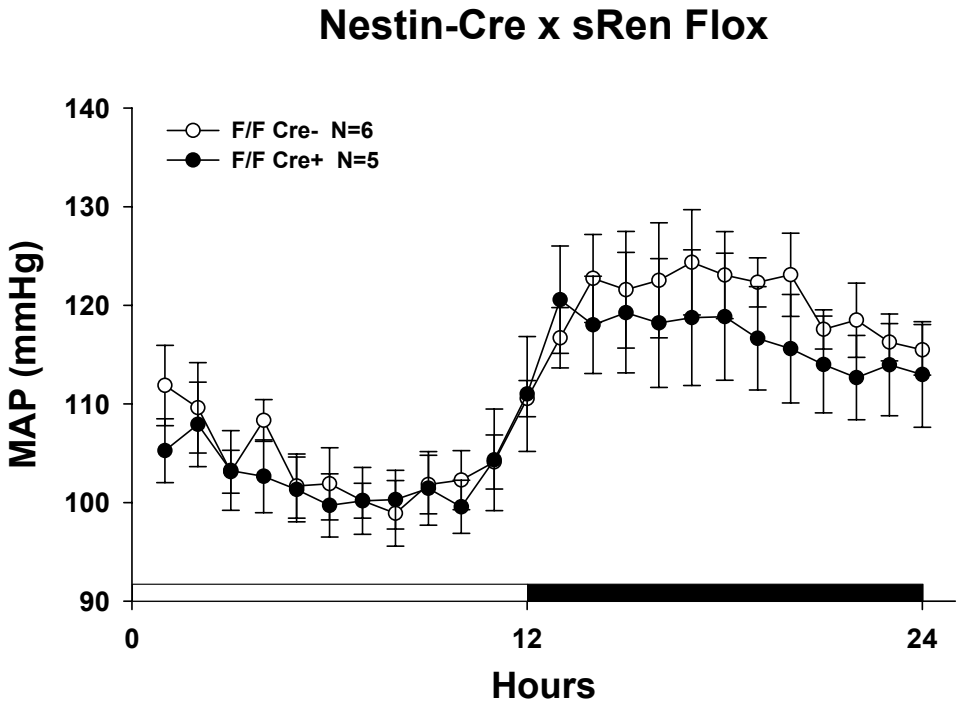
Nestin-Cre x sRen Flox
F/F Cre- N=6
F/F Cre+ N=5
MAP (mmHg)
140
130
120
110
100
90
0
12
24
Hours

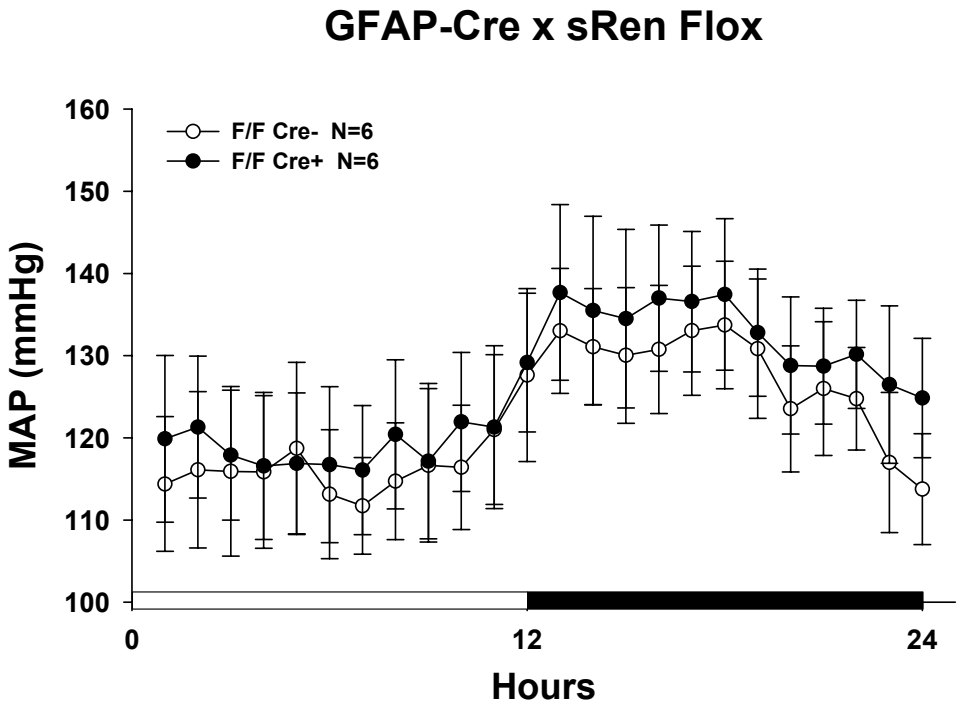
GFAP-Cre x sRen Flox
F/F Cre- N=6
F/F Cre+ N=6
MAP (mmHg)
160
150
140
130
120
110
100
0
12
24
Hours

Figure 42. *Day and Night Averaged MAP and HR Over 10 days.*

Mean arterial blood pressure and heart rate were recorded using radiotelemetry in 2 to 3-month-old knockout and control mice. 10-day average of MAP (day and night) and 10-day summary of HR (day and night) were plotted. The bar graphs demonstrate that there is no significant differences in baseline mean arterial blood pressure and heart rate between F/F Cre+ and F/F Cre- animals (Nestin: Cre+ n=5, Cre- n=6; GFAP: Cre+ n=6, Cre- n=6).

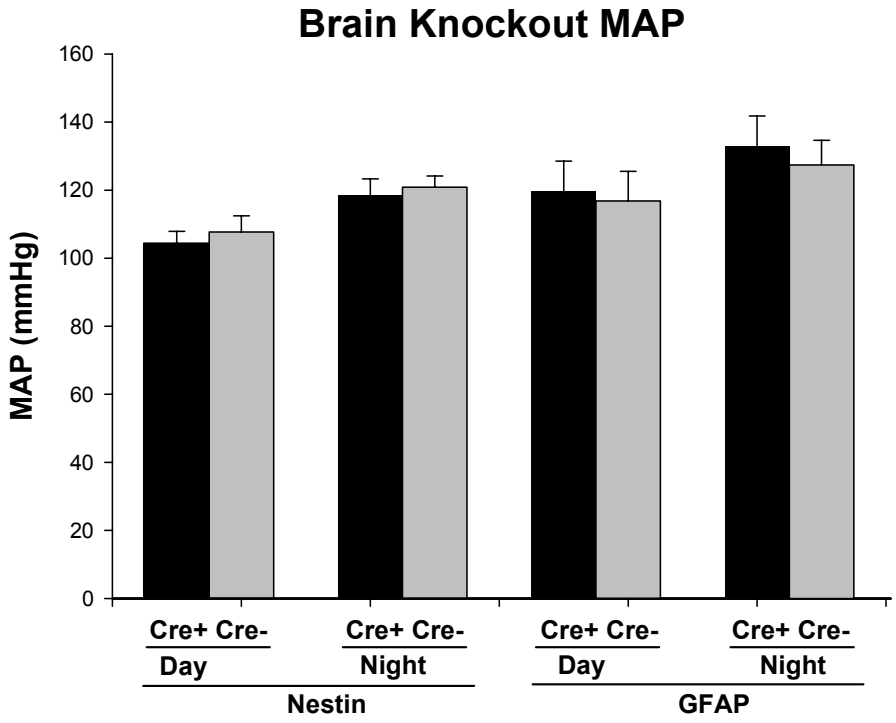
Brain Knockout MAP
MAP (mmHg)
160
140
120
100
80
60
40
20
0
Cre+ Cre-
Day
Cre+ Cre-
Night
Cre+ Cre-
Day
Cre+ Cre-
Night
Nestin
GFAP

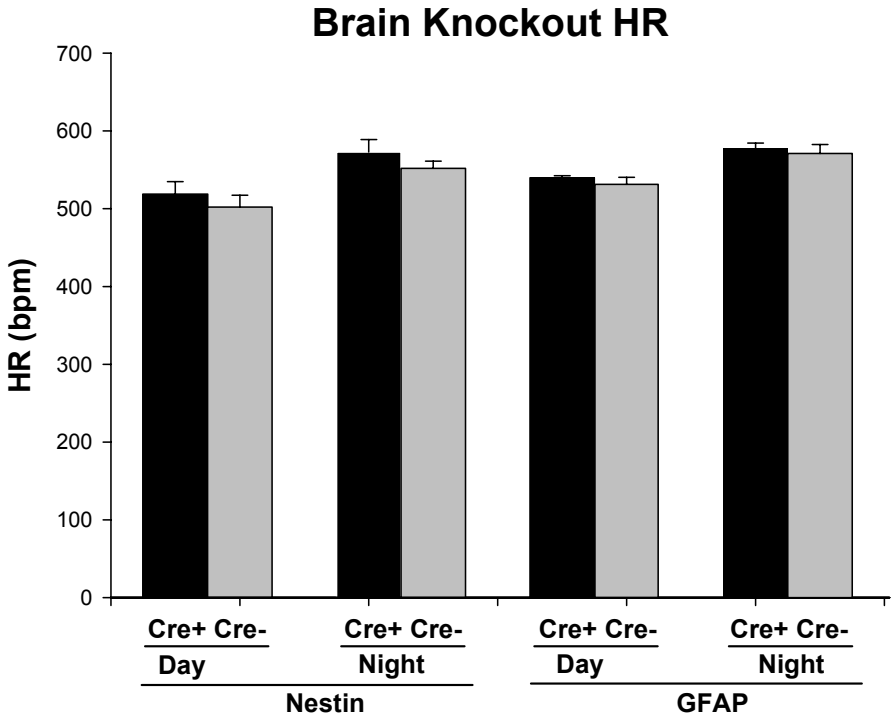
Brain Knockout HR
HR (bpm)
700
600
500
400
300
200
100
0
Cre+ Cre-
Day
Cre+ Cre-
Night
Cre+ Cre-
Day
Cre+ Cre-
Night
Nestin
GFAP

Figure 43. *Resting Oxygen Consumption and Respiratory Quotient (RQ).*

We do not detect a difference in O_2 consumption for either Nestin (n=7 each genotype) or GFAP (n=11 each genotype) lines (2 to 3-month-old). As a comparison, there is also no difference in O_2 consumption in sRen global knockouts (n=8 each genotype). There is no difference in RQ of the GFAP line, but the Nestin line displayed dropped RQ value in F/F Cre+ animals. There is no change in RQ in sRen global knockouts.

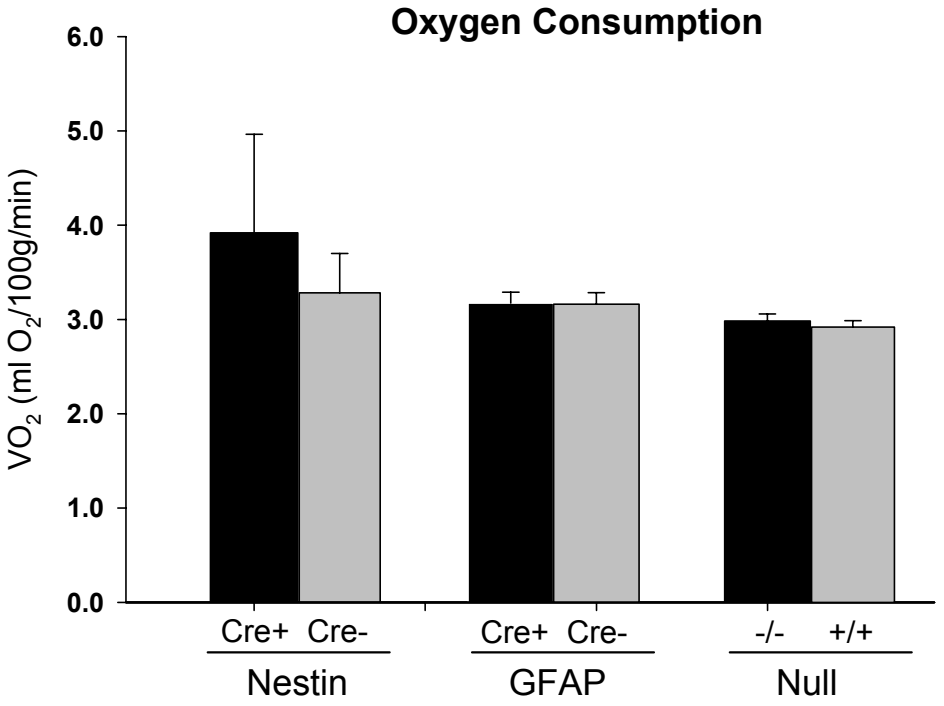
Oxygen Consumption
6.0
5.0
4.0
3.0
2.0
1.0
0.0
VO2 (ml O2/100g/min)
Cre+ Cre-
Cre+ Cre-
-/- +/+
Nestin
GFAP
Null

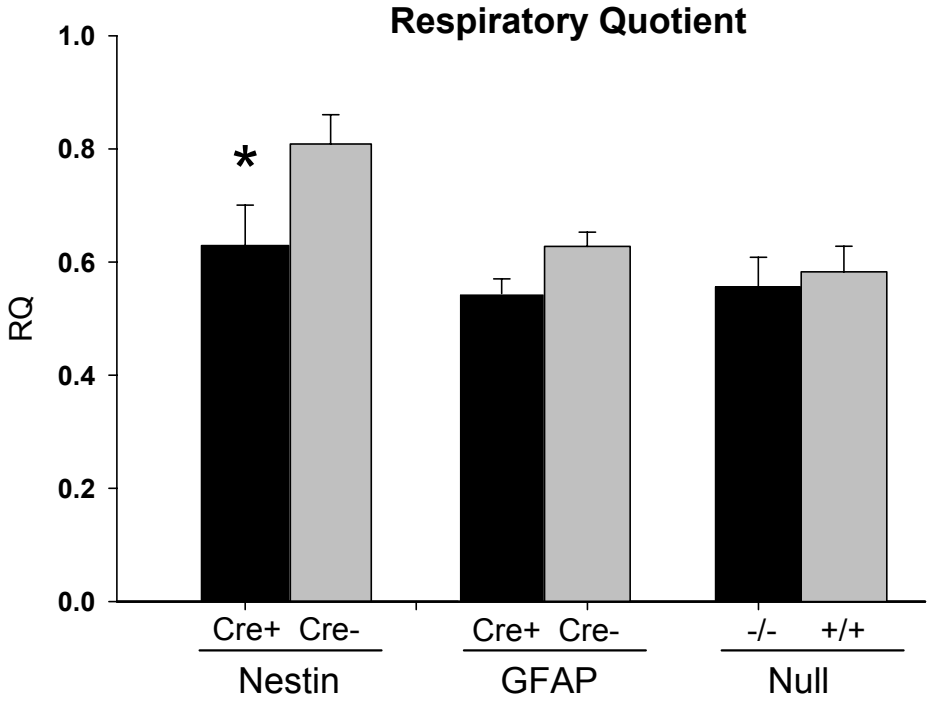
Respiratory Quotient
1.0
0.8
0.6
0.4
0.2
0.0
RQ
*
Cre+ Cre-
Cre+ Cre-
-/- +/+
Nestin
GFAP
Null

Figure 44. *Metabolic Studies.*

Metabolic cage studies from the Nestin line (F/F Cre+ n=8. F/F Cre- n=8) and GFAP line (F/F Cre+ n=6. F/F Cre- n=6) indicate no statistically significant difference in food intake, fecal output, water intake, saline intake, total fluid consumption, urinary output, saline (0.15M NaCl) preference and sodium intake. There is a trend of increased water and saline input, salt intake and urinary output in sRen global knockouts (2~3-month-old, -/- n=4. +/+ n=4).

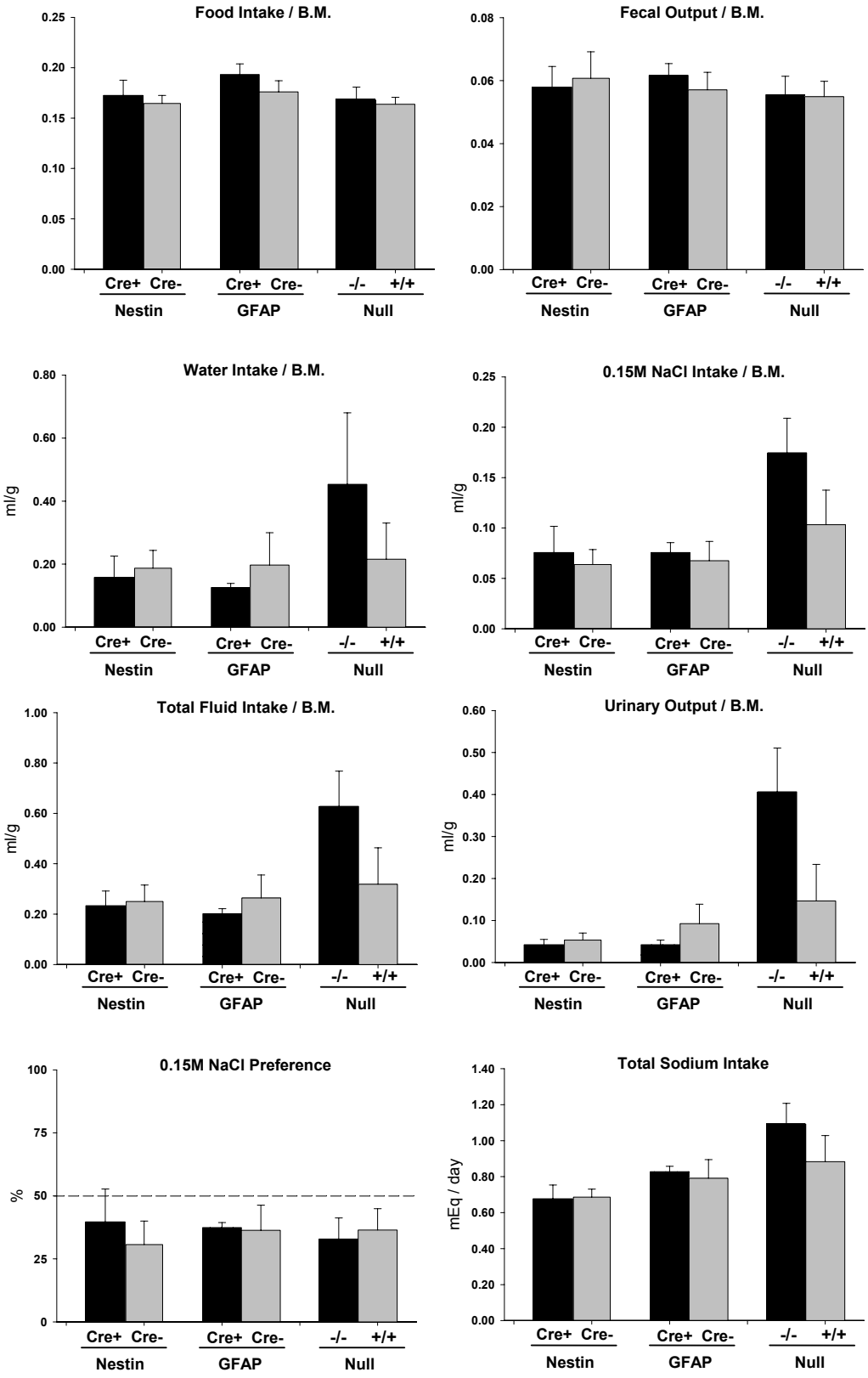
Food Intake / B.M.
0.25
0.20
0.15
0.10
0.05
0.00
Cre+ Cre-
Cre+ Cre-
-/- +/+
Nestin
GFAP
Null
Fecal Output / B.M.
0.08
0.06
0.04
0.02
0.00
Cre+ Cre-
Cre+ Cre-
-/- +/+
Nestin
GFAP
Null
Water Intake / B.M.
ml/g
0.80
0.60
0.40
0.20
0.00
Cre+ Cre-
Cre+ Cre-
-/- +/+
Nestin
GFAP
Null
0.15M NaCl Intake / B.M.
ml/g
0.25
0.20
0.15
0.10
0.05
0.00
Cre+ Cre-
Cre+ Cre-
-/- +/+
Nestin
GFAP
Null
Total Fluid Intake / B.M.
ml/g
1.00
0.80
0.60
0.40
0.20
0.00
Cre+ Cre-
Cre+ Cre-
-/- +/+
Nestin
GFAP
Null
Urinary Output / B.M.
ml/g
0.60
0.50
0.40
0.30
0.20
0.10
0.00
Cre+ Cre-
Cre+ Cre-
-/- +/+
Nestin
GFAP
Null
0.15M NaCl Preference
%
100
75
50
25
0
Cre+ Cre-
Cre+ Cre-
-/- +/+
Nestin
GFAP
Null
Total Sodium Intake
mEq / day
1.40
1.20
1.00
0.80
0.60
0.40
0.20
0.00
Cre+ Cre-
Cre+ Cre-
-/- +/+
Nestin
GFAP
Null

Figure 45. *Adipose Tissue Weights.*

F/F Cre+ (5-month-old) from the Nestin line exhibited increased brown adipose and white adipose components after normalized to body weight, while their total weight and body size remain the same as F/F Cre- controls. This is partially due to contribution from the Nestin-Cre transgene. As for the GFAP line (5-month-old), there is no detectable change in brow adipose, white adipose mass and body weight. The sRen global knockout exhibited significant decrease in white adipose and body mass.

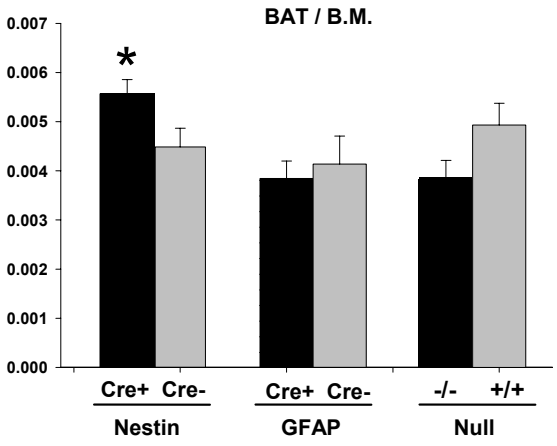
BAT / B.M.
0.007
0.006
0.005
0.004
0.003
0.002
0.001
0.000
*
Cre+ Cre-
Nestin
Cre+ Cre-
GFAP
-/- +/+
Null

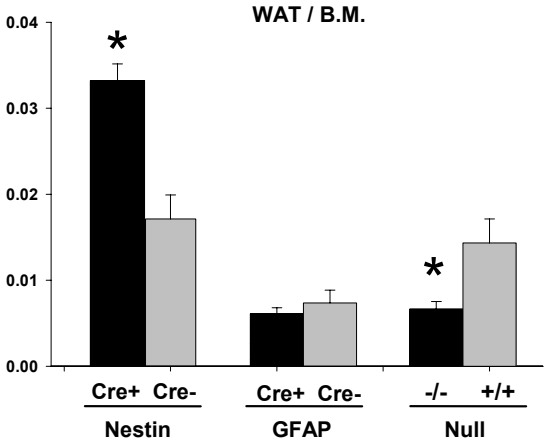
WAT / B.M.
0.04
0.03
0.02
0.01
0.00
*
*
Cre+ Cre-
Nestin
Cre+ Cre-
GFAP
-/- +/+
Null

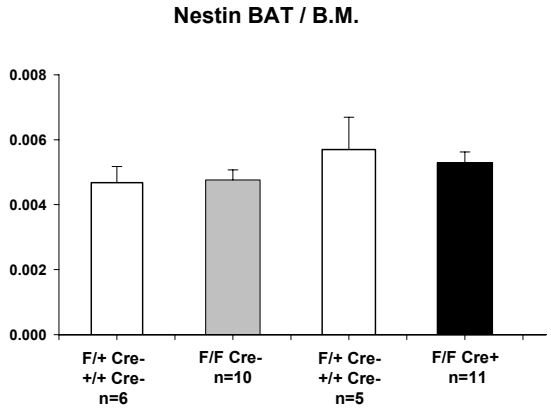
Nestin BAT / B.M.
0.008
0.006
0.004
0.002
0.000
F/+ Cre-
+/+ Cre-
n=6
F/F Cre-
n=10
F/+ Cre-
+/+ Cre-
n=5
F/F Cre+
n=11

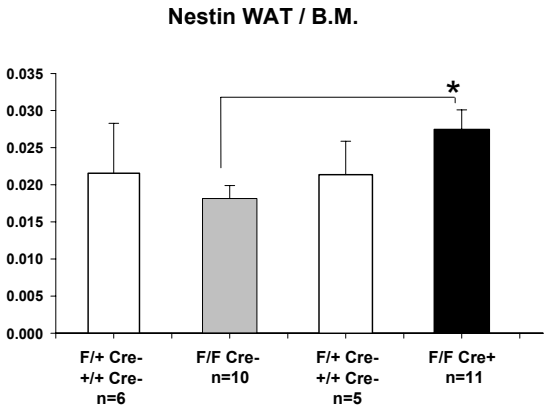
Nestin WAT / B.M.
0.035
0.030
0.025
0.020
0.015
0.010
0.005
0.000
*
F/+ Cre-
+/+ Cre-
n=6
F/F Cre-
n=10
F/+ Cre-
+/+ Cre-
n=5
F/F Cre+
n=11

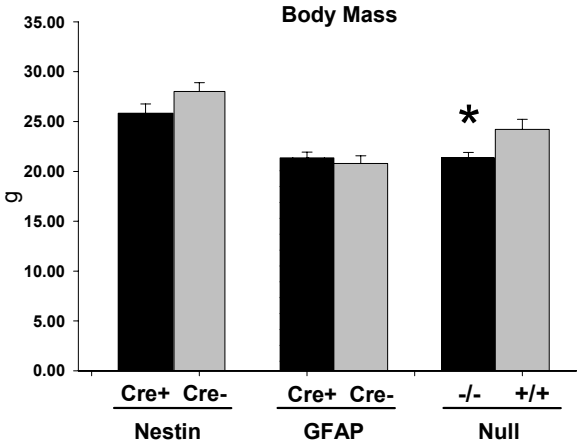
Body Mass
35.00
30.00
25.00
20.00
15.00
10.00
5.00
0.00
g
*
Cre+ Cre-
Nestin
Cre+ Cre-
GFAP
-/- +/+
Null

CHAPTER 5

GENERAL DISCUSSION

Overall Hypothesis

The aim of my dissertation study was to investigate the role of renin isoforms (secreted vs. intracellular) in blood pressure regulation, control of water/electrolyte homeostasis and baseline metabolism. A further goal was to distinguish the functions of sRen vs. icRen within the central nervous system. Based on a large body of aforementioned literature, we hypothesized that sRen and icRen in the brain play differential roles in the central regulation of blood pressure. Either of the renin isoforms, or both of them, may be responsible for generating nerve-activating angiotensin peptides. sRen could potentially process glial-secreted angiotensinogen into angiotensin in the extracellular space between neurons and astrocytes. Subsequently, angiotensin may bind to its receptors in neuronal plasma membranes and activate signaling transduction pathways in neurons. These signaling cascades are potentially involved in neuronal or glial cell proliferation and differentiation[113]. These signaling pathways may also act as neuromodulators. For example, overexpression of AT1R specifically in neurons in the brain leads to increased water and sodium intake[233], as well as increased cardiovascular sensitivity to ICV administration of Ang-II (ligand for AT1R) or losartan (AT1R blocker)[234]. Another possible working mechanism is that icRen cleaves angiotensinogen, mostly likely of neuronal origin, and produces angiotensin peptides in the cytoplasm of neurons. As a result, intracellular angiotensin peptides then exert their function as neurotransmitters to promote or inhibit nerve firing in certain nuclei of the brain and to impact sympathetic outflow, hormone release, and fluid/electrolyte balance.

Evidence to Support General Hypotheses

Our hypotheses that sRen and icRen in the CNS are important for cardiovascular regulation have been supported by expression studies, which demonstrate the existence of all the elements of the RAS within the central nervous system. It has been shown that angiotensin converting enzymes (ACE[235] and ACE2[236]) are ubiquitously expressed in the brain. Given that I have reviewed the RAS in detail in the introduction chapter, herein I will briefly summarize major findings that have brought us to this project. First, we have identified co-localization of angiotensinogen and renin promoter activities in cardiovascular regulatory regions of the brain[102]. It is now accepted that angiotensinogen has a wider expression pattern than that of renin. We have reported that angiotensinogen is mainly synthesized in glial cells throughout the brain, and in some neuronal cells in certain cardiovascular-control nuclei, whereas renin is more strictly expressed in neurons in certain cardiovascular nuclei. In addition, we have shown that sRen and icRen are endogenously expressed in the brain using RT-PCRs in wild type and sRen knockout fetuses and adults[175]. Moreover, functional studies suggest that overexpression of either sRen or icRen leads to increased mean arterial blood pressure[22]. Therefore, it is necessary to utilize isoform-specific knockouts to pinpoint the function of sRen and icRen in the brain.

Development of sRen and icRen Knockout Models

The first half of my dissertation research was to establish genetic mouse models to study the central regulation of cardiovascular function and fluid balance. This would set the stage for various molecular and physiological characterizations to better understand the role of the central RAS in the regulation of blood pressure. The two major models I have been working on were sRen-flox and icRen-flox. These are C57BL/6J mouse models engineered with two identical LoxP sites at the *mRen1*^{c} locus, thus allowing conditional knockout of either isoform using Cre recombinase. After several

generations of breeding, we have successfully developed global sRen knockout and neuronal-/glial-specific sRen knockouts from the sRen-flox model. At the same time, we have been in the process of generating icRen-flox mice. We have obtained correctly targeted ES cells and chimeras with either the (ATG-GCG) mutation or wild type for this codon. Unfortunately, we have encountered difficulties in the process of obtaining germline-transmitted progeny from chimeras. We are continuing to generate new ES clones and chimeras in order to obtain icRen-flox founder mice.

Physiological Roles of sRen vs. icRen

From my dissertation research, we have found for the first time that sRen and icRen have distinguishable roles with regard to blood pressure regulation. We have learned that sRen secreted from the kidney is a crucial component for survival. Similar to other RAS knockouts, the global sRen knockout exhibited less than a 10% survival rate. Given that sRen accounts for more than 99% of total renin in the kidney (unpublished data), depletion of sRen leads to severe renal atrophy, possibly due to the lack of renal Ang-II or systemic Ang-II. Moreover, given that peripheral Ang-II plays an important role in cell proliferation and differentiation during development, and that mouse kidney development has a critical window of two weeks right after birth, the reduction of Ang-II level in the kidney most likely interferes with kidney development. This is in line with what we observed histologically. We have found that sRen knockout (-/-) newborns displayed normal renal morphology, whereas 2-3 months old sRen knockout (-/-) adults showed severe renal atrophy.

Besides renal damage, another striking phenotype we have observed with sRen knockout is hypotension. The chronic 20 mmHg blood pressure decrease could be the result of attenuated renal and/or global RAS activity. From the studies from Crowley S.D. *et. al*, we know that removal of renal AT1R is able to cause decreased blood pressure[30], supporting a contribution of the renal RAS to mean arterial blood pressure regulation.

On the other hand, it has been well acknowledged that circulating RAS is also important for blood pressure regulation[30]. In fact, we have identified vascular dysfunction in this model, for instance, blunted aortic contraction upon serotonin treatment when examined *ex vivo*. This is possibly due to the lack of circulating Ang-II to elicit responses through AT1R in vascular smooth muscle cells[237]. Thus, blood vessels have diminished ability to generate the appropriate level of constriction to respond to the decreased level of blood pressure. Taken together, it is likely that the declined mean arterial blood pressure in sRen knockout is the result of a reduction in vascular reactivity, renal damage, and loss of major portion of Ang-II, which leads to loss of sodium concentration ability and blunted sympathetic activity. Hypotension and renal defects could act synergistically to cause lethality.

It is interesting to note that although sRen global knockouts exhibited decreased mean arterial blood pressure, they did not display any detectable alterations in heart rate. Potential mechanisms to explain this phenomenon include that the loss of sRen (instead of both sRen and icRen) from the brain is not sufficient to result in decreased sympathetic output. We know that sympathetic output from the brain plays an important role in the control of heart rate. Given that in the sRen global knockout model, the icRen expression is not changed (as far as we can detect at mRNA level), the heart rate data indirectly supports the function of icRen in the control of heart rate, possibly by generating intracellular angiotensin as a neurotransmitter to maintain normal sympathetic outflow.

Other phenotypes we have observed in this sRen knockout model include decreased body mass and white adipose mass when compared to littermate controls. The mechanism behind the change in body composition could involve either interference with the brain RAS or hindered peripheral RAS function, or both. Interestingly, we found similar metabolic phenotypes in DOCA-salt treated wild-type mice as well as in an overexpression model (referred as sRA mice) of hyperactive brain

RAS (unpublished data). DOCA-salt treated mice are known to have a hyperactive brain RAS, as when RAS blockers (e.g. ACE inhibitor captopril or AT1R blocker losartan) are administered via ICV (intracerebrolventricular) injection, the hypertension phenotype could be prevented and reversed[21,96-98]. The sRA model expresses a human renin transgene under a brain-specific synapsin promoter, and a human angiotensinogen transgene under the control of its endogenous promoter. Due to the species-specificity of the cleavage of angiotensinogen by renin, sRA mice only have overexpression of RAS in the brain. Despite the difference between the sRen global knockout and DOCA/sRA mice with regard to the brain RAS (depletion of brain RAS vs. hyperactive brain RAS), all three models share one important similarity, that is suppressed peripheral RAS (that is low circulating renin and Ang-II). At this point, one hypothesis is that the lean phenotype does not appear to be a brain-specific effect. Instead, it seems to be a result of a suppressed peripheral RAS. In fact, in support of this, it has been reported that a series of global RAS knockouts have shown alterations in body mass and adipose deposition[172,182,208-211]. Interestingly, however, in contrast to the animal models with suppressed peripheral RAS, Cassis *et al.* have shown that chronic peripheral infusion of Ang-II leads to a decrease in body weight that is independent of blood pressure, but primarily driven by decreased food intake[238]. The discrepancy could arise from the different species used (mouse for suppressed RAS studies vs. rat for chronic Ang-II infusion), or the change in brain RAS (hyperactive brain RAS / RAS knockout vs. no presumed change in brain RAS in the chronic Ang-II infusion study). Furthermore, Poter *et al.* have reported that ICV injection of Ang-II was able to prevent weight gain in both young and adult rats[188,189]. Based on the above studies including the investigation of sRen global knockouts, we speculate that the brain RAS likely interacts with the peripheral RAS to regulate body composition and metabolism. This indirectly suggests that icRen may be a key regulator in adipose metabolism. On the other hand, we cannot exclude the possibility that the lean phenotype in these aforementioned animal models

is a secondary effect of animals suffering from cardiovascular and/or renal defects. For example, most of the homozygous sRen knockout did not survive till weanling. We had to carry on daily saline (0.9% NaCl) injections into neonatal newborns to help them survive the first two weeks. Presumably, the cardiovascular and renal defects in the sRen global knockouts could lead to metabolic changes. One of the metabolic parameters is food intake. We have measured food intake and fecal output of the sRen knockout as compared to those of littermate controls; however, there was no difference between knockouts and wild types. An additional metabolic parameter that could be measured with radiotelemetry is locomotor activity. A third end point would be oxygen consumption, as a marker for basal metabolic rate. There was no difference in O_2 consumed between sRen global knockouts and wild type animals.

We have also observed trends for increased water intake, sodium intake and urinary output in sRen global knockouts. These are most likely physiological responses to renal dysfunction, or more specifically, failure to concentrate urine and retain water. Given the importance of renal renin in fluid/electrolyte balance, lack of sRen from both brain and kidney most likely masks any role of icRen in the brain on hydromineral phenotypes in this model. Even though sRen plays dominant roles in the phenotypes we have observed in this model, and that the other isoform, icRen, is probably not adequate to compensate for the loss of sRen, one cannot exclude the possibility that icRen is also important in specific tissues to mediate certain physiological responses. For instance, icRen has been detected in the heart[164] and adrenal gland[165,166] in several independent studies. We know from mRNA expression studies that icRen is the major form of total renin in the adult mouse brain. As total renin in the brain is expressed at very low levels[239], this makes it challenging to dissect the role of brain icRen. Moreover, icRen share all its amino acid sequences with sRen, lacking only the N-terminal of sRen. This adds to the difficulty to distinguish icRen from sRen at the protein level. Since the function of icRen is masked under the lethal phenotype, it is possible that icRen is

balancing cardiovascular output in a very dedicated way when the system is under pathophysiological conditions.

Molecular Study of the Mouse Renin Gene

In addition to physiological alterations that we have observed, the sRen knockout model has been very useful to provide molecular information with regard to the transcriptional regulation of sRen vs. icRen. We learned for the first time that icRen is independently transcribed using unknown regulatory elements, and that the expression of icRen is not affected by the presence or absence of the classic promoter. It is very likely that icRen uses sequences neighboring exon 1b, the novel first exon, to mediate expression. To examine this, we have designed promoter-bashing experiments at both human and mouse intracellular renin loci. Given that sequence analysis upstream of mouse exon1b using bioinformatic approaches has revealed a potential CCAAT box at -50 and that there is no typical TATA box around this region, in an experiment to locate the mouse icRen promoter, we PCR-amplified and cloned continuous regions varying from 300bp up to 1.1 kb upstream of exon 1b all the way to 3' end of exon1a (Figure 54) into firefly luciferase reporter plasmids and transected them into mouse neuronal cell lines (Neuro2a and GT1-7). Unfortunately, we have not identified any distinguishable promoter activity in this region. Simultaneously, we performed similar assays to identify the human icRen promoter. Since human exon1b is upstream of the classic human exon1a (Figure 55), we have examined promoter activity with fragments upstream of exon1b from 2Kb to 10kb. Again we did not detect significant promoter activity as indicated by the firefly luciferase/renilla ratio. It is likely that there might be a mix of activating and inhibitory cis-regulatory elements in the fragments tested. If we have had a neutralizing effect of positive and negative-reacting sequences in one fragment tested for promoter activity, it is likely that we are not going to have a clear readout with regard to luciferase activity. It is also possible that the cis-

regulatory element of icRen is downstream of exon 1b, though we have not yet investigated this possibility.

Studies from the sRen global knockout have supported the existence of icRen in the brain. It becomes very intriguing to consider where, and how, icRen could be synthesized and packaged to exert its function to cleave angiotensinogen intracellularly. Since the level of icRen is low in the brain and its expression pattern is dispersed in some neuronal cells but not necessarily in all neurons of the cardiovascular control regions (implicated by unpublished data from Dr. Gomez's laboratory), it is not practical to perform immunostaining on brain sections. Therefore, we have utilized the strategy of developing fusion proteins of sRen vs. icRen tagged with DsRed vs. EGFP. Although we have had success in transfections with parent plasmids (DsRed or EGFP only), the transfection with any of the fusion proteins did not succeed. We have carefully examined all cloned coding sequences and junctions, and made sure the fusion proteins were in-frame. Since the failure in fusion protein expression is not likely to be a result of frame-shift mutation, it could probably be because of misfolding of renin fusions and eventually the degradation of fusion proteins by cellular machinery. One of the future experiments we could carry out would be to transfect cells with the same fusion plasmids, in the presence of proteasomal inhibitors[240,241].

Cell Type-specific Functions of sRen vs. icRen

In addition to the sRen global knockout, we have also established two cell type-specific knockout models of sRen. Immunohistological data have provided evidence in support of the tissue-specificity of Nestin-Cre[212] and GFAP-Cre[213] in the central nervous system. In the brain of Nestin-Cre-induced sRen knockouts, mainly neuronal sRen is depleted (unpublished data from our group), while in the brain of GFAP-Cre-elicited sRen knockout, mostly glial sRen is abolished. However, although in both models we have demonstrated that sRen is deleted, as suggested by a null band after Cre-induced

recombination, we did not detect any overt phenotype changes at baseline levels with the lack of sRen in either model. This is consistent with our hypothesis that icRen in the adult brain is the renin isoform most important in mediating cardiovascular functions. We have examined blood pressure and heart rate via radiotelemetry, and electrolyte/fluid balance via metabolic cages. Even though we see alterations of these endpoints in global sRen knockouts, we did not observe any changes with either neuronal or glial-specific sRen knockout. This suggests that brain icRen, or peripheral sRen, or both, are important for cardiovascular and mineral balance. One may argue against the idea that icRen is important because icRen is also present, but insufficient to normalize these physiological endpoints in the sRen global knockouts, but we speculate that since icRen is expressed at a very low level in the brain, the effect caused by loss of peripheral sRen may be overwhelming and thus mask the functions of icRen. Furthermore, we have examined basal metabolic rate by comparing oxygen consumption between brain knockouts and their littermate controls. We have also investigated body mass, body length, brown and white adipose masses, heart weight between neuronal or glial knockouts and their matching littermate controls. There was no difference in any of these parameters. There was a slight contribution of the Nestin-Cre transgene to the increased brown adipose in F/F Cre+ of neuronal sRen knockouts, which complicates the analysis of the impact of sRen neuronal knockout on adiposity. Therefore, it is difficult to evaluate the contribution of the sRen allele alone on body composition.

In addition to the potential homeostatic control mechanisms involving icRen, we cannot exclude the possibility that there may be compensation between neuronal and glial sRen. Therefore, deletion of sRen in either one of the cell types is not adequate to result in any physiological changes at baseline. Indeed, since sRen is secreted, preservation of glial sRen in mice with deficient neuronal sRen could still provide sufficient extracellular renin for cleavage of angiotensinogen. The same argument can

be made for preservation of neuronal sRen in mice lacking glial sRen. Another possible reason for normal phenotypes upon either neuronal or glial depletion of sRen is the compensation from circulating sRen. Indeed, there are regions of the brain, which are important for blood pressure regulation, which lie outside of the blood brain barrier. These circumventricular organs (such as the SFO) have access to the circulation through the blood supply and cerebrospinal fluid. We know that loss of Ang-II production and action in the SFO has profound effects on blood pressure and electrolyte handling[125]. Consequently, angiotensinogen produced in the SFO may be cleaved by renin present which gains access through these circumventricular organs. We would not able to directly test whether circulating sRen leaked into the central nervous system in these models as a mechanism to compensate for the loss of some central sRen. Even if there was a leak, its concentration would be below the detection threshold by immunostaining in the brain. sRen could thus possibly be enriched by (pro)renin receptors located in critical cardiovascular control regions. One potential experiment would be to examine the effects on the experimental end points we employed here in response to IC injection of a renin inhibitor. An alternative possibility is that besides neuronal and glial cells, renin is produced by other cell types. There is literature supporting a vascular renin-angiotensin system[242]. It has also been reported by Müller *et al.* that renin is expressed at vessel wall[243]. Nevertheless, it remains unclear whether blood vessels in the brain express renin, or if renin in the brain vascular beds is functional. On the other hand, studies from Dr. Ariel Gomez's group located brain renin promoter activity primarily in neurons (unpublished data).

Despite the fact that we did not detect baseline phenotypic changes in sRen neuronal- or glial-specific knockouts, it is possible that lack of sRen could have an impact in a single cell, since Ang-II is involved in multiple aspects of cellular physiology, such as proliferation, differentiation and nerve firing. One could carry out primary cell cultures

from the neuronal or glial sRen knockouts and perform patch clamp, single cell RT-PCR or apoptosis assays.

Future Experiments

Development of icRen-flox mice followed by global and cell type-specific icRen knockouts is critical to study the role of icRen in the brain. We would be able to compare and contrast the icRen models to the existing sRen knockout models. We will continue using the ES clones we have already identified, confirmed, and used to generate chimeras and germline transmitted founders. We expect to have the founder in one year and the final icRen knockout models in 2 years.

Once we obtain the icRen brain-specific knockout, it would be interesting to study the cardiovascular response in this model upon DOCA-salt treatment. The sRen brain-specific knockouts would be employed as controls. Since we speculate that icRen is more functionally relevant, depletion of icRen in the brain might be sufficient to block DOCA-salt induced blood pressure increase and white adipose loss. In that case, sRen brain-specific knockouts would act like wild type mice upon DOCA-salt treatment, to display elevated blood pressure, decreased white adipose and perhaps renal hypertrophy. It is also possible that icRen brain-specific knockouts would develop renal hypertrophy upon DOCA-salt stimulation, since icRen is barely expressed in the kidney.

Furthermore, we could also establish 2-kidney-1-clip (2K1C) models on the brain-specific icRen knockout background, since 2K1C-induced experimental hypertension has been shown to be associated with central RAS activity[89,187,244]. Similar to the DOCA experiment, the sRen brain-specific knockouts and wild type C57BL/6J would be used as controls.

Given that the brain-specific sRen knockouts did not exhibit any physiological alteration at baseline, it might be worthwhile to challenge the mice under abnormal physiological conditions. In fact, we have carried out dehydration studies in the GFAP-

Cre x sRen Flox line. There is no difference in drinking when water is provided again after overnight dehydration (F/F Cre+ N=8; F/F Cre- N=9). This indicates that either glial sRen is not important in thirst mechanisms, or neuronal sRen or icRen is compensating for loss of glial sRen during the physiological challenge. We decided to employ dehydration as a challenge for drinking instead of Ang-II infusion for the reason that peripheral Ang-II has been reported to be ineffective at eliciting drinking responses in mice[224]. Indeed, we have confirmed that acute Ang-II intraperitoneal (IP) injections with an extremely high dose of 10ug (Ang-II)/g (body weight) had no dipsogenic effect. A drawback of using dehydration in this type of study, however, is that it also enhances vasopressin release[245]. That would complicate the interpretation of the direct effect of the brain RAS in drinking responses, since hyperactivity of brain RAS is known to promote vasopressin secretion[246]. We are currently waiting for enough Nestin-Cre x sRen-flox offspring for study. If neuronal sRen could compensate for glial sRen in the previous experiment, it is also likely that this would be true vice versa. Moreover, if icRen is indeed important, we are also not likely to see a change in drinking response in neuronal sRen knockouts as compared to littermate controls. Nevertheless, we would still carry out the experiment to confirm that loss of neuronal sRen is not influential on thirst responses. Even though the sRen brain knockouts may not provide interesting phenotypes, they would serve as ideal controls to the icRen brain knockouts.

Clinical Relevance

Hypertension is a multifactorial disease. As previous introduced, the treatment of hypertension has typically focused on targeting different components of the RAS (RAS blockers) as well as balancing electrolyte/fluid homeostasis (diuretics), decreasing cardiac contraction (α-adrenergic blockers) and vasoconstriction (calcium channel blockers & α-blockers), and blocking sympathetic drive (β-adrenergic antagonists). With the identification of a unique isoform of renin in the brain, we could further unmask the

mechanism of how renin contributes to the conversion of angiotensinogen into neurotransmitter peptides and how icRen possibly mediate sympathetic outflow to regulate blood pressure. icRen serves as an additional potential target for antihypertensive treatments that could dramatically benefit patients who are less responsive to current medications.

We have taken advantage of the Cre-LoxP system to conditionally ablate sRen function in whole body or in specific tissue/cell type. The three sRen knockout models (global, neuronal and glial-specific) I have established and characterized during my Ph.D. research have promoted our understanding of the distinct functions of sRen vs. icRen in the periphery as well as in the brain, in cardiovascular regulation and fluid/electrolyte homeostasis. My project also has set the stage for the characterization of icRen knockouts and comparisons between sRen and icRen models. The discovery of icRen-associated neuronal pathways and confirmation of angiotensin as a neurotransmitter in the brain will potentially provide therapeutic targets to treat hypertension and cardiovascular diseases.

Figure 46. *Exon1b Location at Mouse Renin Locus.*

Positions of exon1a and exon 1b are indicated in pink in the *mRen1^{c}* gene. The green bars represent location and length of cloned fragments in the promoter bashing project. The CCAAT motif is 50 bp upstream of exon 1b. (Courtesy of Henry L.Keen, Ph.D.)

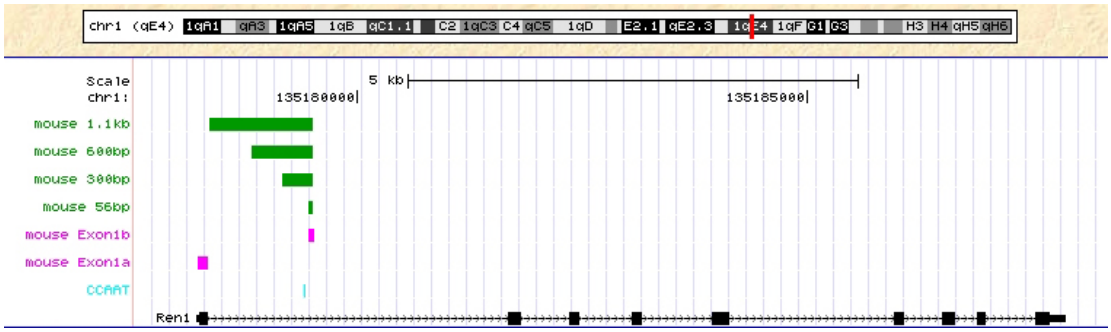
chr1 (qE4)
Scale
chr1:
5 kb
135180000
135185000
mouse 1.1kb
mouse 600bp
mouse 300bp
mouse 56bp
mouse Exon1b
mouse Exon1a
CCAAT
Ren1

Figure 47. *Exon1b Location at Human Renin Locus*

Positions of exon1a and exon 1b are indicated in pink in the human Renin gene. The green bars demonstrate location and length of cloned fragments for promoter bashing. The human kidney enhancer is presented in red. (Courtesy of Henry L. Keen, Ph.D.)

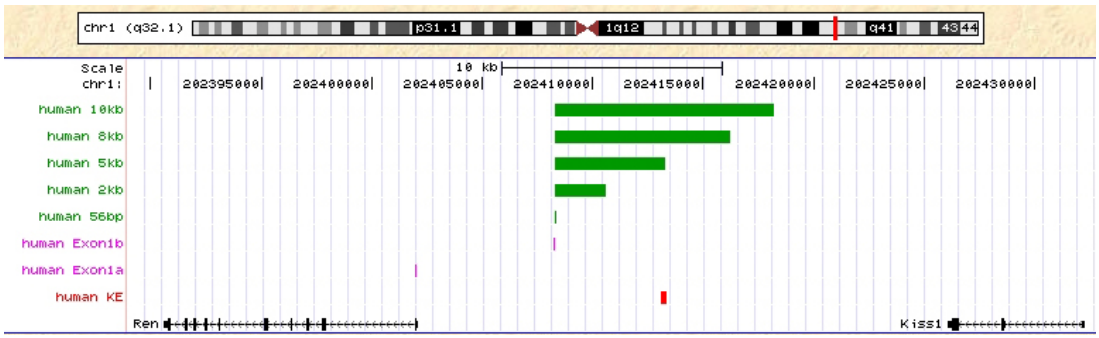
chr1 (q32.1)
p31.1
1q12
q41
43
44
Scale
chr1:
10 kb
202395000
202400000
202405000
202410000
202415000
202420000
202425000
202430000
human 10kb
human 8kb
human 5kb
human 2kb
human 56bp
human Exon1b
human Exon1a
human KE
Ren
Kiss1

APPENDIX A: ESTABLISHMENT OF ICREN KNOCKOUT MICE

Development of icRen-flox with the Gene Targeting Facility

As previously described in Chapter 2, we started the gene targeting of both sRen and icRen simultaneously. Unfortunately, we have encountered a lot of technical problems in generating the icRen knockout. We first collaborated with the Gene Targeting Facility on campus under Dr. Baoli Yang's guidance. We have successfully generated the sRen knockout through the same facility. After screening more than 1000 icRen ES clones that survived Neomycin selection with the initial PCR, we have successfully obtained 16 positive candidates (Clones A5, A7, A10, B3, B5, C1, C8, C9, C11, D4, D5, D11, E1, E2, E5 and E11 from a single plate, they are also coded as FT 605-mut, 607-wt, 610-wt, 615-wt, 617-wt, 625-wt, 632-mut, 633-abnormal, 635-wt, 640-wt, 641-wt, 647-wt, 649-wt, 650-wt, 653-wt, 659-mut) (Figure A1). However, after several rounds of further examination on the integrity of 5' LoxP, 3' LoxP, upstream and downstream FRT sites, neomycin gene, site-directed mutation and both homology arms, we found that most of the clones did not meet the requirement of having all the sites intact. In most cases, the 3' LoxP and its flanking linker region were lost, but the neighboring genomic region was preserved in the targeted allele. This might be a mechanism of how cells recognize/remove unrecognized fragments and protect the original genome from exogenous modifications, for instance, from nucleotide integrations from viruses. Fortunately we did not lose the 3' LoxP or any other regions of the gene in the sRen knockout project, as the capability of the floxed sRen to transcribe into renin mRNA has been established and the flox/flox mice are viable whereas the null/null mice are not[175]. In a few other cases, the 3' homology arm did not perfectly connect to the downstream genomic region that is outside the gene-targeting locus, missing various genomic sequences. Based on examples of a large number of gene-targeting projects, some regions of the genome are more strictly protected than others,

presumably because these regions are more critical for cellular and systemic biological functions. The difficulties we have encountered so far only make the function of icRen more intriguing.

Out of 16 clones we have obtained from the initial PCR screen, we have successfully identified three positive ES clones (FT605, FT632 and FT617) that have all elements intact. FT605 and FT632 are the clones with the introduced mutation, whereas FT617 is the clone that has a wild-type allele at the mutation site. Studying both mutation and wild-type lines would allow us to address the importance of the icRen translation start codon in exon 2. We introduced the ATG->GCG mutation with the purpose of completely abolishing icRen translation. Subsequently, we have brought the three clones into chimeric stages and have had several chimera mice (both males and females) from each clone (Table A1). We then bred all the chimeras with C57 mice to give birth to germ-line transmitted icRen knockout founders. Given there is literature suggesting that male chimeras have a better chance to give normal germ-line transmitted offspring[229], we bred both genders of chimeras just in case. However, after careful PCR screens using tail genomic DNA from hundreds of pups, we did not identify any germ-line transmitted offspring. Now we are continuing the screening, as well as repeating the very first step of transfection of ES cells.

Development of icRen-flox with iTL

While performing gene-targeting of icRen in collaboration with the core facility on campus, we also started generating the same knockout through a commercial company (ingenious Targeting Laboratory). The same targeting construct was linearized and confirmed before shipping it out to iTL. We have experienced similar difficulties in getting intact positive clones through iTL as through the Gene Targeting Facility. Specifically, some of the candidates were missing the 3' LoxP and the correct junction extending from the 3' homology arm to the downstream region. In this project, a

Research Scientist in our laboratory, Dr. Xuebo Liu, has provided a great amount of help in the later stage of PCR screening and Southern Blot confirmation. Eventually, after screening approximate 1500 ES clones in total from iTL, we had obtained 2 potential candidate clones (clone # 4C7 and 4D5: first number as plate #, middle letter and last number as position in a certain plate) that we initially considered intact and complete (Figure A2). We took a step further to examine the integrity of 3' LoxP in PCR-purified large fragment that expands from downstream homology of the targeted region to 3' neighboring sequences in the genome that is not targeted. This allowed us to obtain a PCR product that only reflects the homologous recombination-targeted allele, not any random insertions. However, from this large PCR amplicon, we found the intact 3' LoxP site and its linker regions only in clone 4D5, but not in 4C7. This indicates that clone 4C7 has a homologous-targeted allele that does not include the 3' LoxP site, and that 4C7 has another random integrant that does include the complete 3' LoxP at the mean time. To this date, we have identified 4D5 as a *bona fide* homologous-recombinated ES clone that contains wild-type allele (ATG) at the first in-frame start codon of exon 2. We subsequently verified it again via Southern Blots (Figures A3 and A4). We have now proceeded into the generation of chimeras with this clone.

Figure A1. *Initial Screening of icRen ES Clones from Gene-Targeting Facility.*

In this original screening, 16 ES candidate clones have been identified. The expected band size is 2.15 kb (Figure 15). Clone C9 might be an aberrant clone, thus has been eliminated. The negative control is ddH_2O, where as the two positive controls from left to right are the same positive control plasmid with/without wild type genomic DNA.

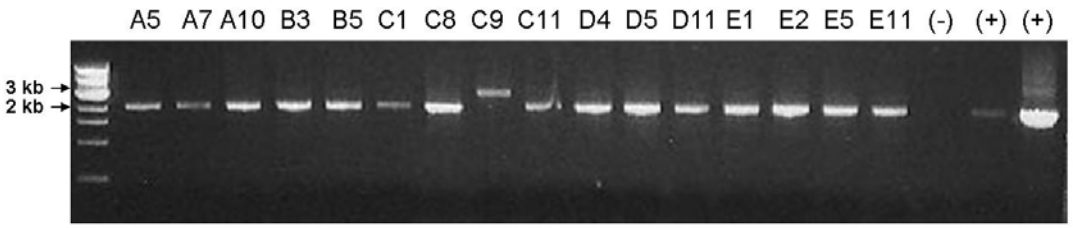
A5 A7 A10 B3 B5 C1 C8 C9 C11 D4 D5 D11 E1 E2 E5 E11 (-) (+) (+)
3 kb
2 kb

Figure A2. *Downstream Homology Junction Confirmation of icRen ES Clones from iTL.*

Clones 4C7 and 4D5 were able to generate a 5.5 kb band that indicates the correct junction between the 3’ end homologous arm and its downstream genomic sequence (Figure 19).

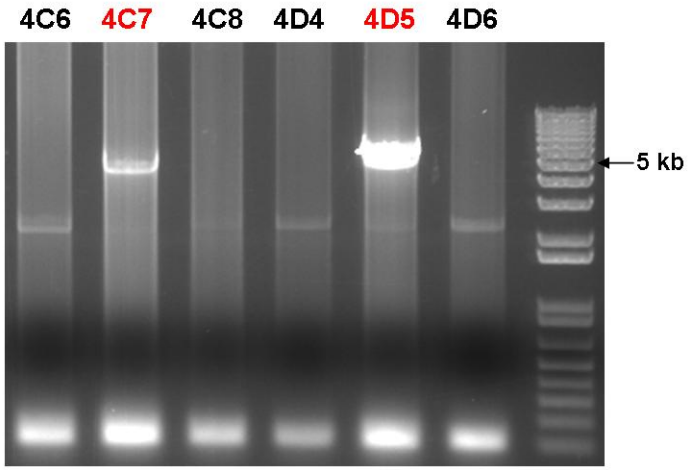
4C6
4C7
4C8
4D4
4D5
4D6
5 kb

Figure A3. *5'-end Southern Blot of iTL ES Clone 4D5.*

The probe was located at the 5' region upstream of the upstream homologous arm, as depicted in Figure 27. Upon SpeI digestion, the probe will detect a targeted band of 4.3 kb and a wild type band of 13.6 kb.

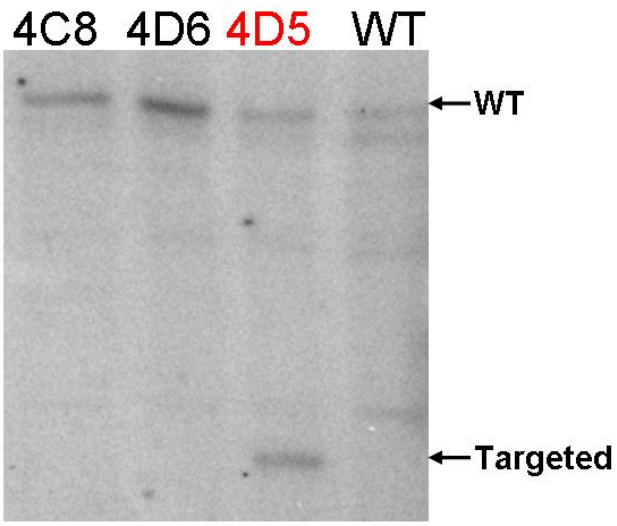
4C8
4D6
4D5
WT
WT
Targeted

Figure A4. *3'-end Southern Blot of iTL ES Clone 4D5.*

The probe was located at the 3' region downstream of the downstream homology, as demonstrated in Figure 27. SpeI digestion will produce a targeted band of 8.7 kb and a wild type band of 13.6 kb that can be detected by the probe.

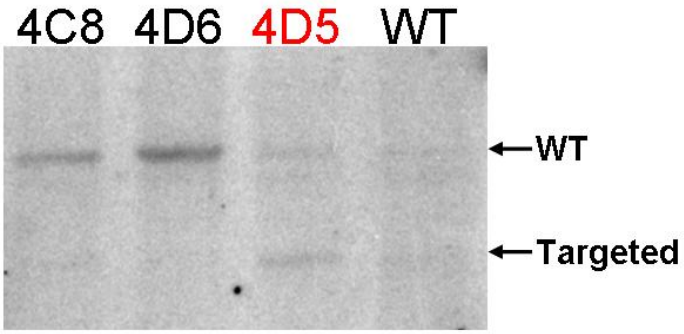
4C8
4D6
4D5
WT
WT
Targeted

Table A1. *List of icRen Chimeras Generated Through Core Facility.*

Chimera	**Gender**	**Chimerism (%)**
605/3	female	5
617/1	male	NA
632/1	female	60
632/2	male	60
632/3	male	50
632/4	female	40
632/5	female	40
632/6	male	10

Note: The three confirmed ES positive clones (FT605, FT617 and FT632) have been used to generate chimeras. FT 632 has been producing more chimeras with higher chimerism.

APPENDIX B: ROLE OF BRAIN RENIN IN DOCA-SALT-INDUCED HYPERTENSION

It has been well documented that DOCA-salt induced hypertension is due in part to the contribution of central RAS activity[21,97,98]. According to our preliminary studies (Figure B1), DOCA-salt induced hypertensive mice exhibited suppressed systemic RAS. Although studies suggested that DOCA-salt animals demonstrated elevated brain Ang-II synthesis[230], it remains largely undefined with regard to the role of brain renin in this model. Even though we have identified both sRen and icRen expression in the mouse brain, it is still unclear which isoform is more important in DOCA-salt hypertension. Therefore, it is of particular interest to dissect the contributions of secreted vs. intracellular renin in the central regulation of blood pressure and heart rate in DOCA-salt mice. We plan to compare the blood pressure of the brain-specific secreted renin knockout to that of wild-type littermate controls and AGT brain-specific knockouts upon DOCA-salt treatment. We expect to observe blunted increases in blood pressure in DOCA-salt treated renin knockouts compared to wild-type controls.

As a collaborative study with postdoctoral researchers Dr. Justin Grobe and Dr. Giulianna Borges in our laboratory, the project was started with wild-type C57 male mice in order to figure out the baseline experimental conditions in our hands. It is suggested in the literature that males exhibited more apparent physiological changes than females with DOCA-salt treatment[231]. We implanted one DOCA pellet (Innovative Research of America, 21-day-release pellet or 60-day-release pellet) into each mouse subcutaneously. Then in the next 3-weeks, DOCA-implanted and sham-operated mice were given saline (0.9% NaCl+0.1% KCl) or regular drinking water, respectively. All animals were singly-housed for the rest of the experiment. At the end of week 3, all measurements were carried on between DOCA-salt treated and control groups.

We have observed that DOCA-salt treated wild-type male mice exhibited decreased white adipose tissue after normalization for body weight, when compared to the control (There is no detectable difference in body weight) (Figure B2). The reduction in white adipose mass is perfectly in line with what we see in another genetic hypertensive model with high central RAS activity (the sRA model, unpublished data). In that genetic model, we overexpressed neuronal human renin (the enzyme) and systemic human angiotensinogen (the substrate), thus allowing increased production of angiotensin (the product and effector peptide) only in the brain. Interestingly, both models also share the similarity of a suppressed peripheral RAS. An analysis of mRNA levels has confirmed a large decline of renin expression in the kidney of DOCA-salt treated mice (Figure B1). In addition, the DOCA-salt treated group also demonstrated renal hypertrophy as indicated by increased kidney mass (Figure B3). This could be partially a result of imbalanced electrolyte homeostasis[232]. Moreover, the oxygen consumption in DOCA-salt group was increased, implicating elevated basal metabolic rate in treated animals (Figure B4). This further supports the hypothesis that the brain RAS is involved in basal metabolic regulation.

Given that we did not observe any phenotypic differences between sRen neuronal- or glial-specific knockouts and wild-type littermate controls as previously described in Chapter 4, we hypothesize that central sRen is not essential for baseline cardiovascular regulation in adults. Therefore, icRen knockout would be a more appropriate model to study the effect of DOCA-salt on hypertension. We speculate that with the lack of icRen in the brain, central RAS activity would be attenuated such that even with DOCA-salt treatment, the phenotypes one would observe in wild-type controls are less likely to be induced in the DOCA-salt treated icRen brain-specific knockouts.

Figure B1. *Renal Renin Levels in DOCA-salt and Sham-operated Mice.*

Total mouse renin mRNA level (normalized to GAPDH mRNA level) is suppressed in DOCA-salt treated male mice (from C57BL6/J background) when compared to that of sham-operated age and gender matched controls.

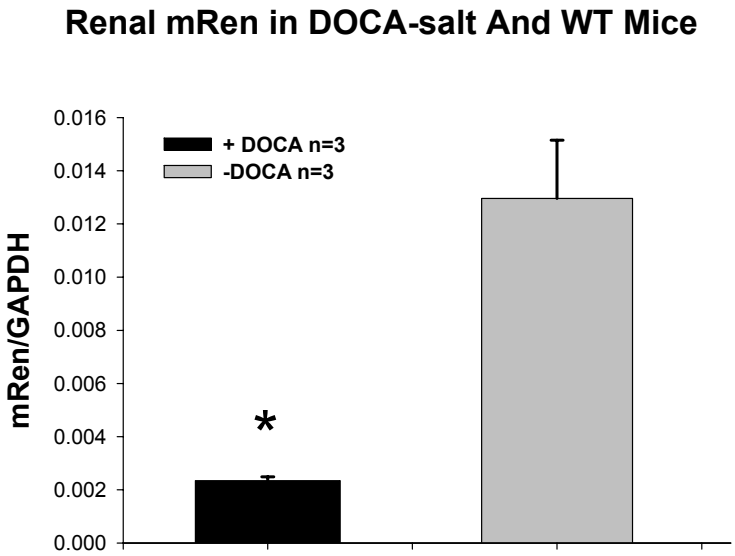
Renal mRen in DOCA-salt And WT Mice
mRen/GAPDH
0.016
0.014
0.012
0.010
0.008
0.006
0.004
0.002
0.000
+ DOCA n=3
-DOCA n=3
*

Figure B2. *Perigenital White Adipose Mass in DOCA-Salt and Sham-operated Mice.*

DOCA-salt-treated male mice exhibited decreased perigenital white adipose after normalization for body weight when compared to sham-operated controls. On the other hand, DOCA-salt-treated female mice showed a trend of decreased white adipose.

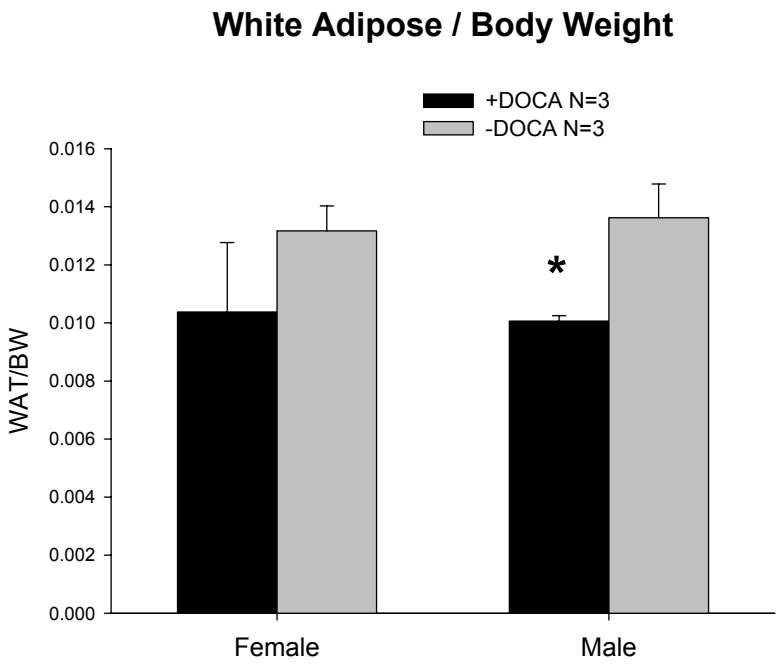
White Adipose / Body Weight
+DOCA N=3
-DOCA N=3
WAT/BW
0.016
0.014
0.012
0.010
0.008
0.006
0.004
0.002
0.000
*
Female
Male

Figure B3. *Kidney Mass in DOCA-salt and Sham-operated Mice.*

Both female and male DOCA-salt-treated mice developed renal hypertrophy, as suggested by significantly increased kidney mass after normalization for body weight.

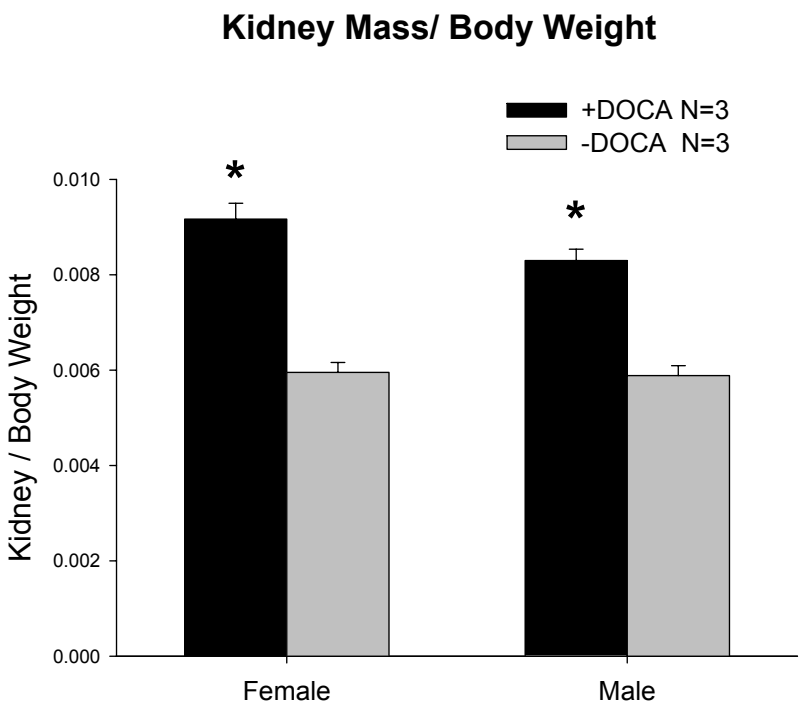
Kidney Mass/ Body Weight
+DOCA N=3
-DOCA N=3
Kidney / Body Weight
0.010
0.008
0.006
0.004
0.002
0.000
*
*
Female
Male

Figure B4. *Oxygen Consumption in DOCA-salt and Sham-operated Mice.*

DOCA-salt-treated male mice displayed increased basal metabolic rate, as indicated by elevated oxygen consumption during rest compared to that of sham-operated controls. (Courtesy of Justin Grobe, Ph.D.)

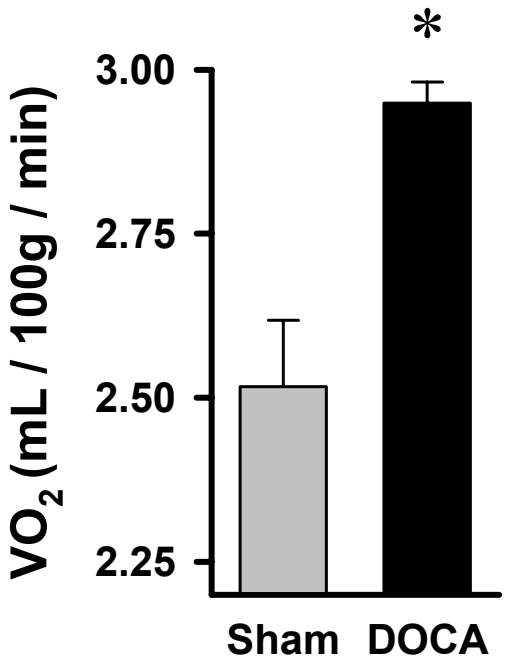
*
3.00
2.75
2.50
2.25
VO2 (mL / 100g / min)
Sham
DOCA

REFERENCES

1. Fernando S.Antezana. Epidemiologic Aspects of Hypertension in the World. World Health Organization . 2010. Ref Type: Internet Communication

2. Kannel,W.B., Vasan,R.S. & Levy,D. Is the relation of systolic blood pressure to risk of cardiovascular disease continuous and graded, or are there critical values? *Hypertension* **42**, 453-456 (2003).

3. Wolf,P.A. Fifty years at Framingham: contributions to stroke epidemiology. *Adv. Neurol.* **92**, 165-172 (2003).

4. Wong,N.D. Intensified screening and treatment of the metabolic syndrome for cardiovascular risk reduction. *Prev. Cardiol.* **8**, 47-52 (2005).

5. American Heart Association. NHLBI unpublished estimates from ARIC, CHS and FHS Cohort and Offspring Studies. 2010. Ref Type: Report

6. American Heart Association. Cause of Mortality. 2010. Ref Type: Internet Communication

7. High Blood Pressure Facts. 2010. Ref Type: Internet Communication

8. Ferguson,R.K., Turini,G.A., Brunner,H.R., Gavras,H. & McKinstry,D.N. A specific orally active inhibitor of angiotensin-converting enzyme in man. *Lancet* **1**, 775-778 (1977).

9. Wong,P.C. *et al.* In vivo pharmacology of DuP 753. *Am. J. Hypertens.* **4**, 288S-298S (1991).

10. Staessen,J.A., Li,Y. & Richart,T. Oral renin inhibitors. *Lancet* **368**, 1449-1456 (2006).

11. Casas,J.P. *et al.* Effect of inhibitors of the renin-angiotensin system and other antihypertensive drugs on renal outcomes: systematic review and meta-analysis. *Lancet* **366**, 2026-2033 (2005).

12. Psaty,B.M. *et al.* Health outcomes associated with various antihypertensive therapies used as first-line agents: a network meta-analysis. *JAMA* **289**, 2534-2544 (2003).

13. Lindholm,L.H., Carlberg,B. & Samuelsson,O. Should beta blockers remain first choice in the treatment of primary hypertension? A meta-analysis. *Lancet* **366**, 1545-1553 (2005).

14. Izzo Jr., Sica & Black. Hypertension Primer, 4th Edition. Council on High Blood Pressure Research, American Heart Association, (2010).

15. Hyman,D.J. & Pavlik,V.N. Poor hypertension control: let's stop blaming the patients. *Cleve. Clin. J. Med.* **69**, 793-799 (2002).

16. NHANES. Hypertension and Treatments. 2010. Ref Type: Internet Communication

17. Myers,M.G. Compliance in hypertension: why don't patients take their pills? *CMAJ.* **160**, 64-65 (1999).

18. Camara,A.K. & Osborn,J.L. AT1 receptors mediate chronic central nervous system AII hypertension in rats fed high sodium chloride diet from weaning. *J. Auton. Nerv. Syst.* **72**, 16-23 (1998).

19. Ferrario,C.M. Angiotension-(1-7) and antihypertensive mechanisms. *J. Nephrol.* **11**, 278-283 (1998).

20. Ganong,W.F. The brain renin-angiotensin system. *Annu Rev Physiol* **46**, 17-31 (1984).

21. Itaya,Y., Suzuki,H., Matsukawa,S., Kondo,K. & Saruta,T. Central renin-angiotensin system and the pathogenesis of DOCA-salt hypertension in rats. *Am. J. Physiol* **251**, H261-H268 (1986).

22. Lavoie,J.L. *et al.* Evidence supporting a functional role for intracellular renin in the brain. *Hypertension* **47**, 461-466 (2006).

23. Morimoto,S., Cassell,M.D. & Sigmund,C.D. Glia- and neuron-specific expression of the renin-angiotensin system in brain alters blood pressure, water intake, and salt preference. *J Biol Chem* **277**, 33235-33241 (2002).

24. Moreira,T.S., Sato,M.A., Takakura,A.C., Menani,J.V. & Colombari,E. Role of pressor mechanisms from the NTS and CVLM in control of arterial pressure. *Am J Physiol Regul Integr Comp Physiol* **289**, R1416-R1425 (2005).

25. Guyton & Hall. Textbook of Medical Physiology. (2010).

26. Molstrom,S., Larsen,N.H., Simonsen,J.A., Washington,R. & Bie,P. Normotensive sodium loading in normal man: regulation of renin secretion during beta-receptor blockade. *Am. J. Physiol Regul. Integr. Comp Physiol* **296**, R436-R445 (2009).

27. Oikawa,Y., Maehara,K., Saito,T., Tamagawa,K. & Maruyama,Y. Attenuation of angiotensin II-mediated coronary vasoconstriction and vasodilatory action of angiotensin-converting enzyme inhibitor in pacing-induced heart failure in dogs. *J. Am. Coll. Cardiol.* **38**, 1188-1194 (2001).

28. Ito,M. *et al.* Regulation of blood pressure by the type 1A angiotensin II receptor gene. *Proc. Natl. Acad. Sci. U. S. A* **92**, 3521-3525 (1995).

29. Sugaya,T. *et al.* Angiotensin II type 1a receptor-deficient mice with hypotension and hyperreninemia. *J Biol Chem* **270**, 18719-18722 (1995).

30. Crowley,S.D. *et al.* Distinct roles for the kidney and systemic tissues in blood pressure regulation by the renin-angiotensin system. *J. Clin. Invest* **115**, 1092-1099 (2005).

31. Wink,D.A. Ion implicated in blood pact. *Nat. Med.* **9**, 1460-1461 (2003).

32. Stauss,H.M., Godecke,A., Mrowka,R., Schrader,J. & Persson,P.B. Enhanced blood pressure variability in eNOS knockout mice. *Hypertension* **33**, 1359-1363 (1999).

33. Falcon,B.L. *et al.* Angiotensin II type 2 receptor gene transfer elicits cardioprotective effects in an angiotensin II infusion rat model of hypertension. *Physiol Genomics* **19**, 255-261 (2004).

34. Metcalfe,B.L. *et al.* Prevention of cardiac hypertrophy by angiotensin II type-2 receptor gene transfer. *Hypertension* **43**, 1233-1238 (2004).

35. Grobe,J.L., Xu,D. & Sigmund,C.D. An intracellular renin-angiotensin system in neurons: fact, hypothesis, or fantasy. *Physiology. (Bethesda.)* **23**, 187-193 (2008).

36. Mohan K.Raizada, M.Ian.Phillips & Colin Sumners. Cellular and Molecular Biology of the renin-angiotensin system. (2010).

37. P.Michael Conn & Shlomo Melmed. Endocrinology: basic and clinical principles. (2010).

38. Sadjadi,J. *et al.* Angiotensin converting enzyme-independent angiotensin ii production by chymase is up-regulated in the ischemic kidney in renovascular hypertension. *J. Surg. Res.* **127**, 65-69 (2005).

39. Rebas,E. & Lachowicz-Ochedalska,A. The effect of angiotensin III on protein tyrosine kinase activity in rat pituitary. *Regul. Pept.* **130**, 14-18 (2005).

40. Esteban,V. *et al.* Angiotensin IV activates the nuclear transcription factor-kappaB and related proinflammatory genes in vascular smooth muscle cells. *Circ. Res.* **96**, 965-973 (2005).

41. Ferreira,P.M., Souza Dos Santos,R.A. & Campagnole-Santos,M.J. Angiotensin-(3-7) pressor effect at the rostral ventrolateral medulla. *Regul. Pept.* **141**, 168-174 (2007).

42. Lee,J. *et al.* Effect of I.C.V. injection of AT4 receptor ligands, NLE1-angiotensin IV and LVV-hemorphin 7, on spatial learning in rats. *Neuroscience* **124**, 341-349 (2004).

43. Danser,A.H. *et al.* Determinants of interindividual variation of renin and prorenin concentrations: evidence for a sexual dimorphism of (pro)renin levels in humans. *J. Hypertens.* **16**, 853-862 (1998).

44. Nguyen,G. *et al.* Pivotal role of the renin/prorenin receptor in angiotensin II production and cellular responses to renin. *J. Clin. Invest* **109**, 1417-1427 (2002).

45. Nabi,A.H. *et al.* Binding properties of rat prorenin and renin to the recombinant rat renin/prorenin receptor prepared by a baculovirus expression system. *Int. J. Mol. Med.* **18**, 483-488 (2006).

46. Stankovic,A.R., Fisher,N.D. & Hollenberg,N.K. Prorenin and angiotensin-dependent renal vasoconstriction in type 1 and type 2 diabetes. *J. Am. Soc. Nephrol.* **17**, 3293-3299 (2006).

47. Ichihara,A. *et al.* Inhibition of diabetic nephropathy by a decoy peptide corresponding to the "handle" region for nonproteolytic activation of prorenin. *J. Clin. Invest* **114**, 1128-1135 (2004).

48. Ichihara,A. *et al.* Nonproteolytic activation of prorenin contributes to development of cardiac fibrosis in genetic hypertension. *Hypertension* **47**, 894-900 (2006).

49. Richoux,J.P. *et al.* Immunocytochemical localization of angiotensinogen in rat liver and kidney. *Cell Tissue Res.* **233**, 439-451 (1983).

50. Balyasnikova,I.V., Yeomans,D.C., McDonald,T.B. & Danilov,S.M. Antibody-mediated lung endothelium targeting: in vivo model on primates. *Gene Ther.* **9**, 282-290 (2002).

51. Pagliaro,P. & Penna,C. Rethinking the renin-angiotensin system and its role in cardiovascular regulation. *Cardiovasc. Drugs Ther.* **19**, 77-87 (2005).

52. Lu,D. & Raizada,M.K. Delivery of angiotensin II type 1 receptor antisense inhibits angiotensin action in neurons from hypertensive rat brain. *Proc. Natl. Acad. Sci. U. S. A* **92**, 2914-2918 (1995).

53. Yang,H., Lu,D., Vinson,G.P. & Raizada,M.K. Involvement of MAP kinase in angiotensin II-induced phosphorylation and intracellular targeting of neuronal AT1 receptors. *J. Neurosci.* **17**, 1660-1669 (1997).

54. Gasc,J.M., Monnot,C., Clauser,E. & Corvol,P. Co-expression of type 1 angiotensin II receptor (AT1R) and renin mRNAs in juxtaglomerular cells of the rat kidney. *Endocrinology* **132**, 2723-2725 (1993).

55. Ramchandran,R. *et al.* Angiotensinergic stimulation of vascular endothelium in mice causes hypotension, bradycardia, and attenuated angiotensin response. *Proc. Natl. Acad. Sci. U. S. A* **103**, 19087-19092 (2006).

56. Coulter,C.L., Myers,D.A., Nathanielsz,P.W. & Bird,I.M. Ontogeny of angiotensin II type 1 receptor (AT1R) in the sheep adrenal gland. *Endocr. Res.* **24**, 935-936 (1998).

57. Kurihara,T. *et al.* Neuroprotective effects of angiotensin II type 1 receptor (AT1R) blocker, telmisartan, via modulating AT1R and AT2R signaling in retinal inflammation. *Invest Ophthalmol. Vis. Sci.* **47**, 5545-5552 (2006).

58. Whaley-Connell,A. *et al.* Effect of renin inhibition and AT1R blockade on myocardial remodeling in the transgenic Ren2 rat. *Am. J. Physiol Endocrinol. Metab* **295**, E103-E109 (2008).

59. Wei,Y. *et al.* Angiotensin II-induced NADPH oxidase activation impairs insulin signaling in skeletal muscle cells. *J. Biol. Chem.* **281**, 35137-35146 (2006).

60. Sakai,K. & Sigmund,C.D. Molecular evidence of tissue renin-angiotensin systems: a focus on the brain. *Curr Hypertens Rep* **7**, 135-140 (2005).

61. Miyake-Ogawa,C. *et al.* Tissue-specific expression of renin-angiotensin system components in IgA nephropathy. *Am. J. Nephrol.* **25**, 1-12 (2005).

62. Navar,L.G., Imig,J.D., Zou,L. & Wang,C.T. Intrarenal production of angiotensin II. *Semin. Nephrol.* **17**, 412-422 (1997).

63. Sander,M. *et al.* The role of the adrenal gland in hypertensive transgenic rat TGR(mREN2)27. *Endocrinology* **131**, 807-814 (1992).

64. Naruse,M. & Inagami,T. Markedly elevated specific renin levels in the adrenal in genetically hypertensive rats. *Proc. Natl. Acad. Sci. U. S. A* **79**, 3295-3299 (1982).

65. Ganten,D., Hayduk,K., Brecht,H.M., Boucher,R. & Genest,J. Evidence of renin release or production in splanchnic territory. *Nature* **226**, 551-552 (1970).

66. Muller,D.N. *et al.* Effects of human renin in the vasculature of rats transgenic for human angiotensinogen. *Hypertension* **26**, 272-278 (1995).

67. Alenina,N., Xu,P., Rentzsch,B., Patkin,E.L. & Bader,M. Genetically altered animal models for Mas and angiotensin-(1-7). *Exp. Physiol* **93**, 528-537 (2008).

68. Kim,S. *et al.* The adipose Renin-Angiotensin system modulates systemic markers of insulin sensitivity and activates the intrarenal Renin-Angiotensin system. *J. Biomed. Biotechnol.* **2006**, 27012 (2006).

69. Engeli,S., Negrel,R. & Sharma,A.M. Physiology and pathophysiology of the adipose tissue renin-angiotensin system. *Hypertension* **35**, 1270-1277 (2000).

70. Cassis,L.A., Police,S.B., Yiannikouris,F. & Thatcher,S.E. Local adipose tissue renin-angiotensin system. *Curr. Hypertens. Rep.* **10**, 93-98 (2008).

71. Sernia,C. A critical appraisal of the intrinsic pancreatic angiotensin-generating system. *JOP.* **2**, 50-55 (2001).

72. Speth,R.C., Daubert,D.L. & Grove,K.L. Angiotensin II: a reproductive hormone too? *Regul. Pept.* **79**, 25-40 (1999).

73. Nielsen,A.H., Schauser,K.H. & Poulsen,K. Current topic: the uteroplacental renin-angiotensin system. *Placenta* **21**, 468-477 (2000).

74. Lee,A.F., MacFadyen,R.J. & Struthers,A.D. Neurohormonal reactivation in heart failure patients on chronic ACE inhibitor therapy: a longitudinal study. *Eur. J. Heart Fail.* **1**, 401-406 (1999).

75. Lavoie,J.L. & Sigmund,C.D. Minireview: overview of the renin-angiotensin system--an endocrine and paracrine system. *Endocrinology* **144**, 2179-2183 (2003).

76. Brunner,H.R. *et al.* Oral angiotensin-converting enzyme inhibitor in long-term treatment of hypertensive patients. *Ann. Intern. Med.* **90**, 19-23 (1979).

77. Dzau,V.J. *et al.* The relevance of tissue angiotensin-converting enzyme: manifestations in mechanistic and endpoint data. *Am. J. Cardiol.* **88**, 1L-20L (2001).

78. Hardman & Limbird. Goodman & Gilman's The Pharmacological Basis of Therapeutics. (2010).

79. Andresen,M.C. & Yang,M. Arterial baroreceptor resetting: contributions of chronic and acute processes. *Clin. Exp. Pharmacol. Physiol Suppl* **15**, 19-30 (1989).

80. Benarroch,E.E., Schmeichel,A.M., Sandroni,P., Low,P.A. & Parisi,J.E. Differential involvement of hypothalamic vasopressin neurons in multiple system atrophy. *Brain* **129**, 2688-2696 (2006).

81. McKinley,M.J. & Johnson,A.K. The physiological regulation of thirst and fluid intake. *News Physiol Sci.* **19**, 1-6 (2004).

82. Nielsen,S., Fror,J. & Knepper,M.A. Renal aquaporins: key roles in water balance and water balance disorders. *Curr. Opin. Nephrol. Hypertens.* **7**, 509-516 (1998).

83. Qadri,F. *et al.* Angiotensin II-induced vasopressin release is mediated through alpha-1 adrenoceptors and angiotensin II AT1 receptors in the supraoptic nucleus. *J. Pharmacol. Exp. Ther.* **267**, 567-574 (1993).

84. Robberecht,W. & Denef,C. Stimulation and inhibition of pituitary growth hormone release by angiotensin II in vitro. *Endocrinology* **122**, 1496-1504 (1988).

85. Spinedi,E. & Negro-Vilar,A. Angiotensin II and ACTH release: site of action and potency relative to corticotropin releasing factor and vasopressin. *Neuroendocrinology* **37**, 446-453 (1983).

86. Steele,M.K., Negro-Vilar,A. & McCann,S.M. Effect of angiotensin II on in vivo and in vitro release of anterior pituitary hormones in the female rat. *Endocrinology* **109**, 893-899 (1981).

87. Martin,P., Massol,J., Scalbert,E. & Puech,A.J. Involvement of angiotensin-converting enzyme inhibition in reversal of helpless behavior evoked by perindopril in rats. *Eur. J. Pharmacol.* **187**, 165-170 (1990).

88. Martin,P., Massol,J. & Puech,A.J. Captopril as an antidepressant? Effects on the learned helplessness paradigm in rats. *Biol. Psychiatry* **27**, 968-974 (1990).

89. Kagiyama,S., Varela,A., Phillips,M.I. & Galli,S.M. Antisense inhibition of brain renin-angiotensin system decreased blood pressure in chronic 2-kidney, 1 clip hypertensive rats. *Hypertension* **37**, 371-375 (2001).

90. Kubo,T., Ikezawa,A., Kambe,T., Hagiwara,Y. & Fukumori,R. Renin antisense injected intraventricularly decreases blood pressure in spontaneously hypertensive rats. *Brain Res. Bull.* **56**, 23-28 (2001).

91. Chen,Y. *et al.* Adenovirus-mediated small-interference RNA for in vivo silencing of angiotensin AT1a receptors in mouse brain. *Hypertension* **47**, 230-237 (2006).

92. Cabassi,A. *et al.* Sympathetic activation in adipose tissue and skeletal muscle of hypertensive rats. *Hypertension* **39**, 656-661 (2002).

93. Arribas,S.M. *et al.* Noradrenergic transmission in the tail artery of hypertensive rats transgenic for the mouse renin gene Ren-2. *J. Auton. Pharmacol.* **16**, 69-77 (1996).

94. Leenen,F.H., Ruzicka,M. & Huang,B.S. The brain and salt-sensitive hypertension. *Curr. Hypertens. Rep.* **4**, 129-135 (2002).

95. Takeda,K. & Bunag,R.D. Augmented sympathetic nerve activity and pressor responsiveness in DOCA hypertensive rats. *Hypertension* **2**, 97-101 (1980).

96. Pochiero,M., Nicoletta,P., Losi,E., Bianchi,A. & Caputi,A.P. Cardiovascular responses of conscious DOCA-salt hypertensive rats to acute intracerebroventricular and intravenous administration of captopril. *Pharmacol. Res. Commun.* **15**, 173-182 (1983).

97. Kubo,T., Yamaguchi,H., Tsujimura,M., Hagiwara,Y. & Fukumori,R. Blockade of angiotensin receptors in the anterior hypothalamic preoptic area lowers blood pressure in DOCA-salt hypertensive rats. *Hypertens. Res.* **23**, 109-118 (2000).

98. Park,C.G. & Leenen,F.H. Effects of centrally administered losartan on deoxycorticosterone-salt hypertension rats. *J. Korean Med. Sci.* **16**, 553-557 (2001).

99. Guzzetti,S. *et al.* Sympathetic predominance in essential hypertension: a study employing spectral analysis of heart rate variability. *J. Hypertens.* **6**, 711-717 (1988).

100. Anderson,E.A., Sinkey,C.A., Lawton,W.J. & Mark,A.L. Elevated sympathetic nerve activity in borderline hypertensive humans. Evidence from direct intraneural recordings. *Hypertension* **14**, 177-183 (1989).

101. Grassi,G., Cattaneo,B.M., Seravalle,G., Lanfranchi,A. & Mancia,G. Baroreflex control of sympathetic nerve activity in essential and secondary hypertension. *Hypertension* **31**, 68-72 (1998).

102. Lavoie,J.L., Cassell,M.D., Gross,K.W. & Sigmund,C.D. Adjacent expression of renin and angiotensinogen in the rostral ventrolateral medulla using a dual-reporter transgenic model. *Hypertension* **43**, 1116-1119 (2004).

103. McKinley,M.J. *et al.* The brain renin-angiotensin system: location and physiological roles. *Int. J. Biochem. Cell Biol.* **35**, 901-918 (2003).

104. atcc. 2010. Ref Type: Internet Communication

105. Allen,A.M. *et al.* Angiotensin receptors in the nervous system. *Brain Res. Bull.* **47**, 17-28 (1998).

106. Saavedra,J.M. Emerging features of brain angiotensin receptors. *Regul. Pept.* **85**, 31-45 (1999).

107. Inagami,T. Molecular biology and signaling of angiotensin receptors: an overview. *J. Am. Soc. Nephrol.* **10 Suppl 11**, S2-S7 (1999).

108. Chappell,M.C. Emerging evidence for a functional angiotensin-converting enzyme 2-angiotensin-(1-7)-MAS receptor axis: more than regulation of blood pressure? *Hypertension* **50**, 596-599 (2007).

109. Wright,J.W. & Harding,J.W. Brain angiotensin receptor subtypes AT1, AT2, and AT4 and their functions. *Regul. Pept.* **59**, 269-295 (1995).

110. Hallberg,M. Targeting the insulin-regulated aminopeptidase/AT4 receptor for cognitive disorders. *Drug News Perspect.* **22**, 133-139 (2009).

111. Shan,Z., Cuadra,A.E., Sumners,C. & Raizada,M.K. Characterization of a functional (pro)renin receptor in rat brain neurons. *Exp. Physiol* **93**, 701-708 (2008).

112. Lazartigues,E. A map and new directions for the (pro)renin receptor in the brain: focus on "A role of the (pro)renin receptor in neuronal cell differentiation". *Am. J. Physiol Regul. Integr. Comp Physiol* **297**, R248-R249 (2009).

113. Contrepas,A. *et al.* A role of the (pro)renin receptor in neuronal cell differentiation. *Am. J. Physiol Regul. Integr. Comp Physiol* **297**, R250-R257 (2009).

114. Lind,R.W., Swanson,L.W., Bruhn,T.O. & Ganten,D. The distribution of angiotensin II-immunoreactive cells and fibers in the paraventriculo-hypophysial system of the rat. *Brain Res.* **338**, 81-89 (1985).

115. Lind,R.W., Swanson,L.W. & Ganten,D. Angiotensin II immunoreactivity in the neural afferents and efferents of the subfornical organ of the rat. *Brain Res.* **321**, 209-215 (1984).

116. Lind,R.W., Swanson,L.W. & Ganten,D. Angiotensin II immunoreactive pathways in the central nervous system of the rat: evidence for a projection from the subfornical organ to the paraventricular nucleus of the hypothalamus. *Clin. Exp. Hypertens. A* **6**, 1915-1920 (1984).

117. Lind,R.W., Swanson,L.W. & Ganten,D. Organization of angiotensin II immunoreactive cells and fibers in the rat central nervous system. An immunohistochemical study. *Neuroendocrinology* **40**, 2-24 (1985).

118. Erdmann,B., Fuxe,K. & Ganten,D. Subcellular localization of angiotensin II immunoreactivity in the rat cerebellar cortex. *Hypertension* **28**, 818-824 (1996).

119. Pickel,V.M. & Chan,J. Co-localization of angiotensin II and gamma-aminobutyric acid in axon terminals in the rat subfornical organ. *Neurosci. Lett.* **193**, 89-92 (1995).

120. Trippodo,N.C. *et al.* Cardiovascular effects of the novel dual inhibitor of neutral endopeptidase and angiotensin-converting enzyme BMS-182657 in experimental hypertension and heart failure. *J. Pharmacol. Exp. Ther.* **275**, 745-752 (1995).

121. Bains,J.S., Potyok,A. & Ferguson,A.V. Angiotensin II actions in paraventricular nucleus: functional evidence for neurotransmitter role in efferents originating in subfornical organ. *Brain Res.* **599**, 223-229 (1992).

122. Gehlert,D.R., Speth,R.C. & Wamsley,J.K. Distribution of [125I]angiotensin II binding sites in the rat brain: a quantitative autoradiographic study. *Neuroscience* **18**, 837-856 (1986).

123. Ferguson,A.V., Washburn,D.L. & Latchford,K.J. Hormonal and neurotransmitter roles for angiotensin in the regulation of central autonomic function. *Exp. Biol. Med. (Maywood.)* **226**, 85-96 (2001).

124. Bohlen und,H.O. & Albrecht,D. The CNS renin-angiotensin system. *Cell Tissue Res.* **326**, 599-616 (2006).

125. Sakai,K. *et al.* Local production of angiotensin II in the subfornical organ causes elevated drinking. *J. Clin. Invest* **117**, 1088-1095 (2007).

126. Sinnayah,P. *et al.* Genetic ablation of angiotensinogen in the subfornical organ of the brain prevents the central angiotensinergic pressor response. *Circ. Res.* **99**, 1125-1131 (2006).

127. Eng,R. & Miselis,R.R. Polydipsia and abolition of angiotensin-induced drinking after transections of subfornical organ efferent projections in the rat. *Brain Res.* **225**, 200-206 (1981).

128. Cato,M.J. & Toney,G.M. Angiotensin II excites paraventricular nucleus neurons that innervate the rostral ventrolateral medulla: an in vitro patch-clamp study in brain slices. *J. Neurophysiol.* **93**, 403-413 (2005).

129. Li,D.P., Chen,S.R. & Pan,H.L. Angiotensin II stimulates spinally projecting paraventricular neurons through presynaptic disinhibition. *J. Neurosci.* **23**, 5041-5049 (2003).

130. Stocker,S.D., Keith,K.J. & Toney,G.M. Acute inhibition of the hypothalamic paraventricular nucleus decreases renal sympathetic nerve activity and arterial blood pressure in water-deprived rats. *Am. J. Physiol Regul. Integr. Comp Physiol* **286**, R719-R725 (2004).

131. Toney,G.M., Chen,Q.H., Cato,M.J. & Stocker,S.D. Central osmotic regulation of sympathetic nerve activity. *Acta Physiol Scand.* **177**, 43-55 (2003).

132. Bains,J.S. & Ferguson,A.V. Paraventricular nucleus neurons projecting to the spinal cord receive excitatory input from the subfornical organ. *Am. J. Physiol* **268**, R625-R633 (1995).

133. Pyner,S. & Coote,J.H. Identification of an efferent projection from the paraventricular nucleus of the hypothalamus terminating close to spinally projecting rostral ventrolateral medullary neurons. *Neuroscience* **88**, 949-957 (1999).

134. Lochard,N., Silversides,D.W., van Kats,J.P., Mercure,C. & Reudelhuber,T.L. Brain-specific restoration of angiotensin II corrects renal defects seen in angiotensinogen-deficient mice. *J. Biol. Chem.* **278**, 2184-2189 (2003).

135. Ganten,D. *et al.* Species specificity of renin kinetics in transgenic rats harboring the human renin and angiotensinogen genes. *Proc. Natl. Acad. Sci. U. S. A* **89**, 7806-7810 (1992).

136. Hatae,T., Takimoto,E., Murakami,K. & Fukamizu,A. Comparative studies on species-specific reactivity between renin and angiotensinogen. *Mol. Cell Biochem.* **131**, 43-47 (1994).

137. Lippoldt,A., Paul,M., Fuxe,K. & Ganten,D. The brain renin-angiotensin system: molecular mechanisms of cell to cell interactions. *Clin. Exp. Hypertens.* **17**, 251-266 (1995).

138. Miyazaki,M. & Takai,S. Tissue angiotensin II generating system by angiotensin-converting enzyme and chymase. *J. Pharmacol. Sci.* **100**, 391-397 (2006).

139. Wright,J.W., Bechtholt,A.J., Chambers,S.L. & Harding,J.W. Angiotensin III and IV activation of the brain AT1 receptor subtype in cardiovascular function. *Peptides* **17**, 1365-1371 (1996).

140. Zini,S. *et al.* Identification of metabolic pathways of brain angiotensin II and III using specific aminopeptidase inhibitors: predominant role of angiotensin III in the control of vasopressin release. *Proc. Natl. Acad. Sci. U. S. A* **93**, 11968-11973 (1996).

141. Santos,R.A. *et al.* Angiotensin-(1-7) is an endogenous ligand for the G protein-coupled receptor Mas. *Proc. Natl. Acad. Sci. U. S. A* **100**, 8258-8263 (2003).

142. Paula,R.D., Lima,C.V., Khosla,M.C. & Santos,R.A. Angiotensin-(1-7) potentiates the hypotensive effect of bradykinin in conscious rats. *Hypertension* **26**, 1154-1159 (1995).

143. Li,P., Chappell,M.C., Ferrario,C.M. & Brosnihan,K.B. Angiotensin-(1-7) augments bradykinin-induced vasodilation by competing with ACE and releasing nitric oxide. *Hypertension* **29**, 394-400 (1997).

144. Ferrario,C.M. *et al.* A hypothesis regarding the function of angiotensin peptides in the brain. *Clin. Exp. Hypertens. A* **10 Suppl 1**, 107-121 (1988).

145. Isa,K. *et al.* Chronic immunoneutralization of brain angiotensin-(1-12) lowers blood pressure in transgenic (mRen2)27 hypertensive rats. *Am. J. Physiol Regul. Integr. Comp Physiol* **297**, R111-R115 (2009).

146. Nagata,S. *et al.* Isolation and identification of proangiotensin-12, a possible component of the renin-angiotensin system. *Biochem. Biophys. Res. Commun.* **350**, 1026-1031 (2006).

147. Ferrario,C.M. *et al.* Differential regulation of angiotensin-(1-12) in plasma and cardiac tissue in response to bilateral nephrectomy. *Am. J. Physiol Heart Circ. Physiol* **296**, H1184-H1192 (2009).

148. Trask,A.J., Jessup,J.A., Chappell,M.C. & Ferrario,C.M. Angiotensin-(1-12) is an alternate substrate for angiotensin peptide production in the heart. *Am. J. Physiol Heart Circ. Physiol* **294**, H2242-H2247 (2008).

149. Fischer-Ferraro,C., Nahmod,V.E., Goldstein,D.J. & Finkielman,S. Angiotensin and renin in rat and dog brain. *J. Exp. Med.* **133**, 353-361 (1971).

150. Ganten,D. *et al.* Renin in dog brain. *Am. J. Physiol* **221**, 1733-1737 (1971).

151. Inagami,T. *et al.* Renin in rat and mouse brain: immunohistochemical identification and localization. *Clin. Sci. (Lond)* **59 Suppl 6**, 49s-51s (1980).

152. Inagami,T. *et al.* Immunohistochemical localization of renin in mouse brain. *Neurosci. Lett.* **18**, 91-98 (1980).

153. Hermann,K., Raizada,M.K., Sumners,C. & Phillips,M.I. Presence of renin in primary neuronal and glial cells from rat brain. *Brain Res.* **437**, 205-213 (1987).

154. Slater,E.E., Defendini,R. & Zimmerman,E.A. Wide distribution of immunoreactive renin in nerve cells of human brain. *Proc. Natl. Acad. Sci. U. S. A* **77**, 5458-5460 (1980).

155. Schweda,F. *et al.* Substitution of connexin40 with connexin45 prevents hyperreninemia and attenuates hypertension. *Kidney Int.* **75**, 482-489 (2009).

156. Wagner,C. Function of connexins in the renal circulation. *Kidney Int.* **73**, 547-555 (2008).

157. Lopez-Bigas,N., Audit,B., Ouzounis,C., Parra,G. & Guigo,R. Are splicing mutations the most frequent cause of hereditary disease? *FEBS Lett.* **579**, 1900-1903 (2005).

158. Newman,A. Molecular biology. RNA enzymes for RNA splicing. *Nature* **413**, 695-696 (2001).

159. Ayoubi,T.A. & Van De Ven,W.J. Regulation of gene expression by alternative promoters. *FASEB J* **10**, 453-460 (1996).

160. Xin,D., Hu,L. & Kong,X. Alternative promoters influence alternative splicing at the genomic level. *PLoS. One.* **3**, e2377 (2008).

161. Lee-Kirsch,M.A., Gaudet,F., Cardoso,M.C. & Lindpaintner,K. Distinct renin isoforms generated by tissue-specific transcription initiation and alternative splicing. *Circ Res* **84**, 240-246 (1999).

162. Sinn,P.L. & Sigmund,C.D. Identification of three human renin mRNA isoforms from alternative tissue-specific transcriptional initiation. *Physiol Genomics* **3**, 25-31 (2000).

163. Morimoto,S., Cassell,M.D. & Sigmund,C.D. The brain renin-angiotensin system in transgenic mice carrying a highly regulated human renin transgene. *Circ. Res.* **90**, 80-86 (2002).

164. Clausmeyer,S., Reinecke,A., Farrenkopf,R., Unger,T. & Peters,J. Tissue-specific expression of a rat renin transcript lacking the coding sequence for the prefragment and its stimulation by myocardial infarction. *Endocrinology* **141**, 2963-2970 (2000).

165. Clausmeyer,S., Sturzebecher,R. & Peters,J. An alternative transcript of the rat renin gene can result in a truncated prorenin that is transported into adrenal mitochondria. *Circ. Res.* **84**, 337-344 (1999).

166. Peters,J., Wanka,H., Peters,B. & Hoffmann,S. A renin transcript lacking exon 1 encodes for a non-secretory intracellular renin that increases aldosterone production in transgenic rats. *J. Cell Mol. Med.* **12**, 1229-1237 (2008).

167. Abel,K.J. & Gross,K.W. Physical characterization of genetic rearrangements at the mouse renin loci. *Genetics* **124**, 937-947 (1990).

168. Sharp,M.G. *et al.* Targeted inactivation of the Ren-2 gene in mice. *Hypertension* **28**, 1126-1131 (1996).

169. Clark,A.F. *et al.* Renin-1 is essential for normal renal juxtaglomerular cell granulation and macula densa morphology. *J. Biol. Chem.* **272**, 18185-18190 (1997).

170. Takahashi,N. *et al.* Ren1c homozygous null mice are hypotensive and polyuric, but heterozygotes are indistinguishable from wild-type. *J Am Soc. Nephrol.* **16**, 125-132 (2005).

171. Yanai,K. *et al.* Renin-dependent cardiovascular functions and renin-independent blood-brain barrier functions revealed by renin-deficient mice. *J Biol Chem* **275**, 5-8 (2000).

172. Takahashi,N. *et al.* Increased energy expenditure, dietary fat wasting, and resistance to diet-induced obesity in mice lacking renin. *Cell Metab* **6**, 506-512 (2007).

173. Sigmund,C.D. & Gross,K.W. Structure, expression, and regulation of the murine renin genes. *Hypertension* **18**, 446-457 (1991).

174. Moriguchi,A. *et al.* Opposing actions of angiotensin-(1-7) and angiotensin II in the brain of transgenic hypertensive rats. *Hypertension* **25**, 1260-1265 (1995).

175. Xu,D. *et al.* Preservation of Intracellular Renin Expression Is Insufficient to Compensate for Genetic Loss of Secreted Renin. *Hypertension* (2009).

176. Borges,G.R. *et al.* Changes in hemodynamic and neurohumoral control cause cardiac damage in one-kidney, one-clip hypertensive mice. *Am J Physiol Regul Integr Comp Physiol* **295**, R1904-R1913 (2008).

177. Halabi,C.M. *et al.* Interference with PPAR gamma function in smooth muscle causes vascular dysfunction and hypertension. *Cell Metab* **7**, 215-226 (2008).

178. Cole,J. *et al.* Lack of angiotensin II-facilitated erythropoiesis causes anemia in angiotensin-converting enzyme-deficient mice. *J Clin. Invest* **106**, 1391-1398 (2000).

179. Oliverio,M.I. *et al.* Reduced growth, abnormal kidney structure, and type 2 (AT2) angiotensin receptor-mediated blood pressure regulation in mice lacking both AT1A and AT1B receptors for angiotensin II. *Proc. Natl. Acad. Sci. U. S. A* **95**, 15496-15501 (1998).

180. Kim,H.S. *et al.* Homeostasis in mice with genetically decreased angiotensinogen is primarily by an increased number of renin-producing cells. *J Biol Chem* **274**, 14210-14217 (1999).

181. Davisson,R.L. *et al.* Complementation of reduced survival, hypotension, and renal abnormalities in angiotensinogen-deficient mice by the human renin and human angiotensinogen genes. *J Clin. Invest* **99**, 1258-1264 (1997).

182. Massiera,F. *et al.* Angiotensinogen-deficient mice exhibit impairment of diet-induced weight gain with alteration in adipose tissue development and increased locomotor activity. *Endocrinology* **142**, 5220-5225 (2001).

183. Ishida,J. *et al.* Rescue of angiotensinogen-knockout mice. *Biochem. Biophys. Res Commun.* **252**, 610-616 (1998).

184. Knudsen,S. Promoter2.0: for the recognition of PolII promoter sequences. *Bioinformatics.* **15**, 356-361 (1999).

185. Mercure,C. *et al.* Molecular analysis of human prorenin prosegment variants in vitro and in vivo. *J Biol Chem* **270**, 16355-16359 (1995).

186. Morimoto,S., Cassell,M.D. & Sigmund,C.D. Neuron-specific expression of human angiotensinogen in brain causes increased salt appetite. *Physiol Genomics* **9**, 113-120 (2002).

187. Nishimura,M., Milsted,A., Block,C.H., Brosnihan,K.B. & Ferrario,C.M. Tissue renin-angiotensin systems in renal hypertension. *Hypertension* **20**, 158-167 (1992).

188. Porter,J.P., Anderson,J.M., Robison,R.J. & Phillips,A.C. Effect of central angiotensin II on body weight gain in young rats. *Brain Res.* **959**, 20-28 (2003).

189. Porter,J.P. & Potratz,K.R. Effect of intracerebroventricular angiotensin II on body weight and food intake in adult rats. *Am. J. Physiol Regul. Integr. Comp Physiol* **287**, R422-R428 (2004).

190. Bunnemann,B., Lippoldt,A., Aguirre,J.A., Cintra,A. & Metzger,R. Glucocorticoid regulation of angiotensinogen gene expression in discrete areas of the male rat brain. An in situ hybridization study. *Neuroendocrinology* **57**, 856-862 (1993).

191. Sangaleti,C.T., Crescenzi,A. & Michelini,L.C. Endogenous angiotensin and pressure modulate brain angiotensinogen and AT1A mRNA expression. *Hypertension* **43**, 317-323 (2004).

192. Stornetta,R.L., Hawelu-Johnson,C.L., Guyenet,P.G. & Lynch,K.R. Astrocytes synthesize angiotensinogen in brain. *Science* **242**, 1444-1446 (1988).

193. Yang,G., Gray,T.S., Sigmund,C.D. & Cassell,M.D. The angiotensinogen gene is expressed in both astrocytes and neurons in murine central nervous system. *Brain Res* **817**, 123-131 (1999).

194. Sherrod,M., Liu,X., Zhang,X. & Sigmund,C.D. Nuclear localization of angiotensinogen in astrocytes. *Am J Physiol Regul Integr Comp Physiol* **288**, R539-R546 (2005).

195. Morimoto,S. *et al.* Elevated blood pressure in transgenic mice with brain-specific expression of human angiotensinogen driven by the glial fibrillary acidic protein promoter. *Circ. Res.* **89**, 365-372 (2001).

196. Sherrod,M., Davis,D.R., Zhou,X., Cassell,M.D. & Sigmund,C.D. Glial-specific ablation of angiotensinogen lowers arterial pressure in renin and

angiotensinogen transgenic mice. *Am J Physiol Regul Integr Comp Physiol* **289**, R1763-R1769 (2005).

197. Francis,J., Wei,S.G., Weiss,R.M. & Felder,R.B. Brain angiotensin-converting enzyme activity and autonomic regulation in heart failure. *Am J Physiol Heart Circ Physiol* **287**, H2138-H2146 (2004).

198. Lenkei,Z., Palkovits,M., Corvol,P. & Llorens-Cortes,C. Expression of angiotensin type-1 (AT1) and type-2 (AT2) receptor mRNAs in the adult rat brain: a functional neuroanatomical review. *Front Neuroendocrinol.* **18**, 383-439 (1997).

199. Ganten,D. *et al.* Angiotensin-forming enzyme in brain tissue. *Science* **173**, 64-65 (1971).

200. Sinn,P.L., Davis,D.R. & Sigmund,C.D. Highly regulated cell type-restricted expression of human renin in mice containing 140- or 160-kilobase pair P1 phage artificial chromosome transgenes. *J. Biol. Chem.* **274**, 35785-35793 (1999).

201. Campbell,D.J. Critical review of prorenin and (pro)renin receptor research. *Hypertension* **51**, 1259-1264 (2008).

202. Nguyen,G. & Danser,A.H. Prorenin and (pro)renin receptor: a review of available data from in vitro studies and experimental models in rodents. *Exp. Physiol* **93**, 557-563 (2008).

203. Batenburg,W.W. & Jan Danser,A.H. The (pro)renin receptor: a new addition to the renin-angiotensin system? *Eur. J. Pharmacol.* **585**, 320-324 (2008).

204. Lavoie,J.L., Cassell,M.D., Gross,K.W. & Sigmund,C.D. Localization of renin expressing cells in the brain, by use of a REN-eGFP transgenic model. *Physiol Genomics* **16**, 240-246 (2004).

205. Kubo,T., Hagiwara,Y., Endo,S. & Fukumori,R. Activation of hypothalamic angiotensin receptors produces pressor responses via cholinergic inputs to the rostral ventrolateral medulla in normotensive and hypertensive rats. *Brain Res.* **953**, 232-245 (2002).

206. Santos,E.L. *et al.* Effect of angiotensin converting enzyme inhibitor enalapril on body weight and composition in young rats. *Int. Immunopharmacol.* **8**, 247-253 (2008).

207. Zorad,S. *et al.* Long-term angiotensin II AT1 receptor inhibition produces adipose tissue hypotrophy accompanied by increased expression of adiponectin and PPARgamma. *Eur. J. Pharmacol.* **552**, 112-122 (2006).

208. Jayasooriya,A.P. *et al.* Mice lacking angiotensin-converting enzyme have increased energy expenditure, with reduced fat mass and improved glucose clearance. *Proc. Natl. Acad. Sci. U. S. A* **105**, 6531-6536 (2008).

209. Kouyama,R. *et al.* Attenuation of diet-induced weight gain and adiposity through increased energy expenditure in mice lacking angiotensin II type 1a receptor. *Endocrinology* **146**, 3481-3489 (2005).

210. Yvan-Charvet,L. *et al.* Deletion of the angiotensin type 2 receptor (AT2R) reduces adipose cell size and protects from diet-induced obesity and insulin resistance. *Diabetes* **54**, 991-999 (2005).

211. Santos,S.H. *et al.* Mas deficiency in FVB/N mice produces marked changes in lipid and glycemic metabolism. *Diabetes* **57**, 340-347 (2008).

212. Tronche,F. *et al.* Disruption of the glucocorticoid receptor gene in the nervous system results in reduced anxiety. *Nat. Genet.* **23**, 99-103 (1999).

213. Zhuo,L. *et al.* hGFAP-cre transgenic mice for manipulation of glial and neuronal function in vivo. *Genesis.* **31**, 85-94 (2001).

214. Sequeira Lopez,M.L., Pentz,E.S., Nomasa,T., Smithies,O. & Gomez,R.A. Renin cells are precursors for multiple cell types that switch to the renin phenotype when homeostasis is threatened. *Dev. Cell* **6**, 719-728 (2004).

215. Sakai,K., Chapleau,M.W., Morimoto,S., Cassell,M.D. & Sigmund,C.D. Differential modulation of baroreflex control of heart rate by neuron- vs. glia-derived angiotensin II. *Physiol Genomics* **20**, 66-72 (2004).

216. Betz,U.A., Vosshenrich,C.A., Rajewsky,K. & Muller,W. Bypass of lethality with mosaic mice generated by Cre-loxP-mediated recombination. *Curr Biol* **6**, 1307-1316 (1996).

217. Forni,P.E. *et al.* High levels of Cre expression in neuronal progenitors cause defects in brain development leading to microencephaly and hydrocephaly. *J Neurosci.* **26**, 9593-9602 (2006).

218. Isaka,F. *et al.* Ectopic expression of the bHLH gene Math1 disturbs neural development. *Eur. J Neurosci.* **11**, 2582-2588 (1999).

219. Hanner,F. *et al.* Connexin45 is expressed in the juxtaglomerular apparatus and is involved in the regulation of renin secretion and blood pressure. *Am J Physiol Regul Integr Comp Physiol* **295**, R371-R380 (2008).

220. Vlasenko,R.I. & Kotov,A.V. [Effector peptides of the brain renin-angiotensin system in central mechanisms of learned and natural forms of drinking behavior in rats]. *Zh. Vyssh. Nerv. Deiat. Im I. P. Pavlova* **56**, 102-110 (2006).

221. Buckley,J.P., Jandhyala,B.S., Doursout,M.F., Huang,Y.K. & Chelly,J.E. Effects of brain renin-angiotensin on cardiovascular function and saline intake in awake dogs. *J. Physiol (Paris)* **79**, 485-490 (1984).

222. Monti,J. *et al.* Glial angiotensinogen regulates brain angiotensin II receptors in transgenic rats TGR(ASrAOGEN). *Am. J. Physiol Regul. Integr. Comp Physiol* **280**, R233-R240 (2001).

223. Fitzsimons,J.T. The physiology of thirst and sodium appetite. *Monogr Physiol Soc.* 1-572 (1979).

224. Rowland,N.E. & Fregly,M.J. Characteristics of thirst and sodium appetite in mice (Mus musculus). *Behav. Neurosci.* **102**, 969-974 (1988).

225. Sweet,C.S., Columbo,J.M. & Gaul,S.L. Central antihypertensive effects of inhibitors of the renin-angiotensin system in rats. *Am. J. Physiol* **231**, 1794-1799 (1976).

226. Singh,V.P., Le,B., Bhat,V.B., Baker,K.M. & Kumar,R. High-glucose-induced regulation of intracellular ANG II synthesis and nuclear redistribution in cardiac myocytes. *Am. J. Physiol Heart Circ. Physiol* **293**, H939-H948 (2007).

227. Grise,C., Boucher,R., Thibault,G. & Genest,J. Formation of angiotensin II by tonin from partially purified human angiotensinogen. *Can. J. Biochem.* **59**, 250-255 (1981).

228. Wahl,M., Gorlach,C., Hortobagyi,T. & Benyo,Z. Effects of bradykinin in the cerebral circulation. *Acta Physiol Hung.* **86**, 155-160 (1999).

229. Bronson,S.K., Smithies,O. & Mascarello,J.T. High incidence of XXY and XYY males among the offspring of female chimeras from embryonic stem cells. *Proc. Natl. Acad. Sci. U. S. A* **92**, 3120-3123 (1995).

230. Rahmouni,K. *et al.* Effects of brain mineralocorticoid receptor blockade on blood pressure and renal functions in DOCA-salt hypertension. *Eur. J. Pharmacol.* **436**, 207-216 (2002).

231. Karatas,A. *et al.* Deoxycorticosterone acetate-salt mice exhibit blood pressure-independent sexual dimorphism. *Hypertension* **51**, 1177-1183 (2008).

232. Wang,Q., Domenighetti,A.A., Pedrazzini,T. & Burnier,M. Potassium supplementation reduces cardiac and renal hypertrophy independent of blood pressure in DOCA/salt mice. *Hypertension* **46**, 547-554 (2005).

233. Lazartigues,E. *et al.* Enhanced water and salt intake in transgenic mice with brain-restricted overexpression of angiotensin (AT1) receptors. *Am J Physiol Regul Integr Comp Physiol* **295**, R1539-R1545 (2008).

234. Lazartigues,E. *et al.* Brain-selective overexpression of angiotensin (AT1) receptors causes enhanced cardiovascular sensitivity in transgenic mice. *Circ Res* **90**, 617-624 (2002).

235. Ganten,D., Mullins,J. & Lindpaintner,K. The tissue renin-angiotensin system: a target for angiotensin-converting enzyme inhibitors. *J. Hum. Hypertens.* **3 Suppl 1**, 63-70 (1989).

236. Xia,H. & Lazartigues,E. Angiotensin-converting enzyme 2 in the brain: properties and future directions. *J. Neurochem.* **107**, 1482-1494 (2008).

237. Tirapelli,C.R., Bonaventura,D., Tirapelli,L.F. & de Oliveira,A.M. Mechanisms underlying the vascular actions of endothelin 1, angiotensin II and bradykinin in the rat carotid. *Pharmacology* **84**, 111-126 (2009).

238. Cassis,L.A., Marshall,D.E., Fettinger,M.J., Rosenbluth,B. & Lodder,R.A. Mechanisms contributing to angiotensin II regulation of body weight. *Am. J. Physiol* **274**, E867-E876 (1998).

239. Davisson,R.L. Physiological genomic analysis of the brain renin-angiotensin system. *Am J Physiol Regul Integr Comp Physiol* **285**, R498-R511 (2003).

240. Dantuma,N.P., Heessen,S., Lindsten,K., Jellne,M. & Masucci,M.G. Inhibition of proteasomal degradation by the gly-Ala repeat of Epstein-Barr virus is influenced by the length of the repeat and the strength of the degradation signal. *Proc. Natl. Acad. Sci. U. S. A* **97**, 8381-8385 (2000).

241. Hershko,A. & Ciechanover,A. The ubiquitin system. *Annu. Rev. Biochem.* **67**, 425-479 (1998).

242. Samani,N.J. & Swales,J.D. Molecular biology of the vascular renin-angiotensin system. *Blood Vessels* **28**, 210-216 (1991).

243. Muller,D.N. & Luft,F.C. The renin-angiotensin system in the vessel wall. *Basic Res Cardiol.* **93 Suppl 2**, 7-14 (1998).

244. Bergamaschi,C., Campos,R.R., Schor,N. & Lopes,O.U. Role of the rostral ventrolateral medulla in maintenance of blood pressure in rats with Goldblatt hypertension. *Hypertension* **26**, 1117-1120 (1995).

245. Kjaer,A., Knigge,U., Jorgensen,H. & Warberg,J. Dehydration-induced vasopressin secretion in humans: involvement of the histaminergic system. *Am. J. Physiol Endocrinol. Metab* **279**, E1305-E1310 (2000).

246. Inoue,M., Crofton,J.T. & Share,L. Interactions between the brain renin-angiotensin system and brain prostanoids in the control of vasopressin secretion. *Exp Brain Res* **83**, 131-136 (1990).